

2014•2015
FACULTEIT INDUSTRIËLE INGENIEURSWETENSCHAPPEN
*master in de industriële wetenschappen: nucleaire
technologie*

Masterproef

Radiological characterization of a cyclotron in view of its dismantling
and final disposal

Promotor :
dr. ir. Herwig JANSSENS

Promotor :
Dhr. PHILIPPE DAMHAUT

Nathan Van Raemdonck

*Scriptie ingediend tot het behalen van de graad van master in de industriële
wetenschappen: nucleaire technologie*

Gezamenlijke opleiding Universiteit Hasselt en KU Leuven

2014•2015

Faculteit Industriële

ingenieurswetenschappen

*master in de industriële wetenschappen: nucleaire
technologie*

Masterproef

Radiological characterization of a cyclotron in view of
its dismantling and final disposal

Promotor :
dr. ir. Herwig JANSSENS

Promotor :
Dhr. PHILIPPE DAMHAUT

Nathan Van Raemdonck

*Scriptie ingediend tot het behalen van de graad van master in de industriële
wetenschappen: nucleaire technologie*

Preface

During my studies in the nuclear sciences I became very interested in the dismantling of nuclear facilities. Proper dismantling and decommissioning of such facilities is nowadays a topical subject and also very interesting from the point of view of an industrial engineer. As a result, it was for me obvious to dedicate my master's thesis to the topic of dismantling a nuclear facility. I am thankful to ONDRAF/NIRAS for giving me the opportunity to contribute to the preparation of the dismantling of the cyclotron facility at Fleurus.

As most information about decommissioning and dismantling of nuclear facilities is available from nuclear power plants, it was a great opportunity to learn about the dismantling of an accelerator facility and the different options to dispose of the activated materials.

This master's thesis was a great opportunity to put the learned theories and methods into practice, but also to learn new approaches and ideas about radiological characterization and final disposal options. Furthermore it was a great opportunity to get to know ONDRAF/NIRAS and their operations.

I would like to thank all the people from ONDRAF/NIRAS for their help and contributions to my master's thesis. In particular I am thankful to Olivier Emond and my promoters Philippe Damhaut and dr. ir. Herwig Janssens for their critical lecture and recommendations.

Furthermore, I am grateful to my parents for giving me the opportunity to follow these studies and to do my master's thesis at Fleurus.

Finally, a special word of thanks goes to my girlfriend Saskia who kept supporting and motivating me to accomplish my studies and master's thesis in the nuclear sciences.

Nathan Van Raemdonck

Table of contents

1	Introduction	15
1.1	The setting	15
1.2	The problem statement	15
1.3	The thesis' objectives	16
1.4	The methods and materials	16
2	ONDRAF/NIRAS	19
3	Cyclotrons	21
4	Dismantling of a nuclear facility	25
5	Cyclotron at Fleurus	27
5.1	General information	27
5.2	Production and operation.....	29
6	Activation	31
6.1	Basic concept.....	31
6.2	Activation in the cyclotron at Fleurus	31
6.2.1	Proton induced nuclear reactions.....	31
6.2.2	Neutron induced nuclear reactions	34
6.3	Inventory of potentially activated materials	37
6.3.1	Metallic parts	37
6.3.2	Non-metallic parts	38
7	Final disposal scenarios of the activated metals	41
7.1	Introduction	41
7.2	Unconditional release	41
7.3	Melting	42
7.3.1	Studsvik Nuclear AB.....	43
7.3.2	EnergySolutions.....	45
7.4	Radioactive waste.....	46
7.4.1	Category A waste	46
7.4.2	Acceptance criteria	47
7.5	Overview of the disposal of activated materials.....	49

8	Methodology.....	51
8.1	Drilling campaign.....	51
8.2	Sample preparation.....	60
8.3	Gamma spectrometry	61
8.3.1	Basic information	61
8.3.2	Detector set-up	62
8.3.3	Calibration	65
8.3.4	Measurement of the samples	68
9	Results and discussion.....	69
9.1	Identified radionuclides.....	69
9.1.1	Metallic samples.....	69
9.1.2	Concrete samples.....	71
9.2	Specific activities of the identified radionuclides.....	72
9.2.1	Deflector area	72
9.2.2	Magnetic channel	78
9.2.3	Beam exit area	79
9.2.4	Switching magnet	80
9.2.5	Ventilation units	83
9.2.6	Internal target area.....	84
9.2.7	High frequency cavity	85
9.2.8	Identified hotspots	85
9.3	Elaboration of the final disposal scenarios of the activated metallic components	86
9.3.1	Deflector area	88
9.3.2	Magnetic channel	90
9.3.3	High frequency cavity 2	90
9.3.4	Beam exit area	90
9.3.5	Switching magnet area	91
9.3.6	Ventilation units	92
9.3.7	Internal target area.....	93
9.3.8	High frequency cavity 1	93
9.3.9	Overview of the final disposal options	95
9.3.10	Additional acceptance criteria for final disposal options	98
10	Conclusion and future work.....	101
10.1	Conclusions	101
10.2	Recommendations and future work.....	102

List of tables

Table 1 - Classification of neutrons by their energy	34
Table 2 - Chemical composition of steel	37
Table 3 - Constituent elements (ppm) in concrete used in IRMM as measured by SCK•CEN	39
Table 4 - Release levels of radionuclides of interest with regard to activation	41
Table 5 - Redistribution of activity (%) of radionuclides over the different melting end products	43
Table 6 - EnergySolutions waste acceptance criteria	45
Table 7 - Allowed metals for A14 and A17; courtesy of ONDRAF/NIRAS	47
Table 8 - Difference between A14 and A17	48
Table 9 - Composition of multi-gamma calibration source	66
Table 10 - Measuring time of the samples	68
Table 11 - Identified radionuclides	69
Table 12 - Possible activation products in metallic components	71
Table 13 - Radionuclides present in concrete samples	71
Table 14 - Specific activities [kBq/kg] at centre of deflector area	76
Table 15 - Comparison between specific activity of copper (Cu) and stainless steel (SS) at right side of the deflector area	77
Table 16 - Specific activities measured in the switching magnet	81
Table 17 - Specific activities in beam pipe supports after the switching magnet	82
Table 18 - Specific activation in the ventilation unit	83
Table 19 - Overview of the three hotspots identified in the cyclotron	86
Table 20 - Acceptance criteria for final disposal options	87
Table 21 - Example of the final disposal evaluation for samples	87
Table 22 - Specific activities at the ventilation units and final disposal options	92
Table 23 - Overview of the optimal final disposal options for each component	95
Table 24 - Overview of the optimal final disposal options for each component – continued	96
Table 25 - Components that need additional sampling	104
Table 26 - Components with decay times to 0.1 kBq/kg lower than 5 years	105
Table 27 - Release levels of radionuclides	106

List of figures

Figure 1 - Durable solutions of ONDRAF/NIRAS	19
Figure 2 – ONDRAF/NIRAS	20
Figure 3 - Schematic principle of a cyclotron	21
Figure 4 - Extraction of positively and negatively charged particles	22
Figure 5 - Number of existing cyclotrons categorized by their energy; reported from an IAEA survey of 2006.....	23
Figure 6 - Drawing of building B14 – Fleurus	27
Figure 7 - CGR-MEV cyclotron accelerator vault and irradiations rooms	28
Figure 8 - 3D view of CGR-MEV cyclotron.....	28
Figure 9 - Number of irradiations January 1988 – April 1988 CGR-MEV	29
Figure 10 - Cross section of ^{52}Cr (p,n) ^{52}Mn reaction	33
Figure 11 - Maxwell - Boltzmann distribution of thermal neutrons	35
Figure 12 - Cross section for ^{59}Co (n, γ) ^{60}Co reaction.....	36
Figure 13 - Melting process of containerized scrap at Studsvik Nuclear AB	44
Figure 14 - cAt surface repository.....	46
Figure 15 - Three caisson types to store cat. A wastes.....	46
Figure 16 - Disposal options for the potential activated metallic materials	49
Figure 17 - Dose rates measured around the CGR cyclotron (values are not corrected for background)	52
Figure 18 - Dose rates measured in the CGR cyclotron	52
Figure 19 - CGR cyclotron sample positions	54
Figure 20 - CGR cyclotron sample positions at deflector	55
Figure 21 - CGR cyclotron sample positions in accelerator room	56
Figure 22 - Example of samples at different distances of the component of interest.....	57
Figure 23 - Drilling campaign	58
Figure 24 - Procedure for depth drilling.....	59
Figure 25 - Samples in concrete (cyclotron vault)	59
Figure 26 - Petri dish geometry.....	60
Figure 27 - Example of prepared sample (top and bottom sides).....	60
Figure 28 - Structure of a gamma ray spectrum [54]	61
Figure 29 - Influence of the surrounding materials on the gamma spectrum.....	62
Figure 30 - Features of HPGe GX 2518.....	62
Figure 31 - Example of a measured spectrum with indication of the radionuclides present.....	63
Figure 32 - Example of a report of measurement.....	64
Figure 33 - Energies of the Eu-152 source used for calibration.....	65
Figure 34 - Result of energy calibration.....	65
Figure 35 - Calculated efficiency from the multi-gamma source.....	67
Figure 36 - Efficiency of the petri dish calibration source	67
Figure 37 - Samples with ^{137}Cs	69
Figure 38 - Sample locations at the left side of the deflector area	73
Figure 39 - Activation at the left side of the deflector area.....	73
Figure 40 - Variation of specific activity with depth	74
Figure 41 - Additional samples at left edge of deflector area	74
Figure 42 - Samples in centre of deflector area.....	75
Figure 43 - Activation at the centre of deflector area.....	75
Figure 44 - Variation of specific activities with depth at position 020	76
Figure 45 - Right side of the deflector area.....	76

Figure 46 - Vertical variation of the specific activity [kBq/kg] in stainless steel and copper	78
Figure 47 - Depth measurement of sample 023.....	78
Figure 48 - Samples and specific activities in the magnetic channel	79
Figure 49 - Beam exit area	80
Figure 50 - Specific activity in beam tube support between beam exit area and switching magnet	80
Figure 51 - Samples taken from the switching magnet	81
Figure 52 - Beam transport set-up at the track 1	82
Figure 53 - Sample locations in cast-iron focus lens and box to stop the beam during emergency	83
Figure 54 - Sample locations at the ventilation units of the cyclotron vault	83
Figure 55 - Internal target area and sample locations.....	84
Figure 56 - Specific activities in stainless steel component at internal target area	84
Figure 57 - Sample 069 at HF cavity 1	85
Figure 58 - Overview of the three hotspots identified in the cyclotron.....	86
Figure 59 - Variation of specific activity with depth	88
Figure 60 - Top of the cyclotron above the deflector area	89
Figure 61 - Beam tube support structure from beam exit to switching magnet	91
Figure 62 - Box and solid iron structure to stop the beam during emergency	92
Figure 63 - Direction of additional samples at internal target area	93
Figure 64 - HF cavity 1	94
Figure 65 - Quantitative overview of the final disposal option.....	96
Figure 66 - Example of method to average specific activity.....	97
Figure 67 - Structure on which the internal target was mounted.....	102
Figure 68 - Specific activities of the concrete samples	103

List of abbreviations

BMB

Best Medical Belgium

FWHM

Full Width at Half Maximum

HPGE

High Purity Germanium detector

IAEA

International Atomic Energy Agency

IRE

Institute for Radioelements

IRMM

Institute for Reference Materials and Measurements

ONDRAF/NIRAS

Belgian Agency For Radioactive Waste and enriched Fissile materials

SCK ° CEN

Belgian Nuclear Research Centre

Abstract

The CGR-MeV cyclotron at Fleurus was used for medical isotope production from 1983 until 1993 and, after more than 20 years of inactivity, is intended to be dismantled. Due to its operation, the internals as well as the surrounding materials of the accelerator are activated. This study's main objective is to determine the radiological characterization of the internal and external metallic parts of the accelerator room as a preparation for their final disposal. The results from this study will give insight into the different options for the disposal of the activated materials based on the Belgian release levels and acceptance limits for nuclear melting facilities.

Based on dose measurements at various metallic parts, 82 samples were drilled in the cyclotron. In addition to those 82 metallic samples, 3 samples were taken from the concrete shield as a first indication of its activation. The samples consist of approximately 1 gram of metal or concrete and were all measured within the same geometry. Finally, the 85 samples were characterized through gamma spectrometry using an HPGe detector.

In the metallic samples, ^{60}Co was the only identified radionuclide with specific activities ranging from non-detectable quantities up to 328 kBq/kg. The deflector, the beam exit and the internal target site were found to be the most activated parts. Based on specific activities, 11% of the samples present values lower than the Belgian release limit for ^{60}Co . The higher activated materials qualify for recycling in melting facilities.

Abstract – Dutch

De CGR-MeV cyclotron in Fleurus werd gebruikt van 1983 tot 1993 voor de productie van medische radionucliden en is nu, na meer dan 20 jaar buiten gebruik, klaar om ontmanteld te worden. Door het gebruik zijn de materialen van de versneller geactiveerd. De focus van deze studie is de radiologische karakterisatie van de interne en externe metallische componenten in de versnellersruimte. Het resultaat ervan zal meer inzicht geven in de verschillende opties voor de behandeling van de geactiveerde metalen. Deze opties zijn gebaseerd op de Belgische niveaus voor onvoorwaardelijke vrijgave en de acceptatiecriteria van gespecialiseerde smelterijen.

Op basis van dosistempo metingen bij verscheidene metallische componenten werden er 82 stalen geboord. Naast deze 82 stalen, werden er nog 3 stalen genomen uit de betonnen muren als een eerste indicatie van de activatie ervan. De stalen bestaan uit ongeveer 1 gram metaal of beton en werden allen gemeten in dezelfde geometrie. Ten slotte werden de 85 stalen gekarakteriseerd door gamma spectrometrie met behulp van een HPGe detector.

In de metallische stalen was ^{60}Co het enige te identificeren radionuclide met een specifieke activiteit variërend tussen niet-detecteerbaar en 328 kBq/kg. De deflector, de bundeluitgang en de interne trefschijf omgeving werden geïdentificeerd als de meest geactiveerde delen. Op basis van de specifieke activiteiten is 11% van de stalen geschikt voor onvoorwaardelijke vrijgave. De hoger geactiveerde materialen zijn bedoeld voor gespecialiseerde smelterijen.

1 Introduction

1.1 The setting

Nuclear power plants, nuclear medicine facilities, research centres with nuclear applications and many other nuclear facilities produce wastes. A fraction of the waste is radioactive and thus requires special attention and treatment. In order to protect the environment and the community, a national management of the radioactive waste is needed. ONDRAF/NIRAS is the Belgian Organism for Radioactive waste and enriched Fissile materials and is responsible for the national management of all the radioactive wastes present on the Belgian territory. Every producer of radioactive wastes has to fulfil the waste acceptance criteria (ACRIA) of NIRAS in order to dispose of their waste. As well as the production of nuclear wastes, every nuclear facility needs to be decommissioned sooner or later. This process is usually accompanied by a decontamination and dismantling process. The execution of such processes produces a lot of radioactive wastes in that matter that those projects are closely linked with ONDRAF/NIRAS to safely manage the wastes, to look over the compliance with the ACRIA's and to assure their final disposal.

At Fleurus, located near the Belgian city Charleroi, the company "Best Medical Belgium S.A." (BMB) was using a cyclotron for the production of radio-isotopes for medical use (mainly Tl-201 and I-123) and research and development. Due to financial problems the commercial court of Charleroi declared the company bankrupt on the 14th of May 2012.

In accordance with the Belgian law of 8 August 1980 and with the Belgian Royal Decree of 30 March 1981, one of ONDRAF/NIRAS's legal assignments is to carry out the decommissioning program and the decommissioning operations of the contaminated facilities belonging to radioactive waste producers in case of failure, which is the case for BMB due to its bankruptcy.

1.2 The problem statement

BMB at Fleurus was a nuclear facility with two cyclotrons that are placed in a vault, surrounded by thick, reinforced, concrete walls. Due to the use of a cyclotron, the reinforced concrete walls and the cyclotron itself are activated. In order to dismantle the facility it is important to characterize the radionuclides that were created in the many years of service of the facility. Besides the radionuclides that were formed in the materials of the accelerator due to its use, there are still some of the produced radionuclides (or by-products) present in the cyclotron. So at one end there are radionuclides due to activation of the materials present and at the other end there are radionuclides present that are leftovers from the production process.

The dismantling of the cyclotron facility, which will take about 5 years and 10 years for the entire project, will produce a lot of radioactive wastes due to the presence of the radionuclides. For the final disposal, the radioactive wastes must be fully characterized. It must be known which radionuclides are present and in which quantity. So this characterization is both quantitative and qualitative. With these radiological characteristics it will be possible to fulfil the waste acceptance criteria of ONDRAF/NIRAS and to define the optimal final disposal scenario of the activated materials. Furthermore this characterization allows a cost estimation for the final disposal of the radioactive wastes. Without the characterization information, ONDRAF/NIRAS will not accept the waste for disposal and it will not be possible to dismantle and therefor decommission the facility. In addition,

the cost estimation is based on the quantity of radioactive waste, without the characterization, it will be impossible to quantify the waste and therefore to estimate the cost to dispose of the waste. Because the wastes and the dismantling of the cyclotron facility are a wide concept, this research project will focus on the activation of one of the two cyclotrons and thus the radionuclides present in it. The central theme of this master project will be the radiological characterization of the cyclotron of ONDRAF/NIRAS – Fleurus Site as a preparation for its dismantling. In correspondence with this central theme the following question will be the main definition of the problem, which the project will try to give an answer to:

Which radionuclides, produced by the cyclotron itself as well as a consequence of the activation of the cyclotron materials, are present in the cyclotron at ONDRAF – Fleurus Site and in which quantity?

1.3 The thesis' objectives

To properly answer this central definition of the problem this thesis has 5 objectives:

The first objective is to perform an extensive literature study in order to learn about the theoretical aspect of the dismantling and decommissioning of a nuclear facility and especially of an accelerator/cyclotron facility.

The second objective is to plan and to take a series of samples of the material of different parts of the cyclotron and analyse them with the proper detection and measurement equipment. This also includes learning how to use this equipment. This has the purpose to obtain a radiological characterization of the cyclotron in order to properly prepare the dismantling operation and to store the nuclear wastes.

The third objective includes the classification of the different materials by their radiological characteristics in order to define the optimal final disposal.

The fourth objective is to make a cost estimation, based on the previous goals, for the future disposal of the radioactive waste coming from the dismantling process.

The fifth and last objective is to get insight of the organisation ONDRAF/NIRAS at Brussels and at Fleurus site, its role in the dismantling operation and the radioactive waste management. This also includes learning about the criteria of acceptance (ACRIA's).

1.4 The methods and materials

In order to obtain the information needed for the theoretical aspects of the thesis, different sources will be consulted and read. Online databases and libraries as well as physical libraries of Hasselt university and university of Leuven and the library of ONDRAF/NIRAS will be consulted. Also, documents and reports concerning the specifications of the cyclotron at Fleurus, the management of radioactive wastes, the organization of ONDRAF/NIRAS, the dismantling and decontamination operations will be looked into. In addition, various people who work at ONDRAF/NIRAS – Fleurus Site will be consulted to get additional information about the subject. Furthermore, various lectures and company visits concerning the decommissioning process, ACRIA's and the management of radioactive waste

will be attended. Once the usefulness of an article, report, book or other source has been verified, the document will be read and summarized. By this way, it is much easier to consult the necessary information when it is needed in the course of this thesis.

The process of taking the samples is preceded by the decision of in which parts of the cyclotron the samples will be taken. The decision making of the location of the samples will be in cooperation with employees from ONDRAF/NIRAS who know most about the specifications of the cyclotron. Depending on those decisions the samples can consist of loose parts of the machine as well as drilled samples in the infrastructure of the machine. The various samples will be measured one by one with a High Purity Germanium detector (HPGe). After the measurement, the obtained spectrum will be analysed with the “Apex Gamma™” software of Canberra industries Inc. The specifications, guidelines as well as the manual of the detector are found in documents provided by NDRAF/NIRAS. To properly classify the different materials which the cyclotron consists of by their radiological aspects and to also make a cost estimate for the final disposal of those materials, internal documents of ONDRAF/NIRAS will be used. Those documents contain and specify the management of radioactive waste.

The first chapter of this thesis will give an introduction about ONDRAF/NIRAS, their mission and their operations. As the focus is on the radiological characterization of a cyclotron, the second chapter discusses the operation of a cyclotron and the most important components of it. This will be useful later on in this study. Chapter four discusses the advantages and disadvantages of the different approaches for the decommissioning and dismantling of a nuclear facility. Because know-how of the site is vital for the preparation of its dismantling, chapter 5 contains information about the site of BMB at Fleurus. Moving on to chapter 6, which is an introduction to the concept of activation. This chapter explains the processes that happened during the operation of the cyclotron and resulted in the activation of the different materials present in the accelerator room. After this the different options for final disposal of the activated materials are discussed. This chapter 7 concludes the theoretical aspect of this study. Next the methodology of the drilling campaign and the methods that were used to identify and quantify the radionuclides in the samples are discussed in chapter 8. The results of the measurements are given and discussed in chapter 9. This chapter first deals with the qualitative analysis of the measured samples. Secondly, a quantitative analysis is made of the different metallic components present in the cyclotron vault. Finally, chapter 9 discusses the current optimal final disposal option of each metallic component. Finally, chapter 10 gives an overview of the conclusions of this master’s thesis and discusses the recommendations for future research.

2 ONDRAF/NIRAS

The management of radioactive waste in Belgium is given by the legislator to the control of ONDRAF/NIRAS: Belgian Organism For Radioactive Waste and Enriched Fissile materials. The organization was created in 1980 by the law of 8 August 1980 and was completed with the Royal decree of 30 March 1981 and with the legal texts that modify and complete this decree [1].

ONDRAF/NIRAS is a public organization in charge of the short and long term management of all the radioactive wastes on the Belgian territory. This management is all-embracing, the final disposal included and is supervised by the ministers who are entitled for economic affairs and energy [1]. In order to manage all the radioactive wastes now and in the future, ONDRAF/NIRAS develops and implements solutions which are regardful for the society as well as for the environment. In doing so, the organisation maintains a system that is based on an equilibrium between the technical, economical, societal and ecological aspect of durable solutions for the management of radioactive waste. Figure 1 visualizes this durable equilibrium [1].

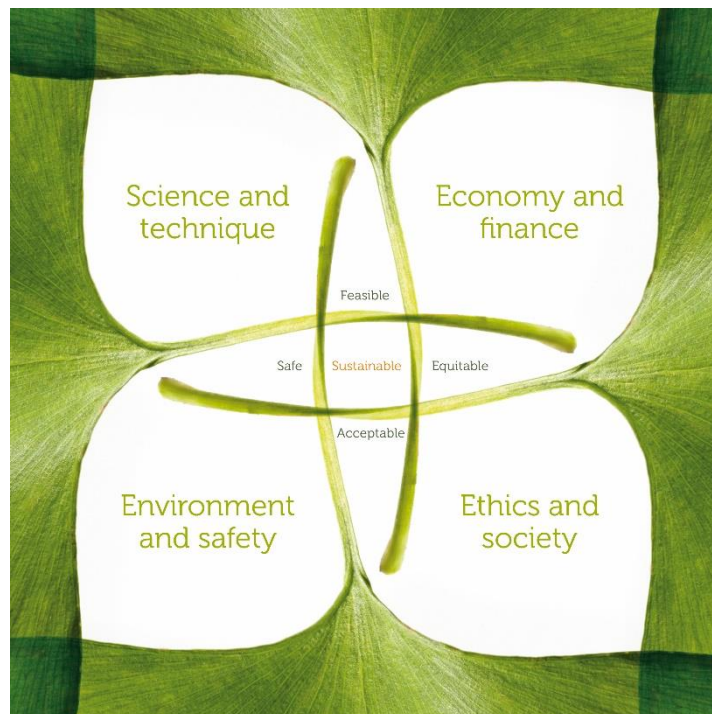


Figure 1 - Durable solutions of ONDRAF/NIRAS [4]

Consequently ONDRAF/NIRAS makes sure that the environment and the society are protected at short and long term against the harmful effects that come along with nuclear and non-nuclear activities [1].

Along with the general management of radioactive waste and enriched fissile materials, ONDRAF/NIRAS also conducts specific tasks with regard to the recognition of nuclear installations. Dismantling and decommissioning of installations, research and development, management of nuclear passive and information to the public are also responsibilities of ONDRAF/NIRAS [2].

Within the global system of radioactive waste management, 4 categories can be distinguished: [3]

- Upward management involves those activities that serve as a preparation for the realisation of the routine management activities. Because it prepares the further steps of the management system, the upward management is of great significance. This management takes place at two different levels: at the customer's level and at ONDRAF/NIRAS's level [4];
- The routine management of radioactive wastes contains the following aspects: acceptance process (based on acceptance criteria), transportation, processing/conditioning and temporary storage. The processing and conditioning of radioactive waste is carried out at Belgoprocess [5]. Belgoprocess (Dessel) is a subsidiary company of ONDRAF/NIRAS and is responsible for the technical operations necessary for the processing and temporary storage of radioactive waste [6], [7];
- The long term management consists in the development of durable solutions for the long term management of radioactive waste. An important property of a durable solution at long term is that the following generations are not excessively charged with problems concerning the management of radioactive waste [8].

Beside the management of radioactive waste on the Belgian territory, ONDRAF/NIRAS is also entrusted with the management of excessive fissile materials and the management of nuclear passives. In addition, one of ONDRAF's legal assignments is to carry out the decommissioning program and the decommissioning operations of the contaminated facilities belonging to radioactive waste producers in case of failure.

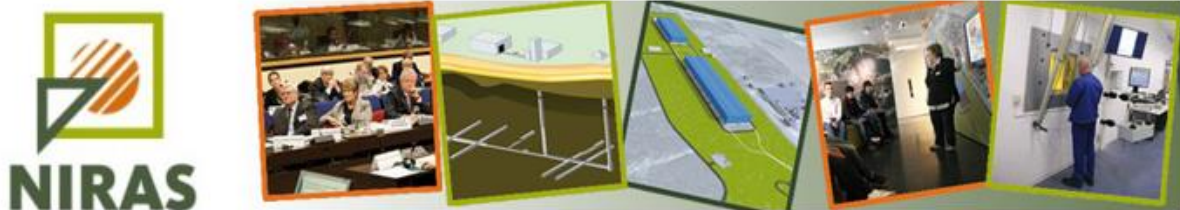


Figure 2 – ONDRAF/NIRAS [19]

3 Cyclotrons

A cyclotron is an accelerator in which a particle is accelerated over a circular trajectory. Each orbit, the particle receives a small voltage increment. Consequently, each particle has to travel many orbits to reach its final and desired energy. The energy is of the order of MeV. The acceleration of the charged particles is done by 2 hollow electrodes. These electrodes are called the “dees” of the cyclotron because of their shape and are connected to a radio frequency power source that gives an alternating voltage. The ion source is located in the centre of the gap, between the two electrodes. That source provides the charged particles of interest to be accelerated. The particle does not feel an accelerating voltage or electric field when it is in one of the hollow D-shaped electrodes. But when it is in the gap between the two “dees”, the particle is subjected to the electric field and feels a small accelerating voltage. Due to the acceleration, the particle has a bigger energy and describes an orbit with a larger radius. When the orbit of the particle has the largest (or desired) radius possible, the particle has reached its maximum velocity and is ready to be extracted from the accelerator. The path of the charged particles is affected by a dipole magnet. This magnet is located under and above the “dees” and provides a centripetal force that curves the trajectory of the particles into a circular orbit [9], [10]. Figure 3 below provides a schematic view of the principle of a cyclotron. It shows in the middle the electrodes or “dees” in which the particles orbit. At the top and bottom, the dipole magnets maintain the circular trajectory of the particles.

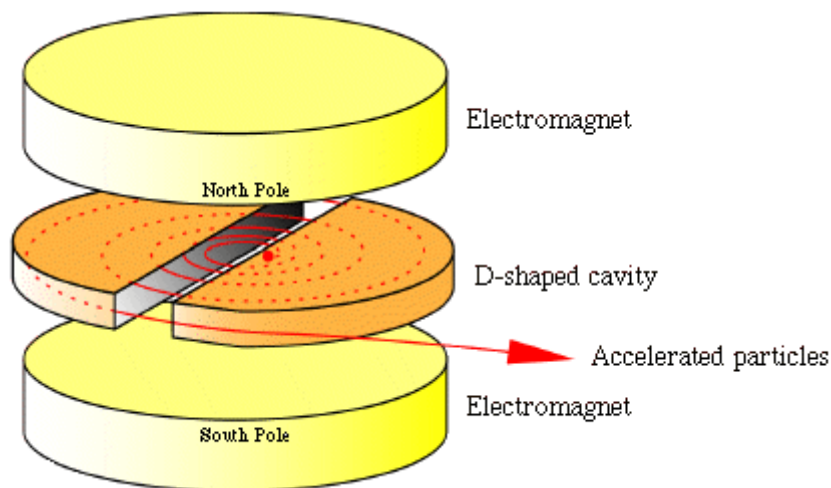


Figure 3 - Schematic principle of a cyclotron. [10]

An important characteristic of the cyclotron is that it's necessary to synchronize the passage of the particle in the gap with the frequency of the alternating voltage in order to accelerate the particle. So it is important that the time it takes for the particle to complete a semi-orbit, remains constant during its acceleration process. This means that the time it takes to complete a semi-orbit is independent of the radius of the orbit. When a particle has a small energy and thus a small velocity it describes a circular path with a small radius, but when the particle describes a larger radius, it has a larger energy and also a larger velocity. The increase in speed compensates the increment in distance that the particle has to cover, so that the time to travel the semi-orbit remains the same when the particle has a smaller orbit to travel. When the half period of the AC voltage, also called the cyclotron frequency, is precisely the same as the semi-orbit time of the particle, they are in synchronization. Thus the particle shows acceleration each time it passes the gap between the “dees” [9].

Another important feature of the cyclotron is the extraction of the particles from the accelerator when they reach the desired energy. This extraction can happen with two different methods. The first is used when the cyclotron accelerates positively charged particles. In this case the charged particles are extracted from the machine using an electric field that deflects the particles from their orbit. The component in the cyclotron that is responsible for this kind of extraction is the deflector. In Figure 4 on the right, a schematic is shown of the extraction of positively charged particles with a deflector [11].

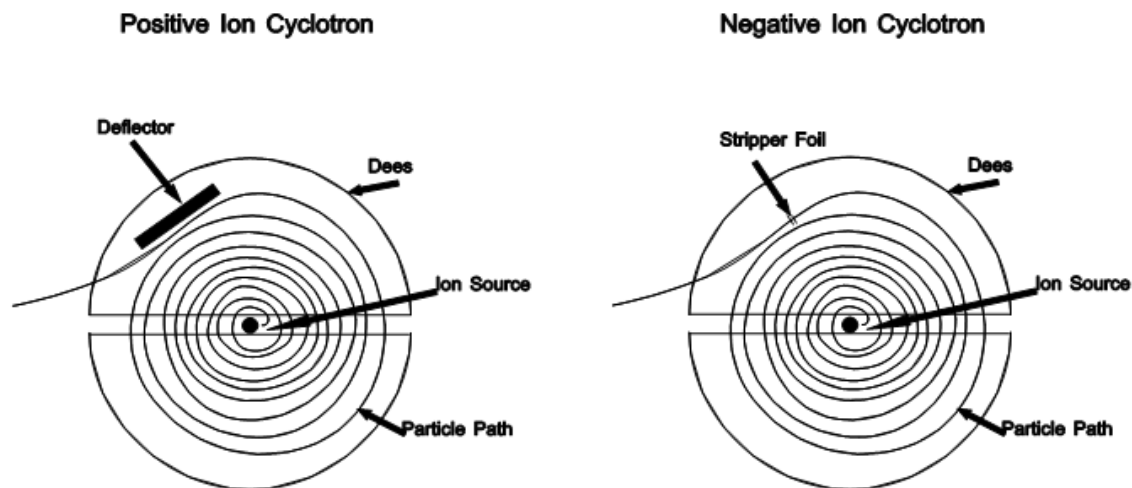


Figure 4 - Extraction of positively and negatively charged particles [11]

When negative ions are accelerated in the cyclotron, a second method is used to extract the charged particles from the machine. This method implies that the negative charged accelerated particles pass through an electron stripper, usually a carbon foil, in which the electrons are taken away from the particles ($H^- \rightarrow H^+$). Then the magnetic field bends them out of the cyclotron. This method is shown in Figure 4 on the left [11]. A great advantage of the electron stripper method is that there are far less interactions between the charged particles and the cyclotron components. This means that there is less activation of the cyclotron with an electron stripper than with a deflector. The disadvantages of using an electron stripper is that the stripper must be replaced regularly and the requirements for the vacuum are also higher than with a deflector [11].

When a cyclotron accelerates positively charged particles and consequently uses a deflector to extract the beam, only one beam exit is possible. To make sure that several targets in different irradiation rooms can be bombarded with the accelerated beam, a switching magnet is used to redirect the beam. This process is not needed when negatively charged particles are accelerated, because multiple beam exits (and multiple electron strippers) are possible with this method.

Cyclotrons are usually characterized by the maximum energy that the charged particles can reach and the beam current that can be obtained. The energy of the particles is usually expressed in MeV and since the beam is in principle a current of charged particles, the beam current is expressed in mA. Depending on the maximum energy of the beam, following categories of cyclotrons are distinguished: [9]

- Low-energy cyclotrons: 10-100 MeV,
- Medium-energy cyclotrons: 100-1000 MeV,
- High-energy cyclotrons: > 1000 MeV.

Since their invention in 1929 by Ernest Lawrence [9], cyclotrons are used on a worldwide scale for a range of applications. These machines are capable of accelerating many sorts of charged particles of a chosen energy to bombard a target for the production of radionuclides. Next to the production of radionuclides, cyclotrons are currently used to perform experiments to get insight in (nuclear) physics and for material science activities [12].

In 2006 the IAEA (International Atomic Energy Agency) published that there were about 350 cyclotrons operated around the world. The largest number of cyclotrons can be found in the United States of America, Japan and Germany [12]. Figure 5 below shows the number of existing cyclotrons collected from an IAEA survey in 2006, categorized by their energy. Because this study is focused on a cyclotron on the Belgian territory, it is useful to know that there are in Belgium approximately 7 cyclotrons (2015) still in operation and someday they also have to be decommissioned and dismantled [12].

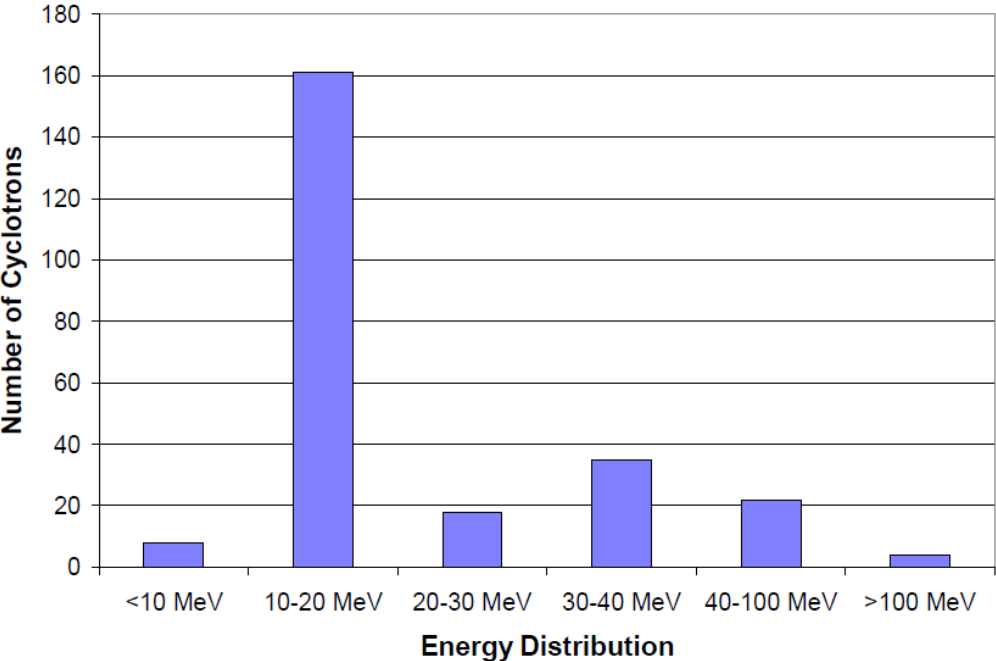


Figure 5 - Number of existing cyclotrons categorized by their energy; reported from an IAEA survey of 2006 [12]

4 Dismantling of a nuclear facility

With the construction and operation of a nuclear facility such as a cyclotron comes the inevitable fact that one day the facility must be decommissioned and dismantled. This means that the nuclear facility is to be removed from the list of registered facilities through several technical and administrative actions. Such actions usually start right after when the facility is definitively taken out of commission [13].

Most of the existing dismantling information and decommissioning techniques are related to nuclear power plants. Although some differences exist, the techniques can also apply for the decommissioning of other nuclear facilities such as accelerators. There are 3 possible strategies to dismantle a nuclear facility: (courtesy of SCK•CEN [14])

- the entombment,
- the storage under surveillance,
- the immediate dismantling.

The first strategy, entombment, places the nuclear facility in a state that it becomes its own final disposal system. Thus, the majority of the radioactive waste remains on-site. Usually the wastes are collected in a particular area of the facility to reduce the total area of radioactive waste. To ensure that the radioactive materials are safely stored for a long term, the facility is put in a permanent enclosure such as a concrete sarcophagus. When applying such a strategy, it is important to make sure that radionuclides with very long half-lives, which normally require a geological repository, are properly removed before the entombment of the facility. Nevertheless, the general parts of nuclear facilities were constructed for operation and not to serve as their own final disposal system. Consequently, the licensing procedure of such a strategy is very complicated. Besides the difficulties for the current generation as a result of entombing, the next generations still hold responsibility for the future evolution of the facility. Finally, this method brings along a lot of financial uncertainties for the current, but also the next generations [14], [15].

The second strategy is to put the nuclear facility into a temporary state of storage with proper surveillance. This strategy needs a procedure that removes all of the radioactive substances that are potentially mobile. After this procedure, the facility is enclosed for several decades to let the most important radionuclides like ^{60}Co , ^{152}Eu , etc. decay. Once those radionuclides are decayed, the dismantling of the facility can begin. Because of the natural decay, the radiation hazard will be reduced for the workers and once activated materials could apply for melting or even unconditional release. It is believed that during the waiting period of several decades, there will be a substantial progress in techniques and knowledge that will improve the dismantling of the facility. Nevertheless, the waiting period could pose a potential risk of losing the (nuclear) knowledge of the facility. Similar to the entombment strategy, storage under surveillance brings along a lot of financial uncertainties for the current, but also the next generations [14], [15].

The third and last strategy is called the immediate dismantling. Like the name suggests, right after the decommissioning of the facility, the dismantling begins without waiting for a certain period of time. This includes that the nuclear and operating knowledge of the staff is still present, as well as the financial funds. But most of all, the responsibility of the dismantling and management of the waste is not passed on the next generations. This fits in the overall slogan of “We clean up what we have built” [14], [15].

5 Cyclotron at Fleurus

5.1 General information

In May 2012, the company Best Medical Belgium S.A. was declared bankrupt. On October 8th, 2012, ONDRAF/NIRAS received from the FANC the authorization for cleaning the facilities and preparing its dismantling.

The facility contains two cyclotrons that were used for the production of radionuclides used in medical diagnosis and therapy. The first cyclotron was built by CGR-MEV and the other one by IBA. Both cyclotrons are located in building B14. Figure 6 below shows the drawing of building B14 which houses both cyclotrons. Only the cyclotron CGR-MEV will be considered in this thesis.

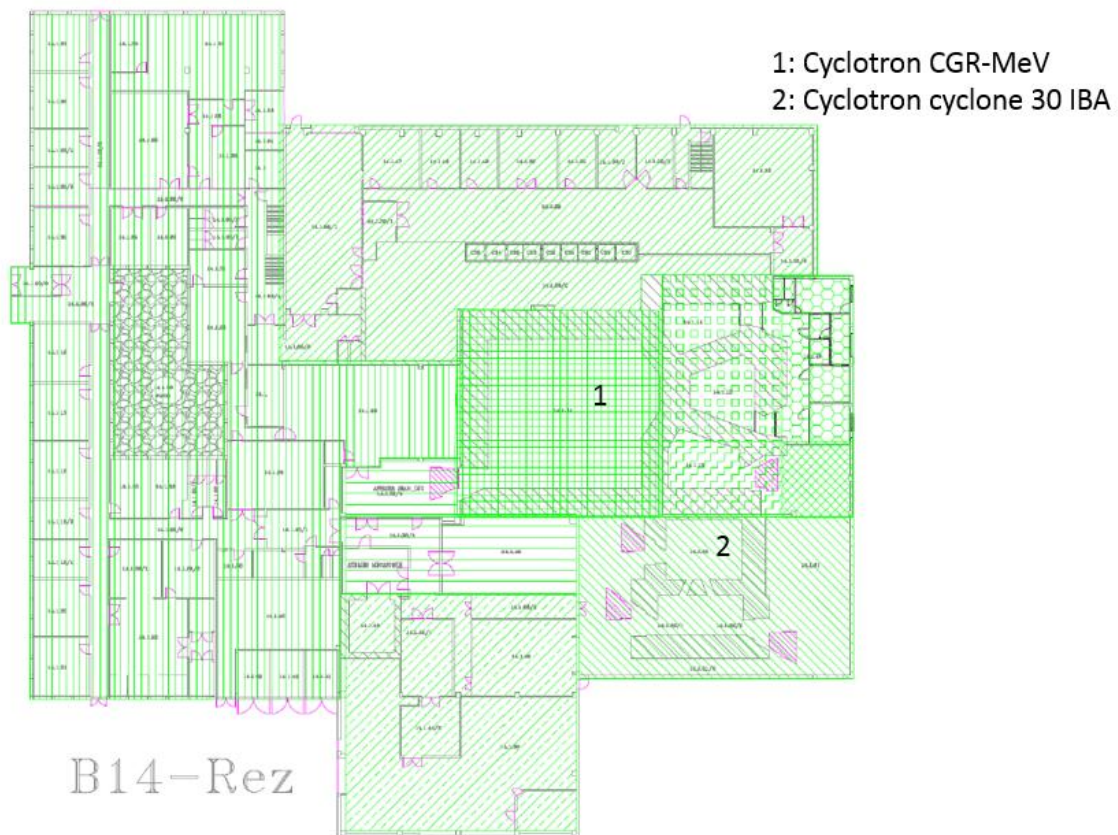


Figure 6 - Drawing of building B14 – Fleurus [16]

The cyclotron 930S CGR-MEV was installed in 1984 and has the following characteristics: [17], [18]

- Isochronous cyclotron;
- Particles to be accelerated: protons, deuterons, tritium and alpha particles;
- Maximum energy: 10-80 MeV for protons;
- Intensity of the extracted beam: 10-20 μA for protons at 65 MeV;
- Intensity of beam at maximum energy for internal target: 100 μA ;
- Total weight: ~250 tons.

An isochronous cyclotron uses mechanically shaped poles for the bending magnets. This to ensure an overall negative magnetic field gradient, which is necessary for vertical focalisation of the beam and to eliminate possible phase shifts between the particle angular frequency and the imposed RF field.

These phase shifts can be due to relativistic effects of the accelerated particles. The negative magnetic field gradient is also obtained by adding concentric circular correction coils [19].

The accelerator CGR-MEV consists out of two major zones, which are also visualized in Figure 7: [16]

- Zone 1: accelerator vault (14m x 14m x 8m) with reinforced concrete walls with thickness varying between 1m and 2.5m;
- Zone 2: three irradiations rooms (6m x 4m x 6m) which contain the external targets. These rooms are also shielded with reinforced concrete walls with a thickness of 1 to 3 m.

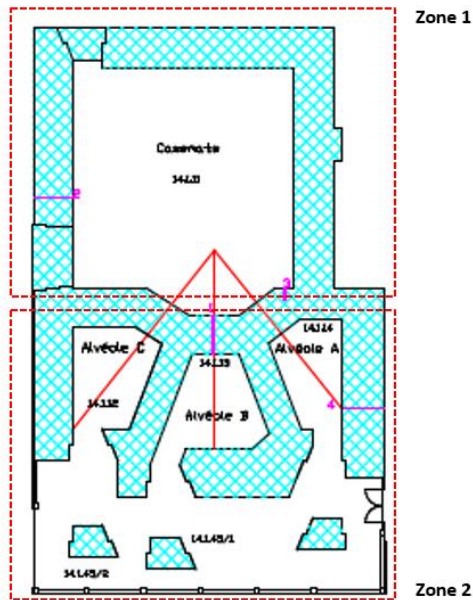


Figure 7 - CGR-MEV cyclotron accelerator vault and irradiations rooms [16]

Figure 8 gives a 3D overview of the CGR-MEV cyclotron:

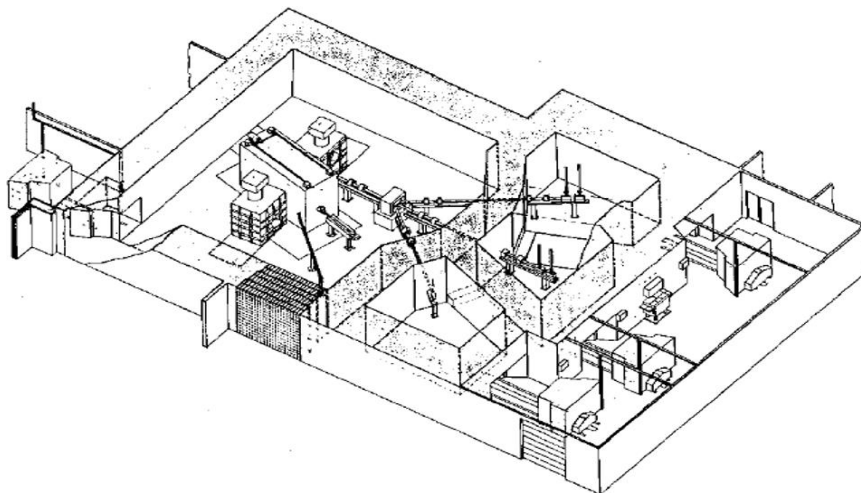
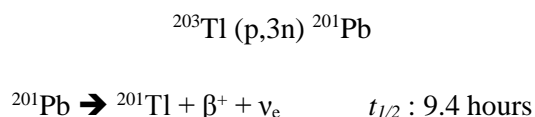


Figure 8 - 3D view of CGR-MEV cyclotron [20]

5.2 Production and operation

Activation of the cyclotron elements and other surrounding materials is a result of the operation of the machine and depends a lot on the type of particles accelerated and their energy. The information given below is useful to well understand the cause of the activation.

The production of radioisotopes, mainly ^{123}I and ^{201}Tl , with the CGR-MEV cyclotron started in 1983. To produce ^{123}I , an external liquid sodium iodide (NaI) target was bombarded with 65 MeV protons to induce a (p,5n) nuclear reaction. This process results in the production of ^{123}Xe , which decays with a half-live of 2.08 hours into ^{123}I . The neutrons that were produced during the reaction activated only the surrounding materials in the irradiation rooms. Of the three irradiation rooms, two were used for this type of production. Room three was only used to perform research and development (R&D) for the production of ^{123}I with 30 MeV protons. R&D was also performed in irradiation room two for approximately 6 irradiations with 55 MeV protons to investigate electrodeposited targets [18]. For the production of ^{201}Tl , an internal rotating target was used in the cyclotron itself. For this purpose, 34 MeV protons were used to induce the following nuclear reaction: [18]



Because the production of ^{201}Tl happened in the accelerator itself, it means that the produced neutrons contributed to the activation of the materials in the accelerator vault. Furthermore, the production resulted in a contamination of the internal parts of the machine.

Because of the very limited information on the runtime of the cyclotron, a detailed overview of the use of the machine is not possible. Instead, Figure 9 gives the use of the accelerator during the period January 1988 – April 1988. It is believed that these 4 months are a good representation of the general use from 1983 until the shut-down in 1993. For the external target, proton energies of 67 MeV were usually reached. For the internal target, the energy was about 30 MeV.

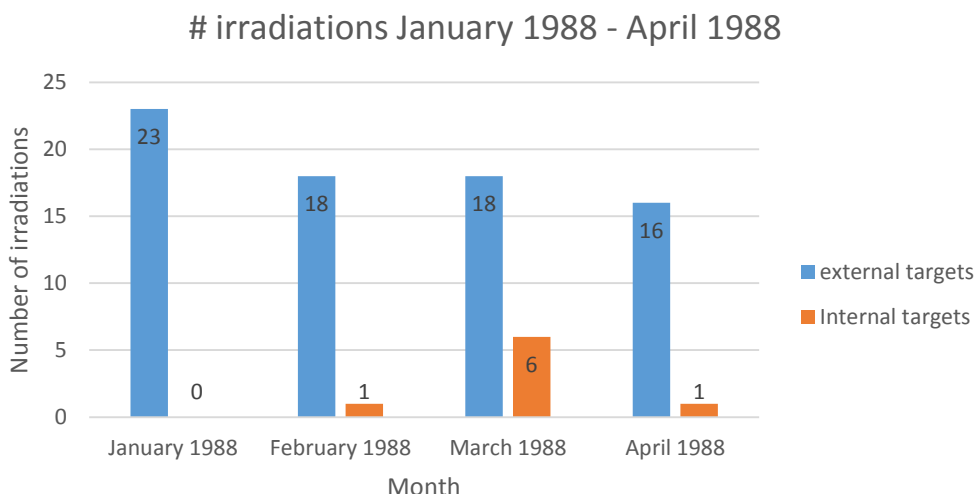


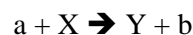
Figure 9 - Number of irradiations January 1988 – April 1988 CGR-MEV [21]

6 Activation

6.1 Basic concept

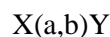
A cyclotron accelerates charged particles to a certain energy. The final goal is to direct these particles to a target in an irradiation room and to produce radionuclides through the process of nuclear reactions. During the acceleration of the particles, there are unwanted but unavoidable collisions between the beam of charged particles and the materials of which the cyclotron consists of. These collisions are the cause of nuclear reactions which results in activation of the materials.

A nuclear reaction is a process in which two or more nuclei collide with each other, resulting in a change of mass, charge or energy state. Due to the interaction a new nuclide can be formed that is different from the initial nuclide [22]. A nuclear reaction is written as follows:



This reaction represents an accelerated particle **a** that is inbound on the target **X**, which is usually stationary. **a** is generally a light particle, **Y** and **b** are the products of the reaction, in which **Y** is usually a heavy product that stays in the target and **b** is a light particle. In many cases the produced nuclide **Y** is radioactive. Because of its radioactivity, **Y** is also called a radionuclide [23]. This process is also called activation of the material **X**. An alternative way to write this nuclear reaction is as follows [24]:

Initial nuclide [incoming particle or photon, outgoing particle(s) or photon(s)] final nuclide



Although formed on an artificial manner, the radionuclide **Y** will decay spontaneously. Like any other radionuclide, **Y** will be characterized by a half-life and a decay mode. This radioactive decay is described by the equation shown below. In which N_0 represents the number of nuclides present at $t=0$. The half-life ($t_{1/2}$) of the nuclide is the time necessary to decay to half of the nuclei originally present. Finally, λ represent the decay constant [25].

$$N(t) = N_0 e^{-\lambda t}$$

6.2 Activation in the cyclotron at Fleurus

6.2.1 Proton induced nuclear reactions

A widely used particle to be accelerated in cyclotrons is the hydrogen ion (H^+). Ionisation of hydrogen gas produces ions and in the case of the Fleurus' CGR cyclotron, these ions (H^+) were accelerated. Furthermore, the acceleration of H^+ particles is the same as accelerating protons.

As mentioned above, the acceleration of positively charged particles is accompanied by the use of a deflector to extract the protons from their circular trajectory. Not all of the accelerated H^+ particles are extracted and transported successfully to the targets in the irradiation rooms. Many high energy protons are "lost" during the acceleration as they interact and collide with the surrounding materials. This causes nuclear reactions and consequently activation of the cyclotron materials.

Not all of the activation in the cyclotron is due to the nuclear reaction with protons. There are two groups of nuclear reactions that play a role in the activation process: proton induced nuclear reactions and neutron induced nuclear reactions.

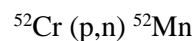
First there are the nuclear reactions in which the accelerated high energy protons interact with the machine's components. The possible proton induced nuclear reactions are: [20]

- (p, α)
- (p,xn) with x the number of neutrons emitted = 1,2,3,...
- (p, γ)
- (p,pn)
- (p,d), but less probable

The activation of the material resulting from the interaction with the protons can be called the direct activation. This category of activation is only applicable on the components that were in direct contact with the protons. Materials that are further away from the beam could not have been activated through a proton induced nuclear reaction because the range of protons in materials is only tens of micrometres and a few centimetres in air. So the activation through proton nuclear reactions is rather limited in comparison with the total activation of the materials present in the cyclotron vault.

The probability of the nuclear reaction (p, α) becomes smaller with increasing atomic number of the target element, because the higher coulomb barrier of heavier nuclei prevents the alpha particle to escape from the nucleus. Nonetheless, the binding energy of the alpha particle becomes smaller with increasing atomic number. These (p, α) reactions are interesting to understand some of the activation processes in the materials (stainless steel and copper) closest to the proton beam [26].

The components of the cyclotron having a direct contact with the proton beam are usually made of stainless steel and copper. A possible nuclear reaction in a stainless steel (which contains > 10.5 % chrome) component subjected to high energy protons is the following:



^{52}Cr is the primary isotope of Cr present in the stainless steel and thus a nuclear reaction with an incident proton is likely to occur. The probability of this reaction – or the cross section – depends on the energy of the incident proton. Figure 10 below shows the cross section of this nuclear reaction in function of the energy of the incident proton.

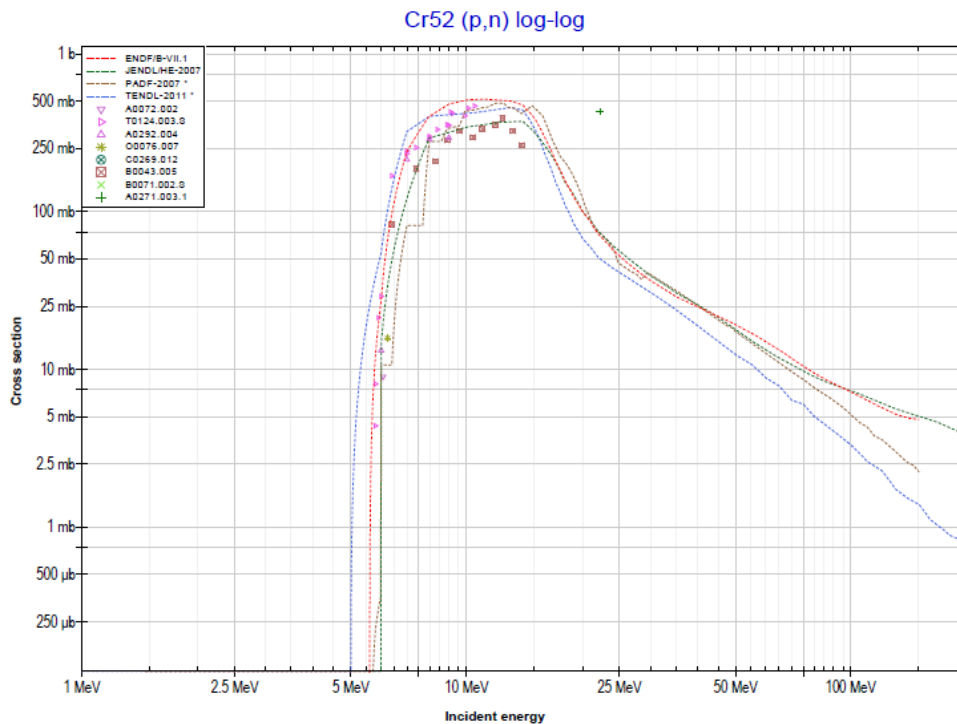


Figure 10 - Cross section of ^{52}Cr (p,n) ^{52}Mn reaction [27]

The different lines in the graph visualize the cross section data from different source installations. The graph shows that a maximum in the reaction's cross section is reached at around 10 MeV. The minimum energy required is about 5 MeV. The product of this reaction is ^{52}Mn with a half-life of 5.6 days. ^{52}Mn is characterized by a β^+ decay and electron capture that can be detected with gamma spectroscopy with a peak at 1434 keV. This radionuclide can be measured in the stainless steel when operating the cyclotron but, due to its short half-life, it will not be measured after a long shut down of the machine. Furthermore, a neutron is produced during the nuclear reaction, which can cause further activation.

The number of neutrons that are emitted during the nuclear reaction depends on the energy of the incident proton. Below 10 MeV the (p,n) reaction is the most relevant. From about 20 MeV the (p,2n) also occurs. In general it can be said that the higher the energy of the incident proton, the higher the probability that more neutrons are emitted during the reaction (p,xn) [20] [27].

The (p,n) nuclear reaction mentioned above is just one of the many reactions that are possible. As the stainless steel components are composed of many different elements, a wide variety of radionuclides is formed as a result of the interactions with the high energy protons. The half-life values of these formed radionuclides varies from several seconds to several years. Two other examples are:

- ^{52}Cr (p,n) ^{54}Mn $t_{1/2}$: 312.2 d
- ^{57}Fe (p,n) ^{57}Co $t_{1/2}$: 271.8 d
- ...

Beside the (p,xn) reactions, the (p, γ) and the (p,pn) reactions are also possible. All of these reactions result in the production of radionuclides in the materials of interest. But, the activation of materials resulting through these reactions is rather limited in comparison with the total activation in the cyclotron facility. Consequently these reactions are less relevant with regard to the dismantling of the facility.

6.2.2 Neutron induced nuclear reactions

An important effect of the (p,xn) reactions is the production of neutrons. Unlike protons, neutrons do not have a charge, they are electrically neutral. As a result, neutrons are not affected by the Coulomb barrier and thus the cross section for reactions at low energies can be much higher than in the case of charged particles. The cross section for neutron absorption usually decreases with increasing energy of the incident neutron: at higher energies, the time of interaction is much shorter and thus the possibility to transfer momentum is smaller [26].

Neutrons have the possibility to travel through many centimetres of material without even interacting with it. These neutrons explain the activation of the materials at distances which could not have been activated through proton nuclear reactions.

Neutron induced nuclear reactions are categorized as follows [26]:

- (n,γ)
- (n,α)
- (n,p)
- (n,2n)
- (n,n'γ)

The energy of the incident neutron defines the type of reaction. Based on the energy of the neutron, following classification can be made:

Table 1 - Classification of neutrons by their energy [28]

Neutron energy	Type
≈ 0.025 eV	Thermal neutrons
~ 1 eV	Epithermal neutrons
~ 1 keV	Slow neutrons
= 100 keV – 10 MeV	Fast neutrons

Neutrons that are in thermal equilibrium with their surroundings are called thermal neutrons. They are characterized by the Maxwellian distribution, which is shown below in Figure 11 (distribution of neutron energy and velocity). The average energy of the neutrons can be calculated with: [20] [29]

$$\langle E \rangle = \frac{3}{2} kT$$

For thermal neutrons:

$$\begin{aligned} \langle E \rangle &= \frac{3}{2} \times 8.1673324 \times 10^{-5} \text{eVK}^{-1} \times 298 \text{ K} \\ \langle E \rangle &= 0.035 \text{ eV} \end{aligned}$$

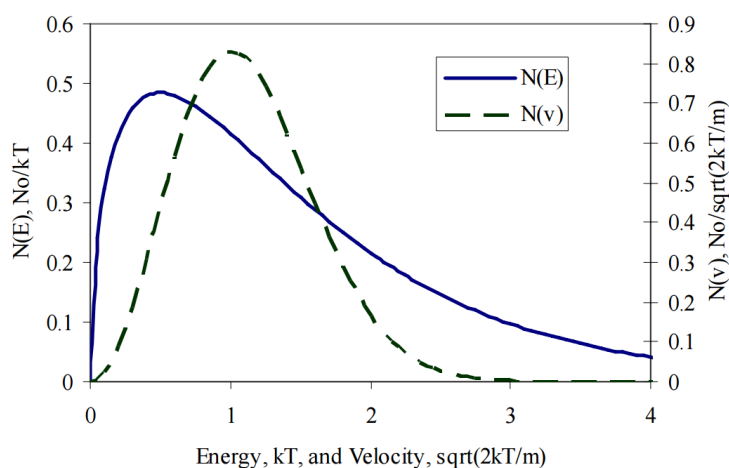


Figure 11 - Maxwell - Boltzmann distribution of thermal neutrons [29]

One of the most important neutron induced nuclear reaction with energies varying between 0 and 500 keV is the (n,γ) reaction, which results in a nucleus with one neutron extra and the emission of gamma radiation. The resulting radionuclide, having a surplus of neutrons, will most probably disintegrate through β^- decay. This type of nuclear reaction is called radiative neutron capture. It is possible that a neutron with an energy of a few keV, can undergo inelastic scattering. In this case the neutrons excite the nucleus. As a result of the excitation, the resulting nucleus stabilizes through the emission of gamma radiation. The emitted neutron is not necessary the same neutron that entered the nucleus. This $(n,n'\gamma)$ reaction requires a minimum neutron energy of 0.1 - 0.5 MeV and depends a lot on the distribution of the excited state levels of the nucleus [26] [30].

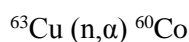
When their energy exceeds 0.5 MeV, neutrons are likely to cause (n,p) and (n,α) reactions. As these nuclear reactions involve the emission of a charged particle, the neutrons must have sufficient energy to ensure that the charged particles can escape from the Coulomb barrier [30].

The $(n,2n)$, $(n,2p)$, $(n,3n)$ reactions become probable with neutron energies higher than 10 MeV. With this energy the incident neutrons have enough kinetic energy to compensate for the binding energy of the extra neutron or proton that is emitted during the reaction [26].

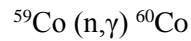
The cyclotron at Fleurus was used to accelerate protons up to 70 MeV, depending on which radionuclide had to be produced. The neutrons produced during the (p,xn) nuclear reactions have a wide range of energies. The neutron induced nuclear reactions discussed above were all relevant during the operation of the machine.

As mentioned earlier, the general activation of the materials present in the cyclotron vault is a result of the neutrons produced during the (p,xn) reactions. The deflector of the cyclotron, where a lot of (p,xn) reactions happened, is a main source of unwanted neutrons. Machine components, located nearby the deflector but not in direct contact with the proton beam, are thus exposed to high energy neutrons. Neutron induced nuclear reactions like (n,α) , (n,p) or $(n,2n)$... that require high energy neutrons of several MeV become relevant.

Copper is a frequently used material in the machine and thus the following reaction is possible:



At different distances from the deflector and after several collisions, the neutrons carry less energy: order of eV to several keV. A possible reaction can be:



Low energy neutrons have a high cross section for this reaction. Consequently, this makes the reaction highly probable in different metallic materials. The variation of the cross section with the energy is shown in Figure 12.

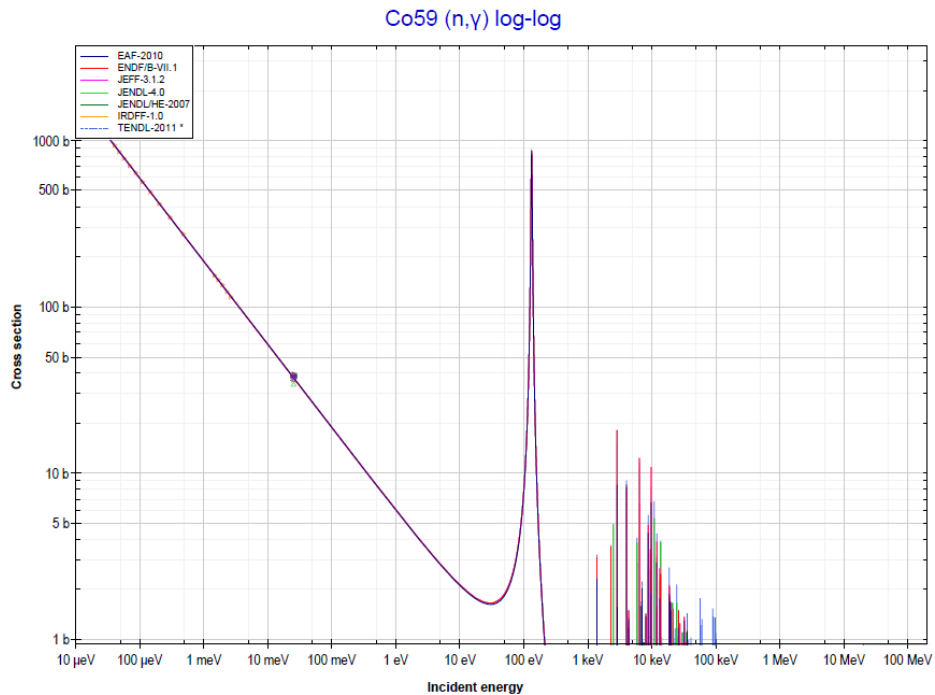


Figure 12 - Cross section for $^{59}\text{Co} (n, \gamma) ^{60}\text{Co}$ reaction [31]

Those two neutron induced nuclear reactions are just a few examples of all the possible reactions, but not all of them are relevant with regard of to the dismantling operation due to their short half-lives.

The resulting radionuclide from those two nuclear reactions is ^{60}Co . It is a β^- emitter with a half-life of 5.3 years. When focussing on dismantling, it is an important radionuclide because of its relatively long half-life. In following section 3.3, a more detailed overview of the radionuclides of interest for the dismantling operation will be discussed.

6.3 Inventory of potentially activated materials

6.3.1 Metallic parts

The materials used for the manufacturing of the cyclotron – and other components present in the cyclotron vault – are primarily: [32] [20]

- Steel + alloys: ± 200 tons
- Aluminium + alloys: ± 25 tons
- Copper + alloys: ± 10 tons

The materials used in the cyclotron vault are not pure. For instance, steel does not only contain iron and carbon, but also many other elements. Because it is a widely used material in the structure of the machine, its activation must be considered. Table 2 gives an overview of the possible chemical composition of steel.

Table 2 - Chemical composition of steel [20] [33]

Iron (Fe)	$\approx 90\%$ [$< 90\%$ (stainless steel)]
Carbon (C)	0.15 – 0.30 %
Manganese (Mn)	0.50 – 1.70 %
Chromium (Cr)	$\approx 8\%$ [$> 10.5\%$ (stainless steel)]
Copper (Cu)	$< 0.20\%$
Molybdenum (Mo)	0.08 – 0.65 %
Nickel (Ni)	0.25 – 1.50 %
Phosphorus (P)	$< 0.04 - 0.05\%$
Sulphur (S)	$< 0.04 - 0.05\%$
Silicon (Si)	$< 0.4\%$
Vanadium (V)	0.02 – 0.15 %
Other: aluminium (Al), niobium (Nb), nitrogen (N), cobalt (Co), selenium (Se), silver (Ag), lead (Pb), tin (Sn), tantalum (Ta)	

The copper and aluminium used in the cyclotron and its surroundings are mainly composed out of the same chemical elements mentioned in Table 2, with copper and aluminium as the dominate elements instead of iron. Titanium (Ti) and magnesium (Mg) can also be found in certain alloys of aluminium [34].

It is not only important to pay attention to the different elements present in steel, copper and aluminium structures, but also to the abundance of the different isotopes naturally present. Furthermore it is also important to take into account the impurities that are present in the metallic structures.

Consequently all of these structures, of which each consists of many elements, isotopes and impurities, can be activated through proton – and/or neutron induced nuclear reactions. Furthermore, it is possible that a nuclear reaction results in the production of a radionuclide and that this newly formed radionuclide is subjected to another nuclear reaction, thus resulting in a new radionuclide. The half-lives of these radionuclides vary from several seconds to several years. It is clear that the possible array of nuclear reactions is extremely wide and too vast to be covered in this study. Therefore, only

those nuclear reactions and radionuclides important in the view of dismantling and decommissioning are considered. This means that radionuclides that were formed during the operation of the cyclotron and have radioisotopes with half-lives of several hours are not relevant in this context.

As it will turn out later in this work, ^{60}Co is one of the most important radionuclides to be considered in the radiological characterization of cyclotron materials and in the dismantling of nuclear installations in general: this particular radionuclide has a half-life of 5.27 years and it is easily produced under neutron activation. This means that even after long period of shut-down, ^{60}Co will be present and must be considered when dismantling the facility.

As mentioned above, ^{60}Co is mostly formed as a result of the following nuclear reactions: [35]

$^{63}\text{Cu} (n,\alpha) ^{60}\text{Co}$	0.037 barn (14 MeV neutrons)
$^{59}\text{Co} (n,\gamma) ^{60}\text{Co}$	37 barn (thermal neutrons)
$^{60}\text{Ni} (n,p) ^{60}\text{Co}$	0.046 barn (14 MeV neutrons)
$^{61}\text{Ni}(n,pn) ^{60}\text{Co}$	0.015 barn (14 MeV neutrons)

^{59}Co is the only stable isotope of cobalt. The (n,γ) nuclear reaction with thermal neutrons has the largest cross section. With higher energy neutrons the cross sections are much smaller. There is also an indirect way to produce ^{60}Co : through the nuclear reaction with ^{58}Fe , which is present in small quantities in steel (abundance of 0.282 %) : [36] [35]

$^{58}\text{Fe} (n,\gamma) ^{59}\text{Fe}$	1.3 barn (thermal neutrons)
--	------------------------------

Two possibilities happen simultaneously:

$^{59}\text{Fe} (p,\gamma) ^{60}\text{Co}$	
$^{59}\text{Fe} \rightarrow ^{59}\text{Co} + \beta^- + \bar{\nu}_e$	$t_{1/2}$: 44.49 days
$^{59}\text{Co} (n,\gamma) ^{60}\text{Co}$	37 barn (thermal neutrons)

The (p,γ) reaction with ^{59}Fe is only possible in those materials that are in direct contact with the proton beam. This reaction does not occur in materials at further distances from the machine.

Next to ^{60}Co , there are also other important radionuclides to consider within the framework of the dismantling operation. Examples are: ^{54}Mn , ^{57}Co , ^{65}Zn , etc. This list is just an indication and will be elaborated in the upcoming chapters.

6.3.2 Non-metallic parts

Non-metallic parts are also present in the cyclotron and were subjected to activation. Among these materials are for example: the rubber insulation of the electric wiring, PVC components, lubricant for moving parts, etc. Out of those non-metallic parts concrete is the most important. It is omnipresent in the cyclotron vault and it is in an considerable extent subjected to neutron activation.

As concrete is used as shielding in the cyclotron vault, it is nowhere subjected to the direct beam of accelerated protons. Consequently, proton induced nuclear reactions and the resulting radionuclides can be ignored. Only neutron induced nuclear reactions must be considered.

Furthermore, the concrete is usually reinforced with steel bars which were also subjected to activation by neutrons and give similar radionuclides as the metallic parts discussed above. Like the different metallic alloys, concrete consists of many chemical elements and impurities that can be activated through neutron induced nuclear reactions. Table 3 below comes from Report EUR 19151: Evaluation of the Radiological and Economic Consequences of Decommissioning Particle Accelerators. It gives an overview of the chemical composition of concrete used in an accelerator at IRMM. It is expected that the concrete in the cyclotron vault at Fleurus has a similar composition.

Table 3 - Constituent elements (ppm) in concrete used in IRMM as measured by SCK•CEN [19]

Constituent element	IRMM concrete
Silicon (Si)	2.4×10^5
Calcium (Ca)	3.7×10^4
Aluminium (Al)	1.8×10^4
Iron (Fe)	1.6×10^4
Potassium (K)	3.8×10^3
Magnesium (Mg)	3.5×10^3
Sodium (Na)	1.3×10^3
Manganese (Mn)	1.1×10^3
Titanium (Ti)	9.5×10^2
Barium (Ba)	2.5×10^2
Nickel (Ni)	3.1×10^1
Cobalt (Co)	6.6
Niobium (Nb)	2.3
Europium (Eu)	1.8
Caesium (Cs)	1.2

It can be learned from the literature that ^{152}Eu is the most dominant and expected radionuclide in the activated concrete shielding. ^{151}Eu , which is a trace element in the composition of concrete (Table 3) has a high cross section (9176 barn) for thermal neutrons and a relatively long half-life of 13.33 years. As with the metallic parts, the diversity of nuclides present in the concrete gives other radionuclides in smaller quantities as a result of activation, for example: ^{54}Mn , ^{154}Eu , etc. A more detailed qualitative report on the radionuclides will follow from the measurements [19].

7 Final disposal scenarios of the activated metals

7.1 Introduction

The activation of the different materials in and around the cyclotron, as mentioned above, results in the production of potential radioactive wastes. In the Belgian royal degree of 30 March 1981 radioactive wastes are defined as:

“Each substance for which no other use is foreseen and which contains radionuclides in a higher concentration in respect with values accepted by the government for substances that may be used without supervision or to be dumped freely. [37]”

It is clear that this definition has two parts: the waste has no other use than to be disposed of and the concentration of radionuclides is higher than standards defined by the Belgian government. This implies that not all of the activated materials in the cyclotron are to be considered as radioactive waste, despite the presence of radionuclides in these materials. In fact there are three possible scenarios to dispose of the activated materials from a nuclear facility:

1. Unconditional release;
2. Melting;
3. Radioactive waste.

7.2 Unconditional release

Unconditional release offers the possibility to recycle the materials or to use them again as raw materials. This means that the materials are no longer considered as radioactive and thus they disappear from the nuclear circuit. In order for that material to be released, some conditions are to be fulfilled. In the ARBIS, the general regulation for the protection of the population, workers and the environment against the harmful effects of ionizing radiation in Belgium, release levels are given for the removal, the recycling and the reuse of solid radioactive wastes originating from nuclear installations class I, II or III. Table 4 below gives an overview of the release levels of several radionuclides that are to be expected with regard to activation of materials in a cyclotron. A more detailed overview of the release levels is given in appendix 1.

Table 4 - Release levels of radionuclides of interest with regard to activation [38]

Nuclide	Release level [kBq/kg]
Mn-52	0.1
Mn-54	0.1
Co-60	0.1
Zn-65	1
Eu-152	0.1
Eu-154	0.1

Two important criteria with regard to those release levels are to be observed [38]:

1. The effective dose per year that can be received by every civilian due to the release or the authorized use of substances coming from a specific activity has to be of the order of 10 μSv or less;
2. The annual collective dose due to the release or the authorized use of substances coming from a specific activity cannot be larger than approximately 1 man Sievert.

Other conditions for the unconditional release of activated materials are: [38]

1. The activity in the material of interest has to be verified with methods that are in accordance with those that are approved by the federal agency for nuclear control (FANC);
2. Only with materials that will be manipulated after release, is it necessary to perform a surface contamination measurement;
3. When the materials contains a mixture of several radionuclides, the following formula must be applied:

$$\sum_j C_j / C_{j,L} \leq 1$$

In which C_j represents the specific activity of the radionuclide j in the mixture and $C_{j,L}$ the release level of radionuclide j .

An exception exists with radionuclides with half-life shorter than 6 months. With these radionuclides it is not sufficient to comply with the specific release levels. To qualify for release it is necessary to store these radionuclides for minimum ten times their half-life until they are fully decayed [38]. Because the half-live of those radionuclides is so short, they are of no significance with regard to the dismantling and decommissioning of the cyclotron facility.

Unconditional release is a very interesting feature with regard to the dismantling operation of a nuclear facility: it is possible to use or recycle the materials in any industry or application. Because the materials qualified for unconditional release are in fact equal to common waste and can be treated through normal waste disposal processes, unconditional release is a financially interesting option to dispose of the wastes of a nuclear facility. Unfortunately it is not always possible to treat all the materials like this and other options are necessary, as described in 7.3 and 7.4.

7.3 Melting

It is also possible that some material are activated to such an extent that it exceeds the release limits. With melting it is possible to process those metals that initially exceed the unconditional release limit. During the melting process there is a repartitioning of the radionuclides across the different end products: melt, slag and dust. This means that it is not only possible to perform a more accurate radiological characterization, but as the repartitioning reduces the activity (= decontamination), it is also possible to reuse and/or recycle materials that were too activated to qualify for that purpose [13], [39]. Table 5 below [13], illustrates the possible redistribution of activity (in %) for some important radionuclides in activated metals. Especially for ^{65}Zn there is large redistribution of the activity in the dust during melting and little activity remains in the melt. For ^{60}Co and ^{54}Mn a large fraction of the

activity remains in the melt. Furthermore, melting is also useful for volume reduction of activated metallic components.

Table 5 - Redistribution of activity (%) of radionuclides over the different melting end products [13]

Nuclide	Melt	Slags	dust
⁶⁰ Co	90	10	< 1
⁵⁴ Mn	95	5	< 1
⁶⁵ Zn	< 1	10	90

Next to unconditional release there is also the possibility for a conditional release of the activated materials. This applies for materials that are still too activated after melting for unconditional release, but provided that the destination is well known, could still be useful for several applications. Conditional release of materials is used especially in the nuclear industry: [39]

- Reuse of metallic components for the production of containers to hold radioactive waste;
- Incorporate metallic components as reinforcement in concrete of radioactive waste repositories or storage buildings;
- Production of reactor vessels out of recycled steel components.

There are two specialized nuclear metal melting facilities that are of interest for this study:

- Studsvik Nuclear AB in Nyköping, Sweden;
- EnergySolutions in Oak Ridge, United States of America.

7.3.1 Studsvik Nuclear AB

The Studsvik melting facility treats low level radioactive contaminated and slightly activated metallic scrap. Before melting the metallic scrap, there are several acceptance criteria that need to be observed: [40]

- The surface dose rate must be ≤ 0.2 mSv/h;
- The dose rate at 1 m must be ≤ 0.1 mSv/h;
- Overall volumetric activity ≤ 100 kBq/kg;
- Hotspots ≤ 0.5 mSv/h are only accepted after permission;
- The dimensions of the metallic scrap must not exceed 0.6 m in diameter/width and 1.2 m in length, otherwise segmentation is needed;
- No free liquids or oils;
- No toxic components;
- No galvanised materials.

Next to those acceptance criteria, there are also several restrictions regarding the contamination of the metallic parts. The contamination is mainly based on ⁶⁰Co as the dominating radionuclide. As guidance for surface contamination Studsvik uses a guiding factor that is defined as follows:

$$\frac{\text{Loose and fixed } \left(\frac{\text{Bq}}{\text{cm}^2}\right)}{\text{Thickness (mm)}} \quad [41]$$

This guiding factor must be smaller than 10 for surfaces without paint and smaller than 15 for surfaces covered with paint for more than 50%. An additional restriction is that the total activity from alpha emitters on the surface cannot exceed 10 Bq/cm². Sometimes the guiding factor is not applicable for certain metallic components. In this case a guide line value for the total specific activity is used in which ⁶⁰Co is usually the most important radionuclide. This total specific activity must not exceed 50 kBq/kg for beta and gamma emitters and a total specific activity of 100 kBq/kg is maintained for alpha emitting radionuclides [41].

Next to the contamination of the metallic scrap, the activation of the metals plays a part in the acceptance criteria for melting. The activation acceptance criteria are mainly concentrated on ⁶⁰Co as the dominating radionuclide. Its specific activity must not exceed 1.2 kBq/kg, otherwise a case-specific acceptance has to be discussed with Studsvik [41]. Figure 13 below gives an overview of the melting process of metallic scrap:

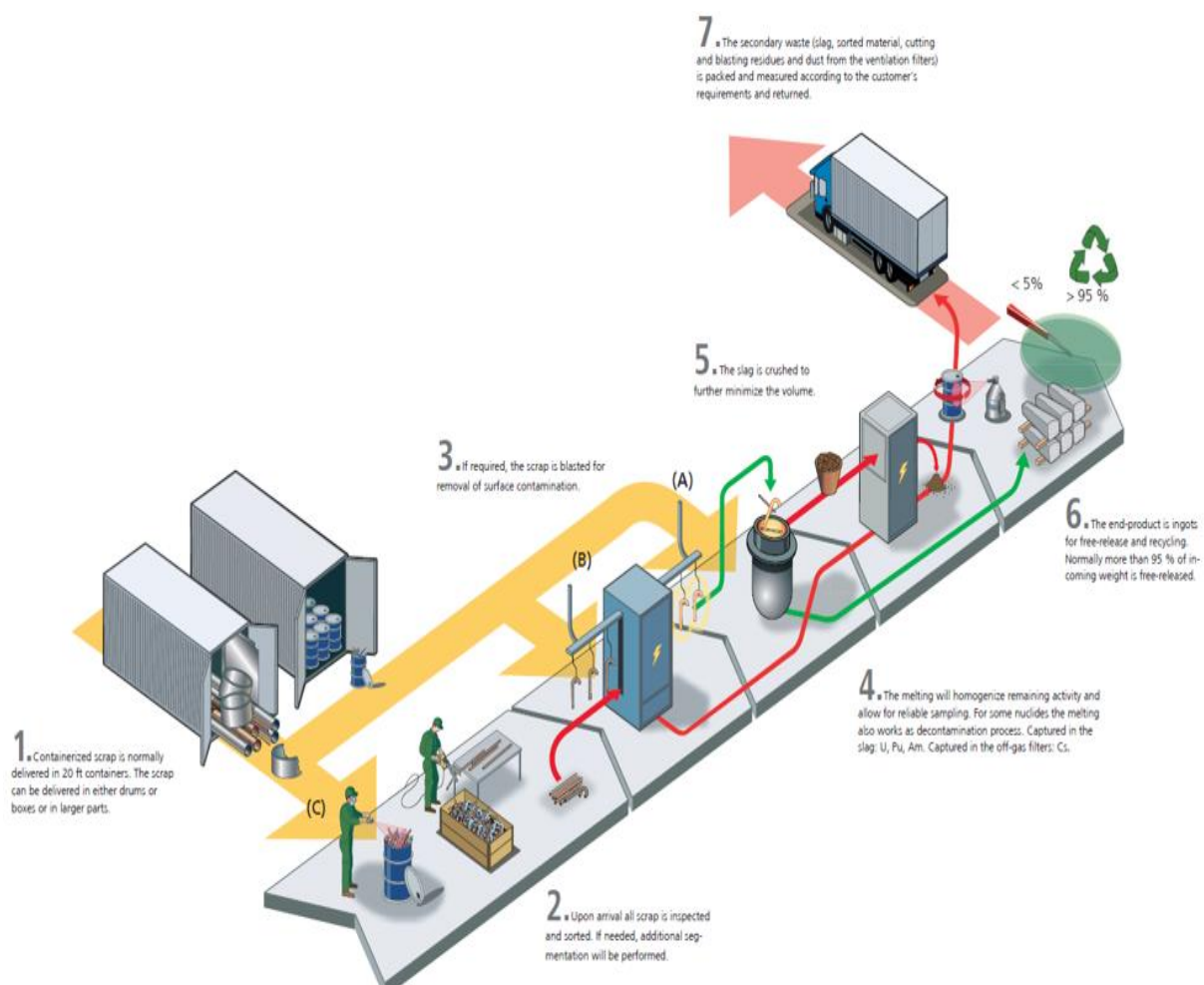


Figure 13 - Melting process of containerized scrap at Studsvik Nuclear AB [40]

The melting process of the metallic scrap results in metal ingots and residual products. These residual products usually consist of slag, dust from the ventilation filters, cutting and blasting residues. Those materials are returned to the original owner of the metallic scrap within 2 years after the melting. It is the responsibility of the owner to properly dispose of those secondary wastes. Metal ingots that have specific activities below the Swedish release level for ⁶⁰Co, which is 1 kBq/kg, are used for free-release and recycling. When a metal ingot is not initially cleared for unconditional release, it is

temporally stored to let them decay until they can be free-released. The maximum time for such storage is 10 years and the annual limit for storing those ingots is 20 tonnes per year. In case that the metal ingots do not qualify for decay storage, they are sent back to the original owner [40], [41].

7.3.2 EnergySolutions

The process of melting the metallic scrap is about the same as in Studsvik, but *EnergySolutions* uses other criteria regarding the acceptance of activated metals. Unlike Studsvik, *EnergySolutions* does not accept non-ferrous metals such as brass, copper, etc. in large quantities. The same applies for: [42]

- Aluminium¹;
- Galvanised metals with zinc weight percentage > 1% of the galvanised metal weight;
- Bulk metals containing > 2% burnable materials by weight;
- Oil or solvent contaminated materials;
- Tungsten;
- Alloys with melting point above 1649 °C;
- Crushed metal items that contain entrained non-metallic materials;
- Zirconium;
- Tin.

With regard to melting, *EnergySolutions* has a limit of 200 µSv/h for the surface dose rate of the metallic waste. With regard to fixed or removable contamination, it must not exceed 8 Bq/cm² for beta and gamma emitters. For alpha emitters a limit of 1 Bq/cm² is applied. In comparison with Studsvik, *EnergySolutions* uses a limit of 11 kBq/cm³ for the total activity density in the metallic waste. This limit holds for all radionuclides with a half-life longer than 5 years, except ³H and ¹⁴C and radionuclides. Furthermore, the specific activity limits for radionuclides in metals are not fixed. They must be derived for each project and are depended upon the radionuclide distributions and final product specifications [42]. Assuming that the 11 kBq/cm³ limit is to be maintained for the radionuclide concentration in metals, specific activity limits are obtained in Table 6 for different metals present in the cyclotron at Fleurus. Although aluminium is excluded from the metals to be melted, *EnergySolutions* declares that special acceptance criteria are always discussable [42].

Table 6 - *EnergySolutions* waste acceptance criteria [42], [43]

Metal	Density (kg/m ³)	Limit (kBq/kg)
Stainless steel	7740	1421.19
Copper	8940	1230.43
Iron	7850	1401.27
Cast iron	7300	1506.85
Aluminium	2712	4056.05

In contrast with Studsvik, *EnergySolutions* does not mention explicitly what they do with the residual products (slag, dust, cuttings, etc.) of the melting process. It might be expected that all of the metallic waste is processed in the USA. No secondary waste resulting from the melting process returns to the original owner. *EnergySolutions* mentions that the metal ingots are used to produce shield blocks for the nuclear industry [44].

¹ *EnergySolutions* is probably going to allow aluminium in the near future.

7.4 Radioactive waste

7.4.1 Category A waste

When the specific activity in the activated materials exceeds both the limits for (un)conditional release and melting, the final option is to treat it as radioactive waste. In general there are three different categories of radioactive waste [45]:

- Category A: short-lived, low-and medium level waste;
- Category B: long-lived, low-and medium level waste;
- Category C: short- or long-lived, high level waste.

With the following distinction between short- and long-lived [45]:

- Short-lived waste: the radionuclides present in the waste have a half-life which is lower than or equal to 30 years;
- Long-lived waste: the radionuclides present in the waste have a half-life which is greater than 30 years.

The activated materials that are not cleared for release or melting are mainly considered as category A radioactive waste. To dispose of this radioactive waste, ONDRAF/NIRAS has started the cAt project in Dessel, Belgium. This project proposes the construction of a long-term surface repository to store exclusively category A radioactive wastes. Figure 14 shows the design of such a repository.



Figure 14 - cAt surface repository [45]

The category A wastes are stored in drums, which in their turn are stored in larger concrete caissons. To immobilize the waste permanently, the caissons are encased with concrete and stored in the repository. To properly store the different types of category A wastes, 3 different caissons were developed. They are shown in Figure 15. The first two caissons are designed to hold respectively standard drums and non-standard drums. The third type is used to store bulk wastes that are especially originating from the dismantling of nuclear facilities [46].



Figure 15 - Three caisson types to store cat. A wastes [47]

7.4.2 Acceptance criteria

In order to properly conduct the management of radioactive waste, ONDRAF/NIRAS created acceptance criteria. These criteria must be respected by the producer of non-conditioned and conditioned radioactive wastes for ONDRAF/NIRAS to accept the wastes for further treatment. The acceptance criteria contain the minimum requirements regarding physical, chemical, biological, thermal, radiological and administrative properties that the waste has to meet [48].

Within the framework of dismantling the cyclotron at Fleurus, the main part of the radioactive wastes will consist out of metallic parts. The following acceptance criteria apply: [49], [50]

- A14: for non-compressible materials;
- A17: for compressible materials.

Although A14 and A17 both apply for metals, some of them are not allowed in one of the acceptance criteria. Table 7 below gives a clearer overview.

Table 7 - Allowed metals for A14 and A17; courtesy of ONDRAF/NIRAS [49], [50]

Description	A14	A17	Description	A14	A17
M0: non-defined metal	X	X	M6: Copper	X	X
M1: lead		X	M7: carbon steel	X	X
M2: aluminium		X	M8: electric cables (with or without insulator)		X
M3: stainless steel	X	X	M9: zinc		X
M4: injection needles		X	MB: beryllium	X	X
M5: cast iron	X	X	MG: galvanised carbon steel	X	X

Both criteria hold the following limits for a drum of 200l radioactive waste: [49], [50]

- Beta/gamma concentration < 40 GBq/m³;
- Maximum surface contamination for beta/gamma emitters < 0.4 Bq/cm²;
- Maximum dose rate at contact < 2 mSv/h.

The fact that A17 applies for materials that are compressible and A14 does not, lies with the different dimensions of metals that are allowed in each category. Table 8 below, courtesy of ONDRAF/NIRAS, gives an overview of those differences.

Table 8 - Difference between A14 and A17 [50]

Physical aspect	Acceptance criterion A17	Acceptance criterion A14
Permitted concentration in one primary package not-conditioned waste of small metallic pieces with a maximal length of 20 cm	≤ 40 m%	≥ 40 m%
Permitted thickness and mass per piece of tubes and solid metals pieces	≤ 20 mm (local maximum of 22 mm) and ≤ 50 kg/piece	> 20 mm and/or > 50 kg/piece
Permitted mass per piece of hollow metal casting	≤ 50 kg/piece	> 50 kg/piece
Permitted quantity, in one primary package of not-conditioned waste, of metals with low redox-potential	≤ 10 kg/primary package not-conditioned waste except separately packed aluminium and zinc	Not permitted
Plumbiferous pieces	To be packed separately	Not permitted

For the above mentioned radioactive wastes, the material will be stored in standard drums. When the cAt-project will be completed, ONDRAF/NIRAS intends to also store the larger pieces of activated materials as bulk in the monoliths (Figure 15). It is expected that by the time the project is finished, an acceptance criterion will be made regarding the acceptance and conditioning of those bulk materials. This will be of particular interest for the dismantling of the cyclotron, because it consists of some large metallic components. Cutting those components to make sure they fit into the standard drums will demand great effort, resources and costs. However, storing them directly as one bigger piece in the monoliths of the repository will both save time and money during the dismantling.

7.5 Overview of the disposal of activated materials

Figure 16 below gives an overview of the possible options, based on the specific activities, for handling the metallic radioactive wastes resulting from the decommissioning and dismantling process of the cyclotron at Fleurus. The limits are based on the specific activity of ^{60}Co as the dominant radionuclide.

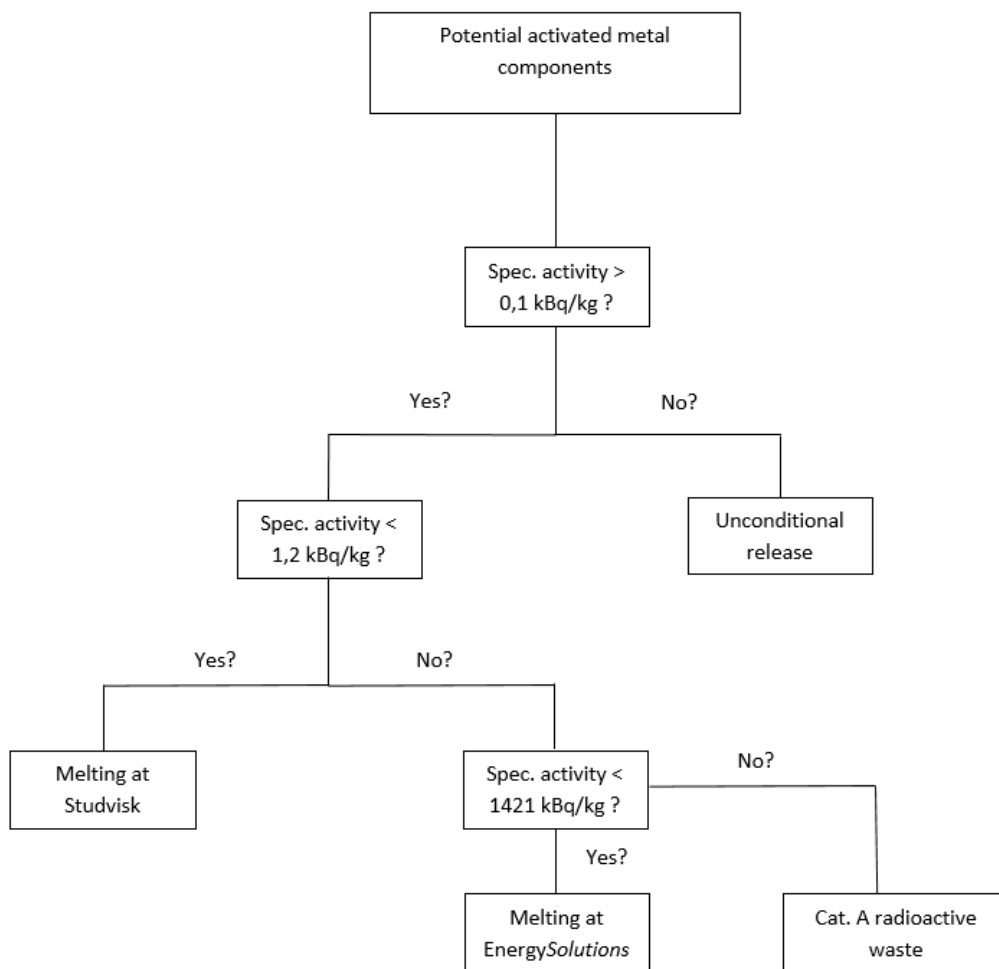


Figure 16 - Disposal options for the potential activated metallic materials

8 Methodology

This chapter elaborates the methods and techniques that were used to identify and quantify the radionuclides that are present in the metallic components of the cyclotron and cyclotron vault. First the process is explained how the sample locations were determined and in which way they were taken from the internal and external metallic components of the accelerator. It contains which factors played a role in the determination of the sample locations and which parts of the cyclotron were most interesting to take samples of.

Secondly, it is explained which techniques were used for the preparation of the samples.

Thirdly, it is explained how gamma spectrometry was used to measure and characterize the samples quantitatively and qualitatively. This includes basic information about the technique of gamma spectrometry and the software program that was used to visualize the spectra and to perform spectrum analysis. Also the detector set-up is discussed. Furthermore, the method for energy calibration and efficiency calibration of the HPGe detector is explained.

Finally, the measuring time of the samples is discussed.

8.1 Drilling campaign

In order to measure the samples correctly and accurately, it is important that the process of collecting them is carefully planned.

The cyclotron is a complex machine with many components. Taking samples of all the different metallic parts of the machine and measuring them is a time-consuming process that falls beyond the scope of this study. The main interests of this project are:

- The hotspots present in the accelerator;
- The quantification and qualification of radionuclides present in each type of metal composing the cyclotron (i.e. copper, aluminium, stainless steel...).

The hotspots were determined with a probe STTC telescopic, energy compensated Geiger-Mueller detector from Canberra that measures the dose rate in sievert per hour (Sv/h). The average measuring time was 60 seconds and the background at the moment of measuring was 1 μ Sv/h. These measurements were then used to map the dose rates in and around the cyclotron. Figure 17 and Figure 18 below show the values measured.

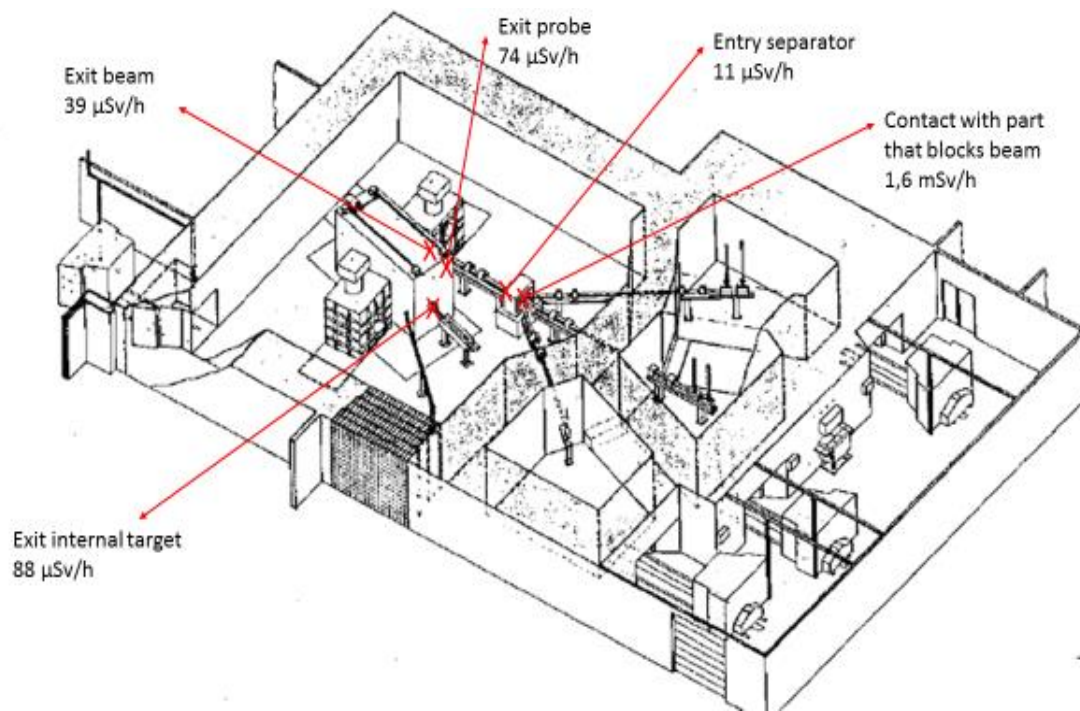


Figure 17 - Dose rates measured around the CGR cyclotron (values are not corrected for background) [20]

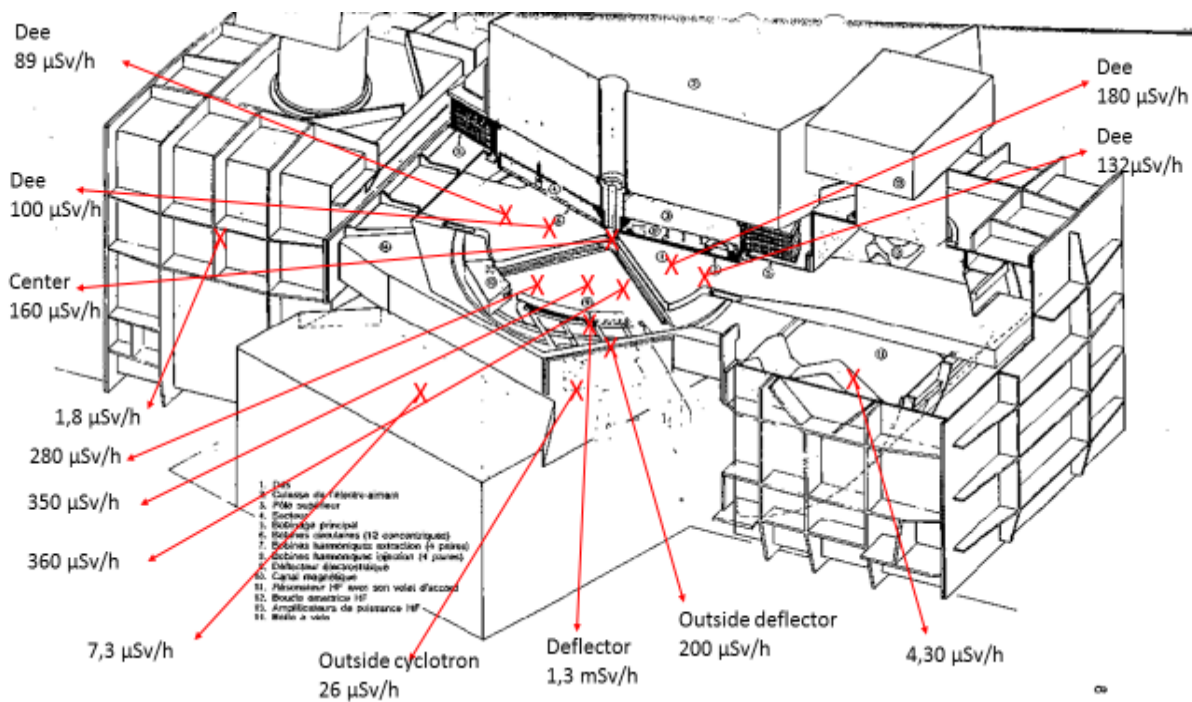


Figure 18 - Dose rates measured in the CGR cyclotron [20]

The highest values were measured at the deflector and the switching magnet with dose rates of respectively 1.3 mSv/h and 1.6 mSv/h. These high dose rates are probably the result of high interaction rates of the beam and secondary neutrons with the components. The remaining values range from background up to 360 μ Sv/h depending on the distance to the centre of the machine and the surrounding components and materials.

Based on these values it was possible to define the hotspots in the machine and thus the most interesting points to take samples of. It must be noted that the samples that were taken for the elaboration of this research study are not sufficient to characterize the entire dismantling project of the cyclotron. To successfully dismantle the facility, all the different metallic and non-metallic parts must be measured to fully characterize them by their chemical, physical and radiological characteristics in order to define the optimal final disposal process of each specific part of the machine.

Based on dose rate values mentioned above, type of metal, nature of the component and several additional factors, the definitive sampling points were determined. Figure 20 to Figure 21 on the next pages show the positions of the sampling points. The majority of samples were planned around the deflector. This component of the machine is one of the most interesting in the view of radiological characterization. As mentioned earlier, the deflector makes sure that the accelerated particles are deviated from their circular trajectory within the cyclotron. This causes some of the accelerated particles to collide with the deflector component and thus activate the material and produce secondary neutrons, which on their turn activate the deflector and other surrounding materials. Therefore, one of the highest activities is expected around the deflector.

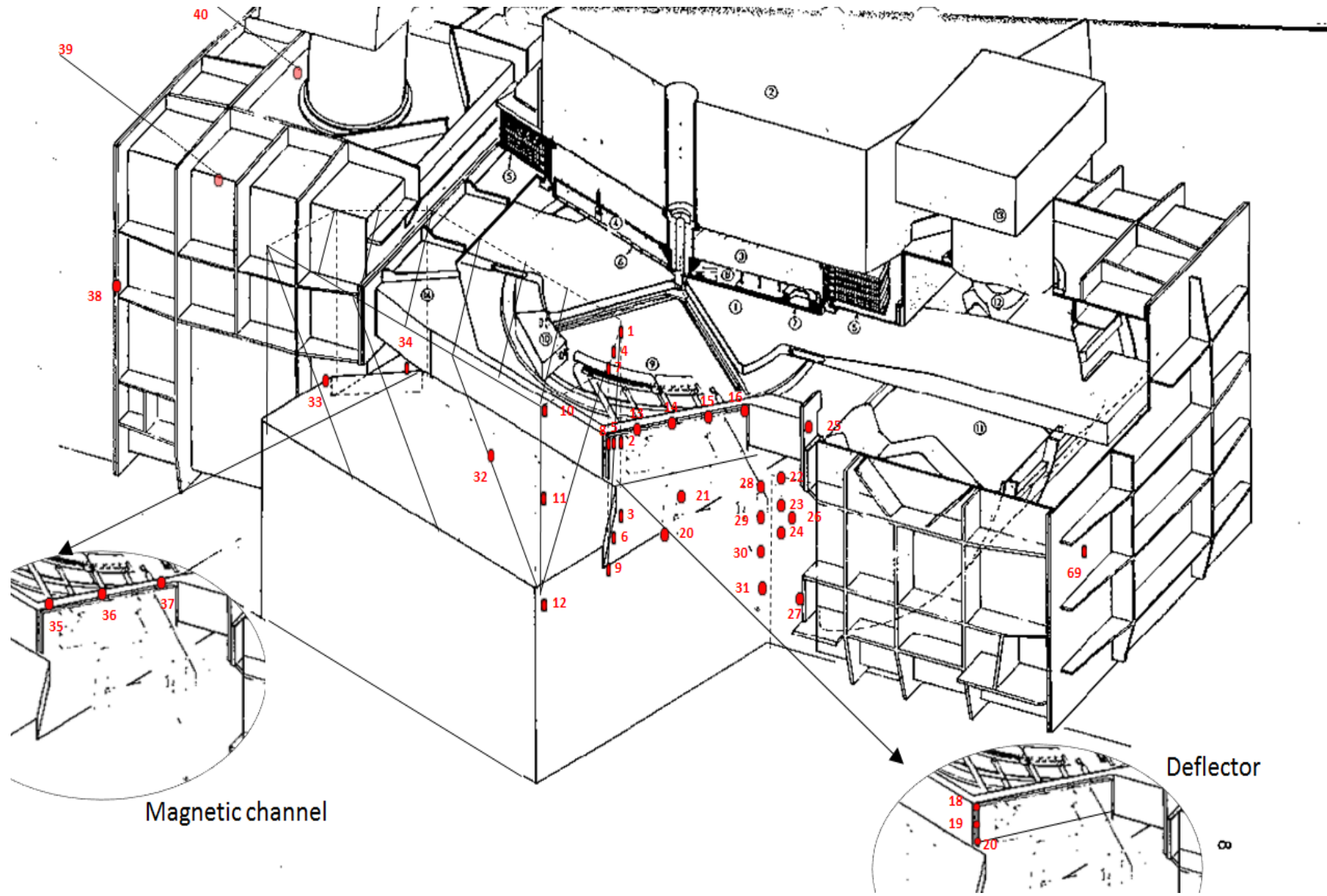


Figure 19 - CGR cyclotron sample positions

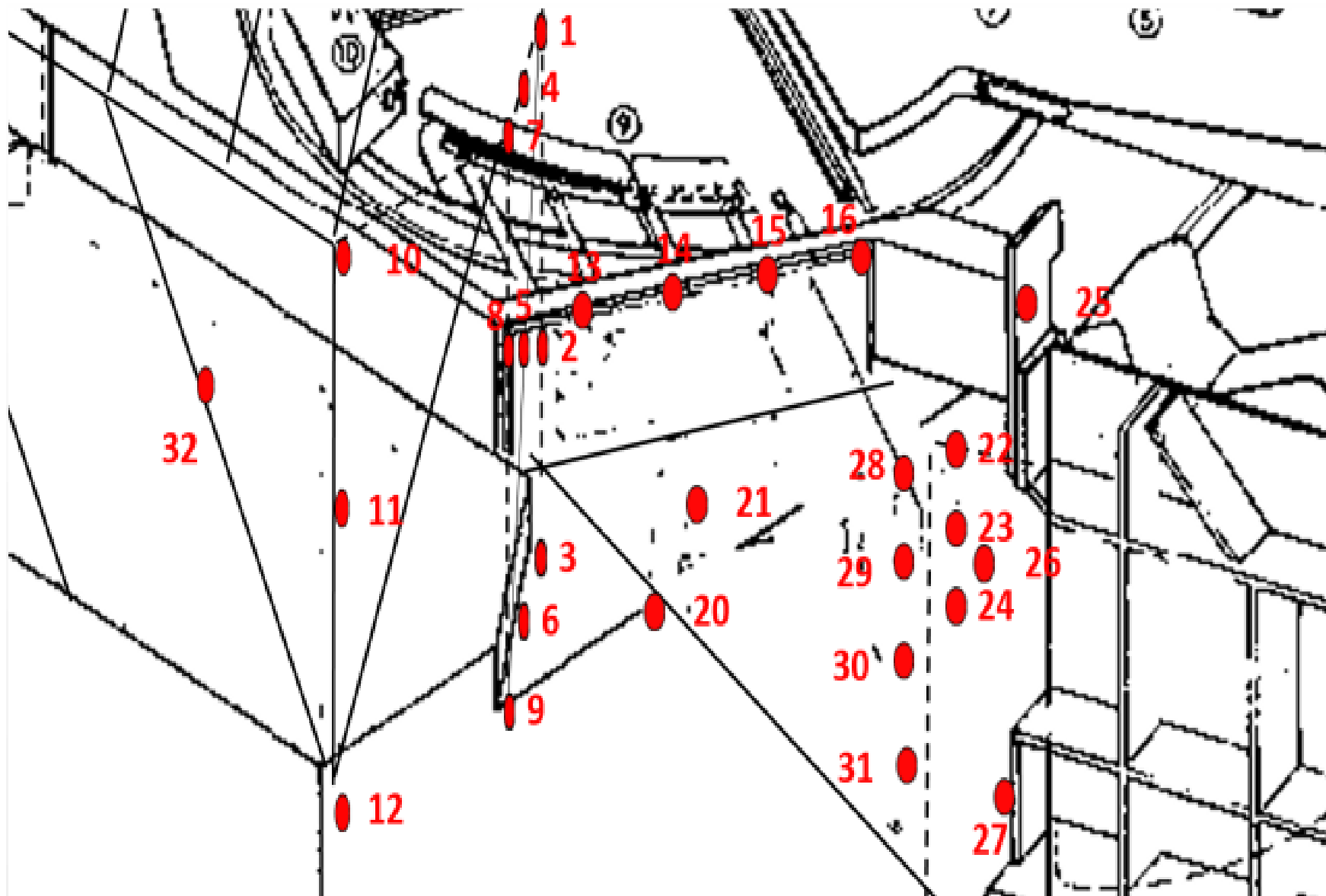


Figure 20 - CGR cyclotron sample positions at deflector

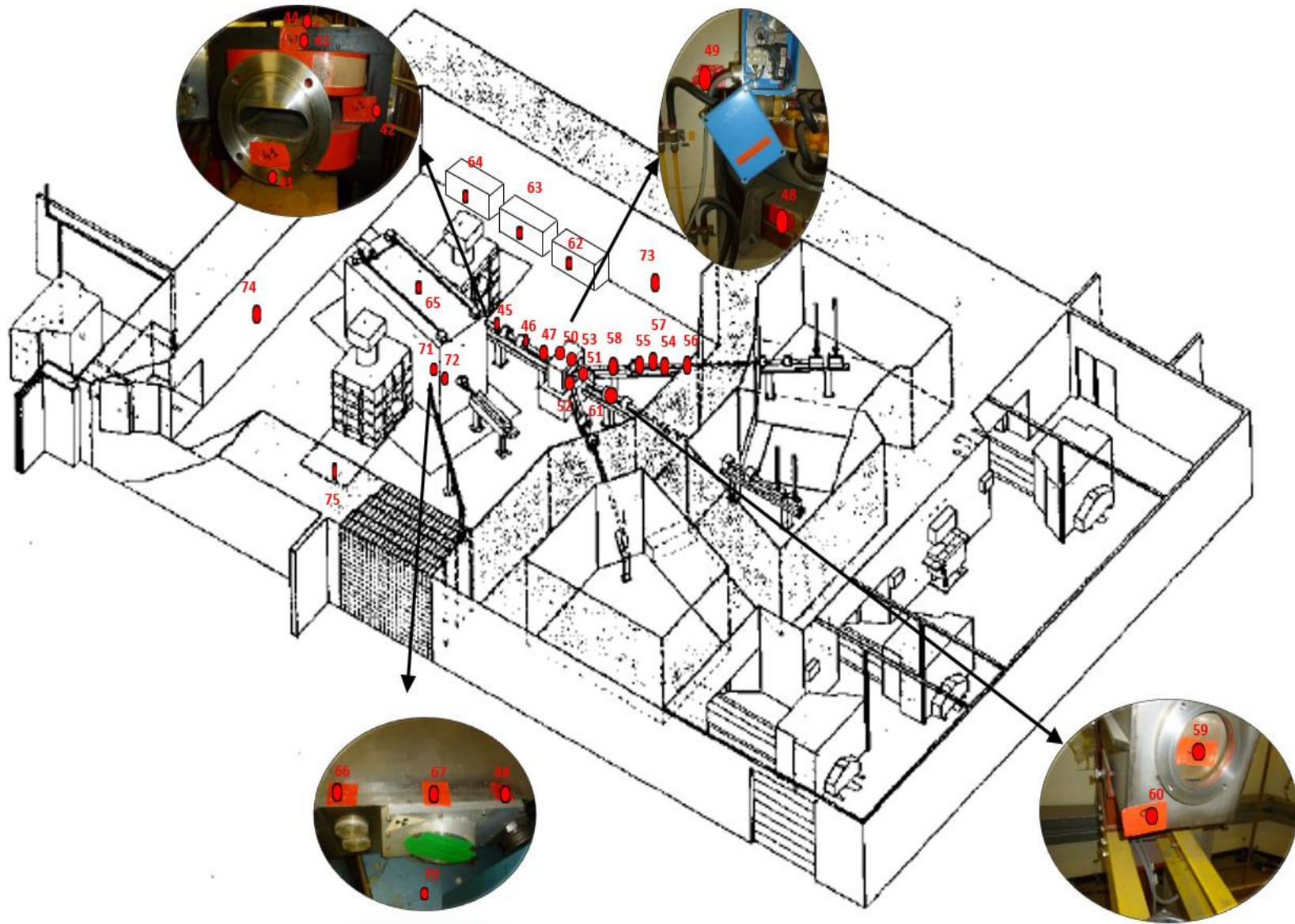


Figure 21 - CGR cyclotron sample positions in accelerator room

As previously mentioned, a number of factors were taken into account for the determination of these sample positions.

Firstly the location of the sample was of great significance with respect to the measured dose rate values. Only places where a lot of collisions were possible between the accelerated particles and the machine materials were selected and this was mainly based on the dose rate.

A second factor that was taken into account was the distance to the component of interest. To see the impact of distance on activation, different sampling points were measured at various distances from the centre of the machine. An excellent example of this factor is shown below in Figure 22. Twelve samples were chosen at increasing distances of the deflector. Each red label in the figures represents a sample location.



Figure 22 - Example of samples at different distances of the component of interest

A third important factor is the accessibility to the component. There are several components within the cyclotron that are interesting to measure, but due to their location and the contamination of these parts it was difficult to include them within the scope of this thesis.

A fourth factor is the type of metal. Different types of metal give different activation products. Therefore it is interesting to take samples of the different metals composing the cyclotron.

A fifth and last factor is the feasibility to take and measure the number of samples. As the period of time for this study was limited, so was the number of samples that could be taken, measured with the HPGe detector and analysed.

An exception was made for 3 sample points at the ventilation unit (samples 062 – 064). Although they are not part of the cyclotron itself, they were selected to measure the radioactivity obtained by activation around the cyclotron because they form a long stretch of metal that is easy to sample. Furthermore, they are located at the largest possible distance from the accelerator. Consequently, these samples are excellent to give an idea of the degree of activation at long distances.

When taking into account those factors, the following site samples were selected:

- Deflector site;
- HF cavity site 1 and 2;
- Exit beam site;
- Beam switching site;
- Box to block beam in case of emergency;
- Beam transport tube;
- Supports of beam tube;
- Magnetic channel site;
- Intern target site;
- Ventilation unit;
- Magnetic lens;
- Top of cyclotron.

The samples were drilled with a common electric drill found in every do-it-yourself shop. For each sampling point a new drill was used in order not to cross contaminate the samples. The drilling into the metallic parts of the cyclotron produced chips that were collected in a plastic cup. The depth of each sample varies between 4 and 8 mm. When the drilling of a specific sample didn't produce enough material for the measurement, a second hole with the same depth was drilled right next to the previous one. Figure 23 below shows the process of taking samples and the plastic bags in which the metal chips were collected. Each plastic sample bag contains the metal chips, the used drill and the little cup that was used to collect the chips. As shown in the figure, each sample has a reference number: 141127 represents the date in the format YYMMDD, 14.1.11 is the location number of the cyclotron vault in building B14 and 010 is the serial number of the sample.



Figure 23 - Drilling campaign

As a result of the methods stated above, 72 samples were taken from the various metallic parts. To see the influence of depth on the activation of a metallic part, 10 additional samples were taken. These were drilled at some earlier defined points:

- 002 : 3x 7.6 mm
- 005 : 3x 8.2 mm
- 011 : 3x 4.0 mm
- 021 : 3x 6.0 mm
- 023 : 3x 4.5 mm

First the exact depth of the first sample was measured and then 2 separate samples with exactly the same depth as the first one were drilled in the same hole. This procedure is illustrated below in Figure 24.

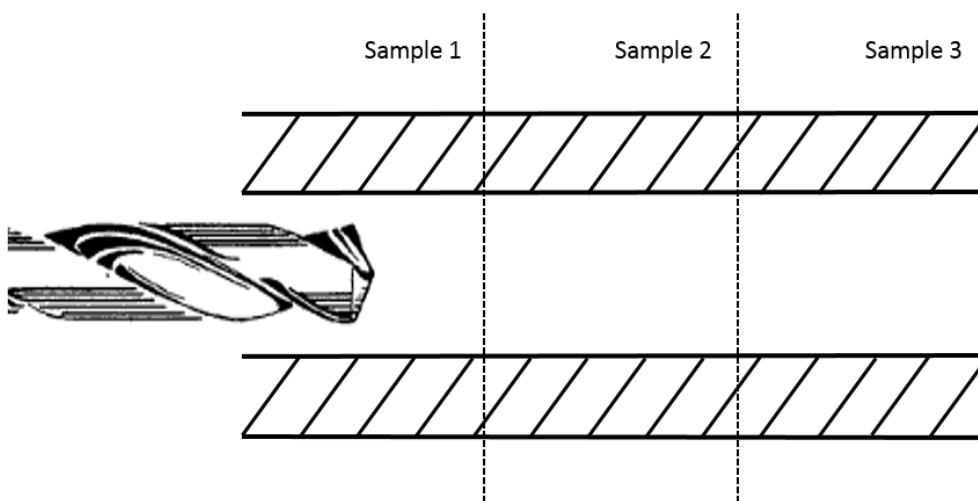


Figure 24 - Procedure for depth drilling

To conclude the drilling campaign, three additional samples were drilled from the concrete shield surrounding the cyclotron. These will only serve as an early indication of the activation in the concrete. These three points were selected at three different locations in the accelerator vault which are shown in Figure 25. The three points were selected in accordance with their position to the deflector and the components that can act as a shield between that point and the deflector.

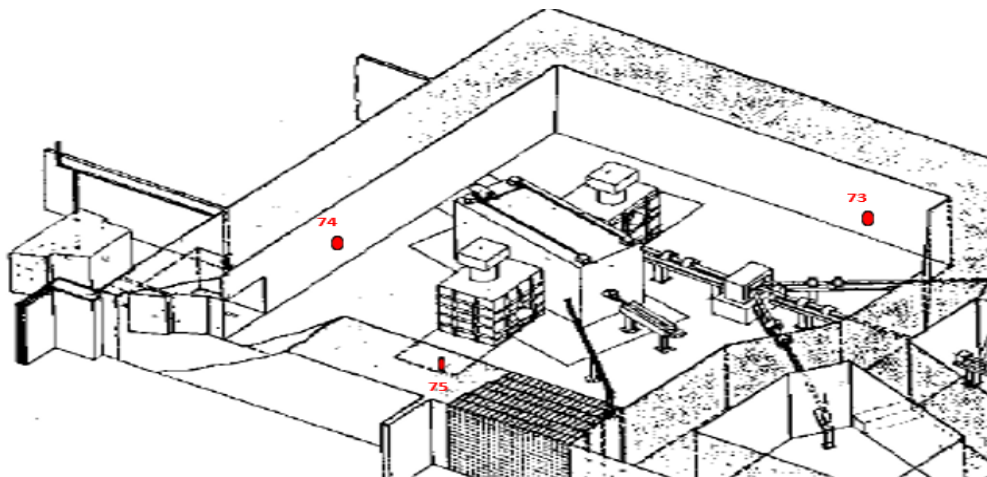


Figure 25 - Samples in concrete (cyclotron vault)

8.2 Sample preparation

In order to measure and compare the 85 samples, they were all prepared with the same methodology. First a unique geometry was defined. A specific box was designed to hold the metallic and concrete samples. There were several requirements that needed to be fulfilled:

- To hold ≈ 1 gram of metallic/concrete sample;
- To fit in the HPGe detector;
- To make sure that the metallic/concrete sample is in a fixed position;
- To be easy to build.

This resulted in a petri dish with a glued cylinder (PVC) in its centre. Figure 26 below shows the developed “petri dish geometry”.

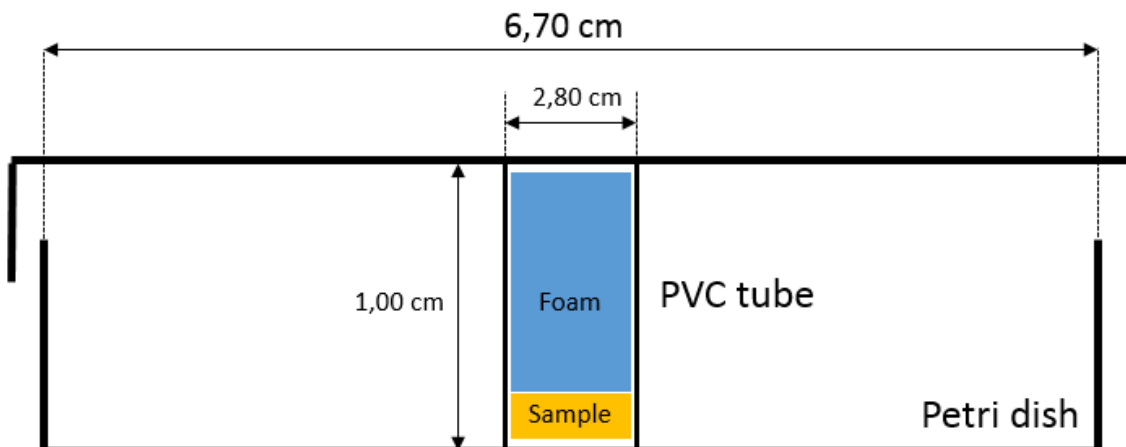


Figure 26 - Petri dish geometry

Secondly, approximately one gram of each sample was exactly weighted and put into the little PVC tube of the petri dish geometry. To permanently fix the position of the sample in the geometry, a little piece of foam was used that fitted into the PVC cylinder. Finally the petri dish was sealed with adhesive tape. An example of a prepared sample is shown below in Figure 27.

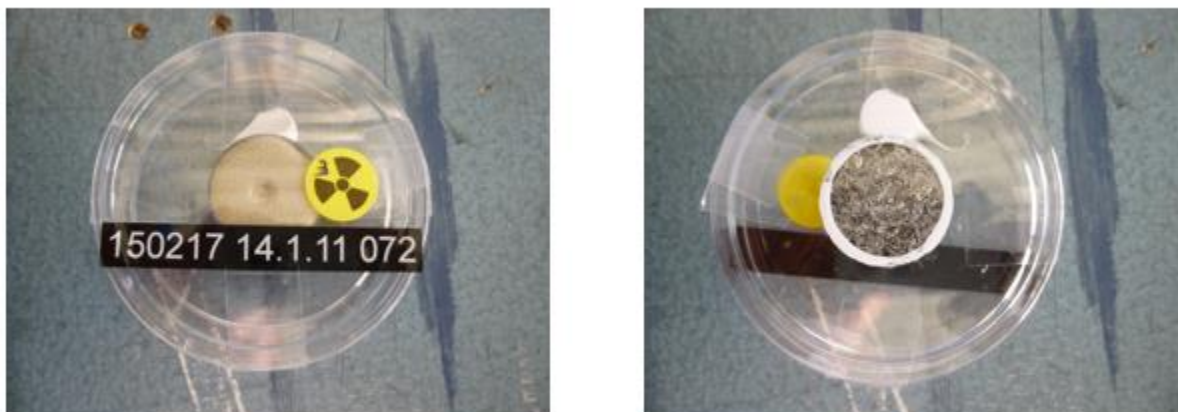


Figure 27 - Example of prepared sample (top and bottom sides)

8.3 Gamma spectrometry

8.3.1 Basic information

The goal of the measurements is to identify the radionuclides present in the metallic and concrete samples as well as their specific activity. This is obtained through gamma spectrometry using an High Purity Germanium (HPGe) detector. Each sample was measured to get a gamma spectrum of the radionuclides present in it. The spectrum consists of a variety of peaks of which the amplitudes give an idea of the activities of the radionuclides. Further, the position against the horizontal axis gives information about the energy of the gamma rays. This information is valuable for the identification and quantification of radionuclides in the concrete and metallic samples.

Gamma rays coming from the sample interact in three different ways with the materials of which the detector is built of: [51]

- Photoelectric absorption;
- Compton scattering;
- Pair production.

The three types of interaction give the gamma spectrum, as illustrated below in Figure 28. When a gamma ray is fully stopped in the medium of the detector, it will result as a full energy peak in the spectrum. In the case of Compton scattering in which the photon is scattered and possibly leaves the medium, a Compton continuum will be seen in the spectrum. Furthermore, when the energy of the gamma rays is higher than twice the rest mass of an electron, a pair of one electron and one positron will be created. This phenomenon is known as pair production. This positron will annihilate rapidly into two photons of 511 keV. When one of those photons leaves the medium, it will appear as a single escape peak in the spectrum. When both of the annihilation photons leave the detector a double escape peak will be visible. When a detector is large enough, it is theoretically possible that all of the photon energy is stopped in the detector. In this case the gamma spectrum will consist of only photo peaks. Unfortunately, building a detector that is large enough to stop even the most energetic gamma rays is not feasible and practical [51]. Thus spectra like the one shown in Figure 28 are the most common.

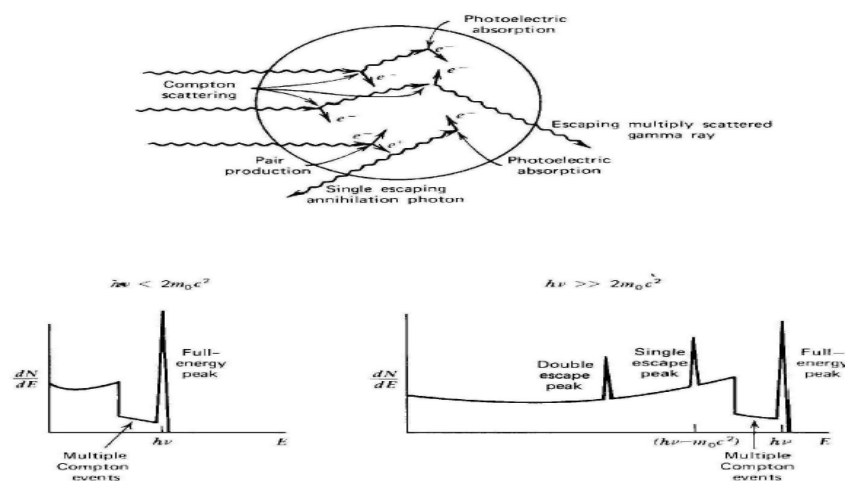


Figure 28 - Structure of a gamma ray spectrum [54]

In addition to the interactions inside of the detector, there are also possible interactions between the gamma rays and the surrounding materials of the detector. These interactions can form secondary particles that can enter into the detector. A schematic of this phenomenon is given below in Figure 29. A common material used to surround the detector is lead. Consequently, characteristic x-ray peaks of lead are frequently seen in gamma spectra.

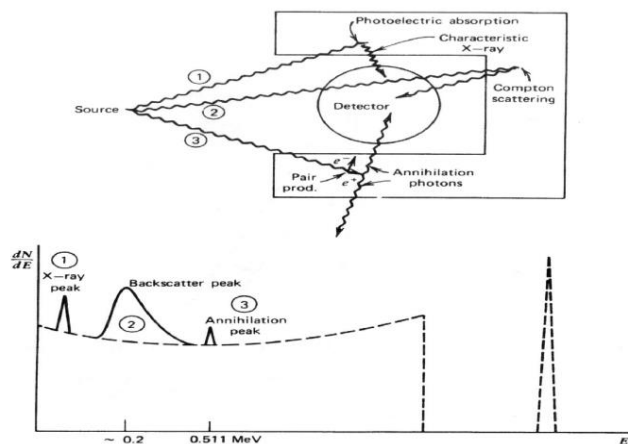


Figure 29 - Influence of the surrounding materials on the gamma spectrum [51]

When two gamma rays arrive simultaneously in the detector, it is possible that the detector sees these two photons as just one. The energy of those two gamma rays is consequently seen as one energy deposition and appears as one peak in the spectrum. However, this peak does not correspond to a characteristic gamma ray from a radionuclide, but is in fact the summation of the energies of the two photons. For this reason such peaks are called sum peaks and they have to be taken into account during gamma spectrometry. [51]

8.3.2 Detector set-up

To measure the gamma spectrum of a sample, a high purity germanium detector model GX 2518 from Canberra Industries Inc. was used. It is an extended range coaxial germanium detector with the following features: (courtesy of Canberra Industries Inc.)

Model Number	Relative Efficiency (%) \geq	Full Width Half Max (FWHM) Resolution (keV)		Peak to Compton Ratio (P/C)	Peak Shape	Endcap diameter mm (in.)
		At 122 keV energy	At 1.3 MeV energy		FWTM/FWHM	
GX2518	25	0.850	1.8	54	1.90	76 (3.0)

Figure 30 - Features of HPGe GX 2518 [52]

To complete the set-up for performing gamma spectrometry some additional components were used:

- High voltage power supply: 3000 V
- Amplifier: position 50
- Multichannel analyzer

To visualize the gamma spectrum and to perform spectra analysis, the software package Apex-Gamma™ from Canberra Industries Inc. was used. After a sample is measured, the program first identifies the peaks found in the spectrum. Based on information available in the library of the software and the specified detection limits, the software compares the peak in the spectrum and identifies the corresponding radionuclides. After the identification of the radionuclides, the software

calculates the specific activity from the photo peak counts based on the peak efficiency and the mass of the sample [53]. Simultaneously, the software produces a spectrum with the labels of the found radionuclides. Next to the spectrum it also produces a report of the measurement that contains all the information concerning the different calibrations and the specified parameters for the measurement. It also contains a complete list of the peaks and the corresponding radionuclides. For each radionuclide, the software indicates which gammas were detected. Furthermore, the program indicates the confidence for a certain radionuclide (see column “taux de confiance” in Figure 32) along with the uncertainty of the specific activity. Figure 31 below shows an example of a measured spectrum (sample 044) with the indication of the radionuclides.

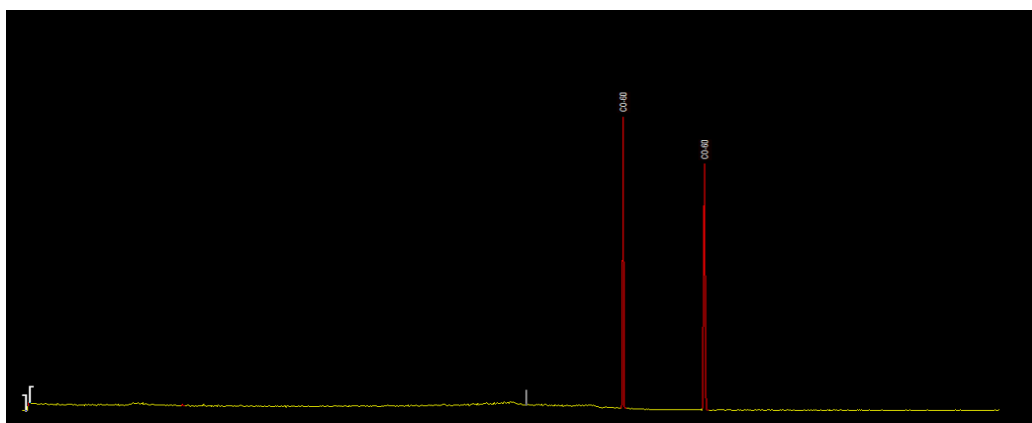


Figure 31 - Example of a measured spectrum with indication of the radionuclides present

The report of the measurement gives more detailed information about the peaks, as illustrated in Figure 32 on the next page. Firstly, information is given about the peaks that were found in the spectrum. For each peak, the beginning and the end of the region of interest (RI) is indicated along with the surface area and the uncertainty for that surface. The full width at half maximum (FWHM) is also given for each peak. Secondly, the peaks that were found in the spectrum are compared with an internal library, which results in a list of identified radionuclides. The little star next to the energy of the peak means that the gamma energy mentioned in the library for that particular radionuclide also appears in the spectrum. The percentage in the fourth column gives the branching ratio of that defined gamma energy. Finally, the bottom of the figure gives a summary of the identified radionuclides along with the average specific activity and the uncertainty, both expressed in Bq/g.

The uncertainty (Bq/g) that is given for the activity of each radionuclide is a value that is calculated with multiple elements: [54]

- uncertainty of the net peak area;
- uncertainty of the activities of the multi gamma calibration source (Table 9);
- uncertainty of the branching ratio;
- uncertainty of the sample quantity;
- uncertainty of the effective efficiency;
- half-life uncertainty;
- user defined random uncertainty.

The total uncertainty of the activity C is calculated as follows:

$$\sigma_{c(\text{tot})} = \sigma_c + \frac{\sigma_{\text{sys}} \times C}{100}$$

Where σ_c is random uncertainty of the activity that takes the uncertainties mentioned above into account and σ_{sys} is the user defined uncertainty (%) [54].

Rapport Recherche des pics

Pic No.	Energie (keV)	Début RI	Fin R.I.	Centroïde Pic	Surface Area	Incertitude Surface	Fond sous le pic	FWHM (keV)
1	75,01	163 -	174	166,28	5,58E+01	9,43	7,86E+01	0,68
2	77,23	163 -	174	171,04	7,30E+01	10,72	8,10E+01	0,69
3	295,28	633 -	642	637,50	8,63E+01	16,84	8,67E+01	1,00
4	352,01	753 -	764	758,86	8,79E+01	16,59	7,41E+01	1,04
5	609,56	1306 -	1314	1309,90	9,75E+01	14,66	5,45E+01	1,40
6	1173,46	2508 -	2525	2516,61	1,32E+03	37,99	3,98E+01	1,65
7	1332,76	2850 -	2866	2857,57	1,07E+03	33,56	1,79E+01	1,86
8	1764,85	3778 -	3786	3782,49	1,88E+01	5,59	5,21E+00	0,70

Nucléides identifiés

Nom Nucléide	Taux de Confiance	Energie (keV)	Embr (%)	Activité (Bq/grammes)	Incertitude Activité
CO-60	0,98	1173,22 *	100,00	1,72E+01	5,94E-01
		1332,49 *	100,00	1,62E+01	6,03E-01
BI-214	0,37	609,31 *	46,30	1,29E+00	1,96E-01
		768,36	5,04		
		806,17	1,23		
		934,06	3,21		
		1120,29	15,10		
		1155,19	1,69		
		1238,11	5,94		
		1280,96	1,47		
		1377,67	4,11		
		1385,31	0,78		
		1401,50	1,39		
		1407,98	2,48		
		1509,19	2,19		
		1661,28	1,15		
1729,60	3,05				
PB-214	0,72	1764,49 *	15,80	2,37E+00	7,09E-01
		1847,44	2,12		
		2118,54	1,21		
		74,81 *	6,33	9,66E-01	1,67E-01
		77,11 *	10,70	7,51E-01	1,13E-01
		87,20	3,70		
		89,80	1,03		
		241,98	7,49		
		295,21 *	19,20	1,35E+00	2,65E-01
		351,92 *	37,20	8,35E-01	1,59E-01
		785,91	1,10		

Nom Nucléide	Nucléide Taux de Confiance	Activité moyenne (Bq/grammes)	Incertitude Activité moyenne	Note
CO-60	0,989	1,67E+01	4,23E-01	
BI-214	0,376	1,37E+00	1,89E-01	
PB-214	0,729	8,68E-01	7,73E-02	

Figure 32 - Example of a report of measurement

Because the software can misinterpret or ignore certain peaks, an individual check of each spectrum and report was carried out. Luckily, these cases of misinterpretation are rare, but the check is nevertheless done to avoid false data in the results. First the spectrum is manually searched for peaks to confirm the identified peaks by the software. Secondly, the identified peaks were checked if they were assigned to the proper radionuclide. This was done by using the data from the website “The Lund/LBNL Nuclear Data search” [55] where detailed information about radionuclides is available.

8.3.3 Calibration

To properly measure the samples and to ensure that the found data are correct, the detector needs to be calibrated. The method for the energy calibration was already present in the facility at Fleurus and was executed with a ¹⁵²Eu source. Figure 33 below shows the energies of the source used for the energy calibration. The europium source has the advantage to present peaks with energies varying from low to high values, making it an excellent calibration source for a wide range of energies.

	Energie (keV)	Canal	FWHM (Ch)
1	121.8	266.4	1.71
2	244.7	529.5	2.08
3	344.3	742.7	2.20
4	411.1	885.7	2.82
5	444.0	956.0	2.82
6	778.9	1673.0	3.15
7	867.3	1862.3	3.85
8	964.0	2069.4	3.39
9	1085.8	2330.1	3.60
10	1112.0	2386.3	3.66
11	1408.0	3020.0	4.07

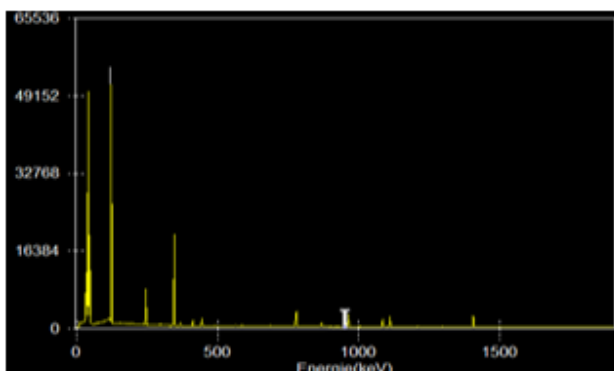


Figure 33 - Energies of the Eu-152 source used for calibration

The calibration results in a graph, visualized in Figure 34. This graph illustrates the relation between the energy and the channel number of the detector. As shown, the channel number is directly proportional to the energy. The straight line in the figure has the following equation:

$$E(\text{keV}) = 2.720 + 0.467 \cdot \text{ch} + (-5.06\text{E-}08) \cdot \text{ch}^2$$

With E = energy and ch = channel number

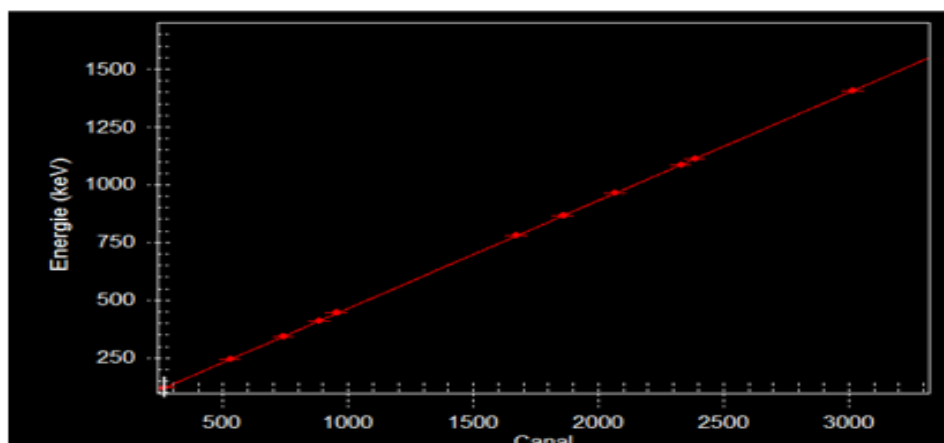


Figure 34 - Result of energy calibration

The energy calibration was manually validated by inserting a ^{60}Co source in the detector and by checking if the two dominant peaks of ^{60}Co were exactly at 1173.2 keV and 1332.5 keV. To ensure that the detector is always well calibrated, the Apex Gamma™ software has a build-in function that warns the user when the calibration is no longer valid (normal period of validity is 36 hours). Furthermore, when there is a shift of energy with the channel number due to, for example, a heating up of the detector, the software gives a warning.

The energy calibration makes it possible to identify the radionuclides in the measured spectrum. In order to quantify those radionuclides in kBq/kg an additional efficiency calibration is needed. For that, it is required to measure the calibration source in exactly the same geometry as the samples. Consequently the calibration source was put into the same petri dish as illustrated in Figure 26. The source used is a multi-gamma source that consists of multiple radionuclides, which are listed in Table 9. The full calibration certificate can be found in Appendix 2.

Table 9 - Composition of multi-gamma calibration source [56]

Radionuclide	Energy (keV)	Specific activity (kBq.g ⁻¹)	Extended relative uncertainty (k=2, %)
^{241}Am	59.5409 ± 0.0001	3.17 x 10 ¹	± 4
^{109}Cd	88.0336 ± 0.0001	2.78 x 10 ²	± 5
^{57}Co	122.06065 ± 0.00012	1.560 x 10 ¹	± 3
	136.47356 ± 0.00029		
^{139}Ce	165.8575 ± 0.0011	1.645 x 10 ¹	± 4
^{51}Cr	320.0835 ± 0.0004	2.35 x 10 ²	± 4.5
^{113}Sn	391.698 ± 0.003	4.62 x 10 ¹	± 4
^{85}Sr	514.0048 ± 0.0022	4.89 x 10 ¹	± 3,5
^{137}Cs	661.657 ± 0.003	6.08 x 10 ¹	± 3
^{60}Co	1173.228 ± 0.003	8.78 x 10 ¹	± 3
	1332.492 ± 0.004		
^{88}Y	1836.052 ± 0.013	9.62 x 10 ¹	± 3

Originally, the multi-gamma source was delivered as a liquid in a 20-ml bottle. To match the calibration source geometry with that of the samples, 32.95 mg of the same multi-gamma source was fixated in the petri dish geometry. Like the samples, this calibration source was measured in direct contact with the HPGe detector. The results from this calibration are shown below in Figure 35.

RESULTATS ETALONNAGE EN EFFICACITE					
Energie	% Efficacit�	Incert.	Eff. Calcul�	Incert.	% Diff�rence
59,54	2,39E+01	9,57E-01	2,40E+01	9,53E-01	-1,17E-01
88,03	2,42E+01	1,21E+00	2,44E+01	8,43E-01	-1,47E-01
122,06	2,09E+01	6,30E-01	2,01E+01	4,61E-01	-8,55E-01
165,86	1,44E+01	5,07E-01	1,56E+01	3,98E-01	-1,21E+00
320,08	9,04E+00	4,24E-01	8,60E+00	2,19E-01	-4,38E-01
391,70	7,30E+00	2,93E-01	7,10E+00	1,53E-01	2,03E-01
514,01	5,32E+00	1,87E-01	5,42E+00	1,07E-01	-9,99E-02
661,66	4,34E+00	1,31E-01	4,14E+00	7,90E-02	-2,03E-01
898,04	2,63E+00	7,92E-02	2,92E+00	4,96E-02	-2,87E-01
1173,23	2,19E+00	6,59E-02	2,13E+00	4,03E-02	6,07E-02
1332,49	1,92E+00	5,78E-02	1,84E+00	3,71E-02	7,92E-02
1836,05	1,33E+00	4,01E-02	1,35E+00	4,02E-02	-2,18E-02

Figure 35 - Calculated efficiency from the multi-gamma source

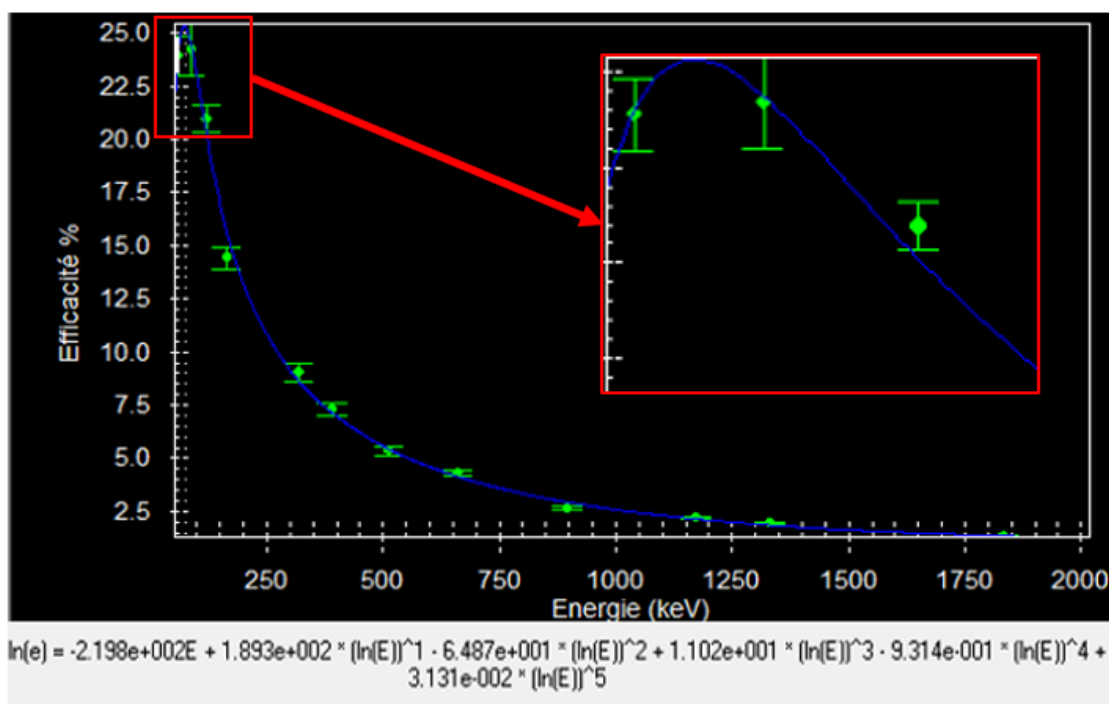


Figure 36 - Efficiency of the petri dish calibration source

The curve resulting from the calibration shows (Figure 36) that the efficiency is maximum at low energies, but decreases rapidly towards zero. The efficiency curve plotted through the measured points is a polynomial function of the 5th order with the equation that is mentioned in the figure. The equation is used by the software to calculate the efficiency of each peak. This efficiency along with the measuring time, the branching ratio of the peak and the peak counts is used for the determination of the activity expressed in becquerel. Thereafter this activity is divided by the mass of the sample to obtain the specific activity of the corresponding radionuclide in the sample. This procedure is done for every identified peak in the spectrum. Finally the software gives an overview of the specific activities for each peak for every radionuclide and an average activity of every identified radionuclide, as shown in Figure 32.

As mentioned above, the software also calculates the uncertainty of the specific activity. Uncertainties that come along with small variations in the positioning of the sample on the detector (user defined random uncertainties) are not included in the report. However these are considered as insignificant with regard to the context in which the results are used. As it will be explained later on, the goal is to obtain a result and a corresponding uncertainty that allows making a decision about the final disposal option of the activated material.

8.3.4 Measurement of the samples

The metallic and concrete samples are taken from various components in the accelerator with the expectation that the specific activity varies significantly between them. To obtain good results with an uncertainty that is between acceptable limits, it is necessary to measure the samples long enough. The time necessary to measure the sample was roughly estimated based on the location where the sample had been taken. After the first measurement, the results were analysed to see if a longer measurement was necessary to have more precise data. The goal of the measurements is to obtain results with uncertainties that allow taking a decision on the subject of the different disposal scenarios discussed in 6.3. Table 10 gives an overview of the measurement time for each sample to have sufficiently precise data.

Table 10 - Measuring time of the samples

1 hour measurement	001 – 005 (2) ² ; 006-009; 013 – 030; 035 – 037; 041 – 044; 058; 060; 066 – 068; 070 – 071;
2 hours measurement	005 (3); 010 – 011 (2); 012; 031; 034; 045 – 047; 054;
3 hours measurement	011 (3); 032 – 033; 056 – 057; 072;
12 hours measurement	038 – 040; 048 – 051; 053; 059; 061 – 063; 065; 069; 073 - 075
24 hours measurement	064
48 hours measurement	052; 055

² The number between parentheses indicates that it concerns a depth measurement in an existing drill hole.

9 Results and discussion

9.1 Identified radionuclides

9.1.1 Metallic samples

In total 82 samples were taken in the various metallic components of the cyclotron. There were several radionuclides identified in the samples, but only one results from the activation process. Table 11 below gives an overview of the different radionuclides found in the samples. The radionuclides both identified in the background measurement (48 hours) and the metallic samples are represented in green. The radionuclide in red was only identified in the metallic samples.

Table 11 - Identified radionuclides

^{40}K	^{214}Bi
^{60}Co	^{214}Pb
^{137}Cs	^{226}Ra
^{212}Bi	^{208}Tl
^{212}Pb	^{228}Ac

The majority of the identified radionuclides, as indicated in green, are radionuclides that occur naturally and are not the result of an activation process in the different components of the cyclotron. They originate from several decay series like the thorium, uranium and radium decay chain. An overview of those decay chains and their resulting radionuclides can be found in Appendix 3.

On the contrary, ^{137}Cs is not a naturally occurring radionuclide and yet it was identified in both the background measurement and some of the metallic samples. The presence of it in the measured samples is very concentrated at two locations in the cyclotron as it can be seen in Figure 37. All of these samples were measured for 12 hours or more.

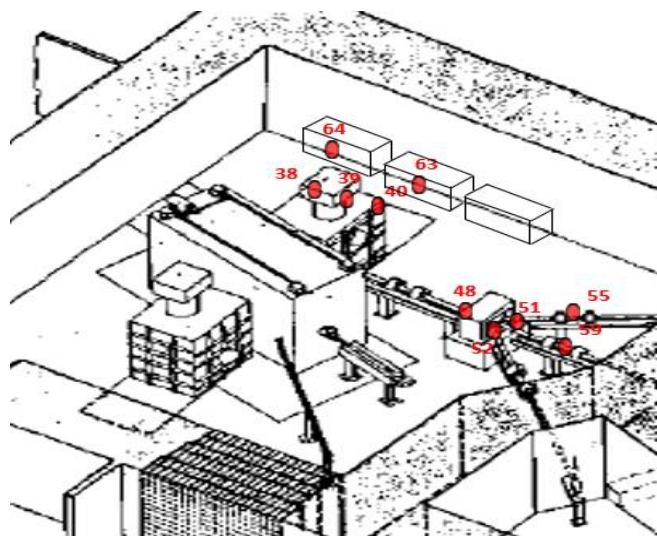


Figure 37 - Samples with ^{137}Cs

To verify if the ^{137}Cs originates from the samples or from somewhere else, the Cs^{137} measured in the background is compared with the ^{137}Cs identified in the metallic samples. The results from the background measurement showed a ^{137}Cs peak of $6.48 \cdot 10^{-4}$ cps. Compared with the metallic samples 052 and 055, which were also measured for 48 hours, $6.31 \cdot 10^{-4}$ cps were measured for ^{137}Cs . From this data it can be concluded that ^{137}Cs is not present in the samples, but originates from the surroundings of the detector. The origin of this ^{137}Cs is not exactly known, but it can be the result of a cross-contamination.

The radionuclide indicated in red, ^{60}Co , is not naturally occurring and was only detected in the metallic samples. As discussed above in 6.2 and 6.3, the presence of ^{60}Co is definitely a result of an activation process. It is also the only radionuclide that is present in all of the measured samples. Consequently it is possible to conclude that out of the two not naturally occurring radionuclides, ^{60}Co , resulting from the activation process, is the only one present in the metallic samples.

Furthermore, there are three samples (038 – 040, corresponding to the backside of the second HF cavity) where no ^{60}Co was detected, although measured for 12 hours. This is somewhat bizarre because the ventilation units that are located behind the HF cavity 2 contain ^{60}Co . One would expect that the cavity acts as a barrier for the neutrons coming from mainly the deflector and the beam exit and thus more interactions and consequently activation would occur in the cavity instead of the ventilations units. A possible explanation of that difference could come from the fact that the cavity and the ventilation unit are composed out of two different materials. The cavity is made of aluminium and the ventilation pipe of cast iron. Because iron is the main element present in cast iron, the probability for nuclear reactions that lead to the production of ^{60}Co is higher than in aluminium which only contains a percentage of iron.

Because the cyclotron was shut-down in 1993, more than 20 years ago, ^{60}Co is the only activation product that remains in the metallic parts. Table 12 gives a better overview of the possible activation products in the metallic components, based on the Karlsruher chart of the nuclides [57] and the chemical composition of the metal components (see Table 2). Especially the radionuclides with half-lives of a few days are fully decayed now and are not detectable anymore. Consequently, only the radionuclides indicated in red have a half-life sufficiently long to be detected after more than 20 years of inactivity. Yet only one of the three indicated radionuclides is visible in the samples, because ^{55}Fe and ^{63}Ni emit no gamma radiation and are thus not detectable with a HPGe detector. Even when ^{63}Ni would emit gamma radiation, it will not be detectable in large quantities due to long half-life and the resulting low activity. In contrast with ^{63}Ni , ^{55}Fe has a half-life of only 2.73 years. It is primarily produced by the (n,γ) reaction of ^{54}Fe and the (p,n) reaction of ^{55}Mn nearby the proton beam. The cross section for the (n,γ) reaction is 2.25 b for thermal neutrons and approximately 10 mb for the (p,n) reaction with 65 MeV protons [27], [31].

Compared with ^{60}Co , which has a half-life of 5.27 years and is mainly produced from the (n,γ) reaction on ^{59}Co with a cross section of 37 barns, the dominant cross section of 2.25 barn for ^{55}Fe is rather small, but not negligible. However, this lower cross section is compensated with the vast larger presence of ^{54}Fe compared with ^{59}Co , as iron and its isotopes are the dominant nuclides in the cyclotron materials. Nevertheless, 20 years of inactivity represent approximately 7 half-lives of ^{55}Fe and only 4 of ^{60}Co . It is possible to conclude that ^{55}Fe could be present in the metallic components, but even when it would emit gamma radiation it will be in very small quantities. Therefore it will not interfere with the decisions regarding the optimal final disposal scenario, because its limit of 100 kBq/kg for unconditional release is probably not exceeded.

Table 12 - Possible activation products in metallic components

Activation product	Half-life	Activation product	Half-life
⁵⁶ Co	77.24 days	⁵⁹ Fe	44.49 days
⁵⁷ Co	271.80 days	⁹⁵ Nb	34.97 days
⁵⁸ Co	70.86 days	¹⁸² Ta	114.43 days
⁶⁵ Zn	244.3 days	¹²⁴ Sb	60.3 days
⁵⁵ Fe	2.73 years	⁵¹ Cr	27.70 days
⁵⁴ Mn	312.2 days	⁴⁹ V	330 days
⁴⁶ Sc	83.79 days	⁶³ Ni	100 years
⁶⁰ Co	5.27 years	⁷ Be	53.22 days

9.1.2 Concrete samples

As a preliminary study, 3 samples were taken from three different locations in the concrete shield (wall of the cyclotron vault). There is a variety of radionuclides detected, but the majority of them are, similar to the metallic samples, naturally occurring and thus not the result of an activation process. With the natural radionuclides left out of consideration, 2 radionuclides remain that are the result of activation: ⁶⁰Co, ¹⁵²Eu and possibly ¹³⁷Cs. The results of the three samples are shown in Table 13.

Table 13 - Radionuclides present in concrete samples

	⁶⁰ Co	¹⁵² Eu	¹³⁷ Cs
Sample 073		X	X
Sample 074	X	X	X
Sample 075	X	X	

As cobalt and europium are already in the concrete (Table 3), it is no surprise that ⁶⁰Co and ¹⁵²Eu are present in the drilled samples. Especially ¹⁵²Eu is an important radionuclide in activated concrete. As it will be shown later from the specific activities, ¹⁵²Eu is more present than ⁶⁰Co, because one of the stable nuclides of europium, ¹⁵¹Eu, has a very high cross section for a (n,γ) reaction with thermal neutrons: 9176.49 b [31]. Furthermore, ¹⁵²Eu has a half-life of 13.33 years, so depending on the activity at the start, it is possible to detect it after 20 years of shut-down. Next to ¹⁵¹Eu, there is also ¹⁵³Eu as stable nuclide. This nuclide has only a cross section of 312 b for the (n,γ) reaction that results in the production of ¹⁵⁴Eu [31]. Furthermore, ¹⁵⁴Eu has a half-life of 8.8 years and thus its gamma emission is certainly detectable with the HPGe. The reason that it is not detected in the spectra is probably due to the fact that it is not present in the samples.

Finally, ¹³⁷Cs is also detected in 2 of the 3 samples. The stable nuclide, ¹³³Cs, is present in concrete, but as ¹³⁷Cs is located far from its stable nuclide it is unlikely that ¹³⁷Cs is formed from ¹³³Cs through neutron nuclear reactions. Reference [19] proposes a possible explanation for the presence of ¹³⁷Cs in the concrete. It suggests the (n,p) nuclear reaction of ¹³⁷Ba with the production of ¹³⁷Cs. The reaction has only a cross section of 3.7 mb with neutrons of 16 MeV [19]. Additional ¹³⁷Ba can be formed through a (n,γ) reaction of ¹³⁶Ba, which has a cross section of 0.4 b [19]. Therefore it is possible that ¹³⁷Cs is present as a result from activation. A second explanation was described above in paragraph 9.1.1: the presence of ¹³⁷Cs originates from the surroundings of the detector.

9.2 Specific activities of the identified radionuclides

The identification, or in other words the qualitative analysis, is not sufficient to take decisions with regard to the disposal of the activated materials. As discussed in chapter 7 Final disposal, the scenarios for disposal are primarily based on the specific activities of the identified radionuclides.

Throughout the whole cyclotron the maximum specific activity found in a sample was $3.28 \times 10^2 \pm 4.78$ kBq/kg. As mentioned before, there were samples with no detectable amount of ^{60}Co . This was the case with three samples (038 – 040) taken at the back side of the second HF cavity. However, when ^{60}Co was not detectable in these samples, it does not mean that there is no ^{60}Co in it. If the samples 038 – 040 are measured for 2 days instead of 12 hours it is likely that ^{60}Co is detected, but this is unnecessary to do. Because in a similar case, sample 052 was measured for 12 hours and as in the samples 038 – 040 no ^{60}Co was detected. However, sample 052 was re-measured for 48 hours and $3.58 \times 10^{-2} \pm 6.03 \times 10^{-3}$ kBq/kg of ^{60}Co was found. Although some activity of ^{60}Co was detected, it is very small and well below the unconditional release level of 0.1 kBq/kg for this radionuclide. Similar cases were found with samples 055 and 064.

So with the current information it is possible to say that for the samples 038 – 040 no longer measurements are necessary to properly classify them for a final disposal scenario. Furthermore, other cases indicate that when there is no ^{60}Co detected during a 12-hour measurement, the specific activity of ^{60}Co in it is well below the clearance level.

9.2.1 Deflector area

The deflector area is a location where many samples were taken from, in fact almost 50% of them originate from this area. Although taken from a relatively small area, the results present large differences. Figure 38 shows that the deflector area can be divided into three major zones:

- Samples taken from the left side of the deflector area which is manufactured out of iron;
- Samples from the deflector itself, which is in the centre and is made out of stainless steel and iron;
- Samples taken from various components at the right side of the deflector, which are made out of copper, stainless steel and aluminium.

The samples 001 – 012 taken from the left side of the deflector indicate the vertical variation of activation, but also the effect of distance. Figure 38 and Figure 39 show the variation of the average specific activity of ^{60}Co in the iron component at the left side of the deflector. The maximum specific activity of $2.58 \pm 1.49 \times 10^{-1}$ kBq/kg was measured at the most right side, closest to the deflector. The smallest amount of ^{60}Co was found at the most left side of the component and is $3.40 \times 10^{-1} \pm 4.51 \times 10^{-2}$ kBq/kg.



Figure 38 - Sample locations at the left side of the deflector area

Both figures indicate that the level of activation is approximately the same at the vertical level for each 'column', except for the samples 001 to 003 where there is a small vertical variation in the specific activity of ^{60}Co . However, the horizontal variation shows a very significant decrease of the specific activity with increasing distance from the deflector. Over approximately 1 m (distance between 002 and 011), the specific activity decreases with 85%. The three lines in Figure 39 indicate the three horizontal lines of samples taken in the component: top, centre and bottom. The arrow indicates that the deflector is located on the right side of the graph.

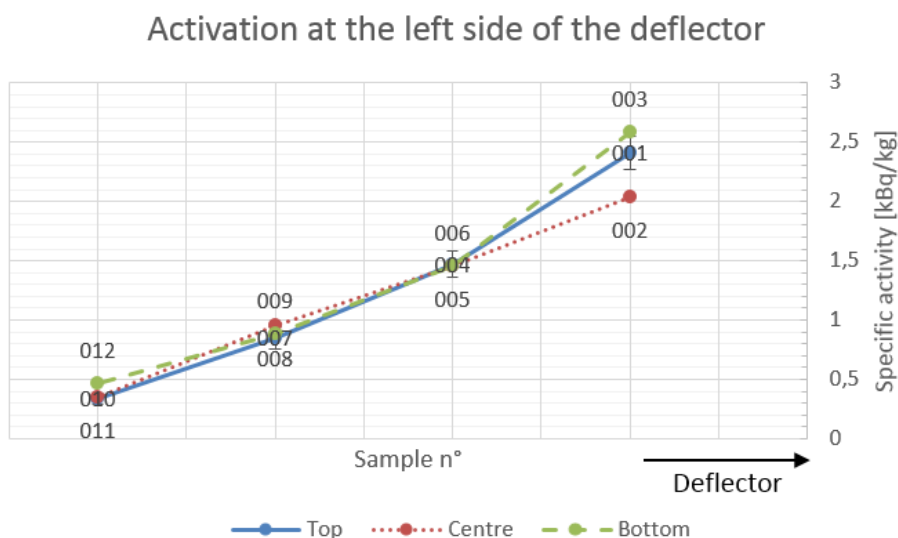


Figure 39 - Activation at the left side of the deflector area

The twelve samples discussed above were all taken from the surface of the component. To obtain the depth variation of the activation, 6 additional samples were taken as described in 8.1. The samples chosen for this procedure were all located on the centre horizontal line: 002 – 011. Figure 40 shows the result of those measurements. For sample 002, the specific activity decreases slowly after a depth of 15.2 mm. Over the distance of 22.8 mm, the specific activity only decreases with 15%. This is less than the samples of 005, which was drilled at approximately the same depth. In 005 the specific activity decreases with 35% over a depth of 24.6 mm. Finally, the green line represents the depth measurement of sample 011, which is located at the most left side of the deflector area. Although these samples were drilled shallower than the other ones, the slight decrease of the specific activity can also be observed.

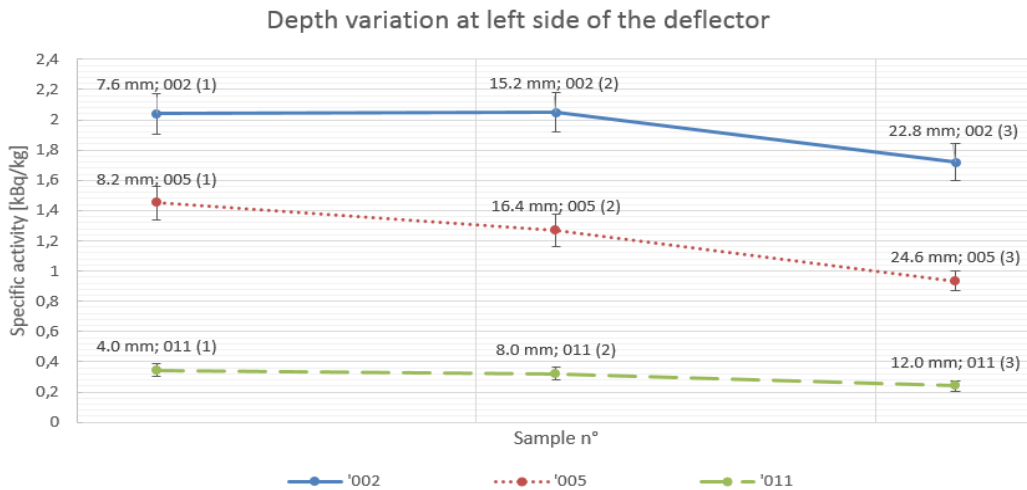


Figure 40 - Variation of specific activity with depth

Additionally, two samples were taken from the left edge of the same iron component to see the activation at even further distances of the deflector area. As can be seen in Figure 41, the two samples were taken at the same centre level as the measurements mentioned above. The average specific activities of 032 and 033 are respectively $2.09 \times 10^{-1} \pm 2.92 \times 10^{-2}$ kBq/kg and $1.28 \times 10^{-1} \pm 2.54 \times 10^{-2}$ kBq/kg. These are the lowest levels of activation measured in the entire deflector area. Because these points are located far away from the deflector, they represent the smallest activity in the entire left side of the component. It can be expected that samples from various depths in 032 or 033 would show an increase of the specific activity, because the distance to the deflector will be decreased by doing so.

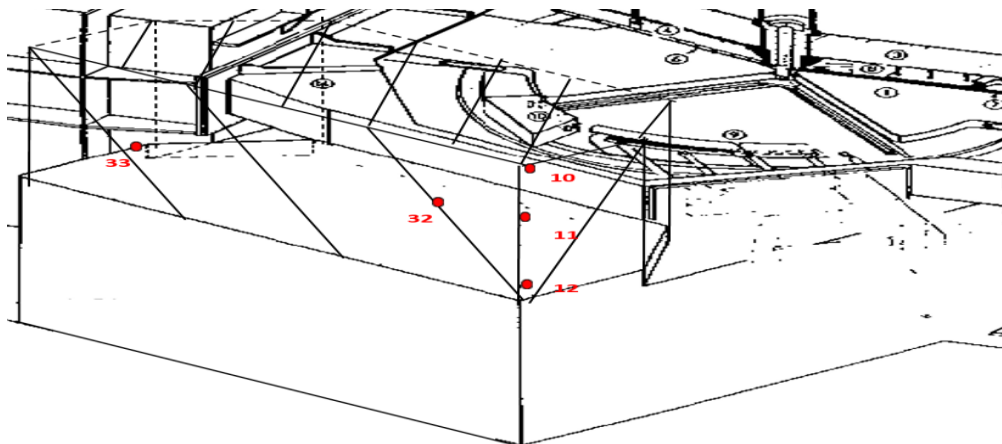


Figure 41 - Additional samples at left edge of deflector area

The second zone of interest is the centre of the deflector area. In contrast with the other zones, there is also the possibility of activation through proton induced reactions. The majority of the samples in this area were taken from the stainless steel component of the deflector, but 3 samples originate from an iron component nearby. The proton induced reactions are only possible in the stainless steel component, because it was in direct contact with the accelerated beam. This means that the activation in the iron component is completely caused by neutron interactions.

Figure 42 shows the 7 samples that were taken from the deflector itself, which is made out of stainless steel. The two samples at the bottom of the figure were drilled in iron.

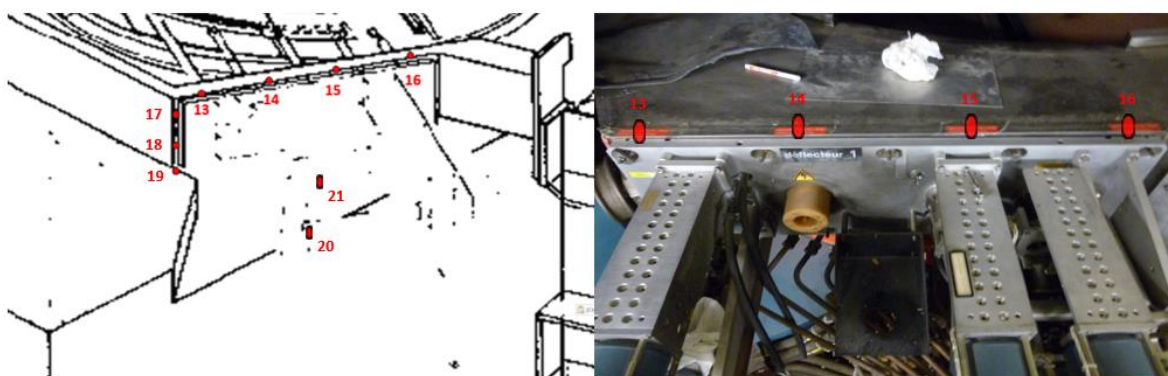


Figure 42 - Samples in centre of deflector area

The maximum specific activity was measured at the top of the deflector (015) and is $1.93 \times 10^2 \pm 2.92$ kBq/kg. The smallest amount of activity (020) was found in the iron sample at the bottom of the deflector and is $3.24 \pm 1.66 \times 10^{-1}$ kBq/kg. For such a small surface, the level of activity varies significantly as shown in Figure 43 and Table 14. The size of the spots in Figure 43 is an indication of the level of specific activity: the higher the specific activity, the larger the size of the spot. Firstly it is clear that the top of the deflector is the most activated part of the deflector with the specific activity varying horizontally. The distance between 013 and 016 is approximately 1.00 m and the activity increases with almost 50%, meaning that the majority of the reactions occurred around the location of samples 015 and 016.

Secondly, the specific activity in sample 017 is a factor 5 lower than sample 013, which is located only a few centimetres from 017. Additionally, there is almost no vertical variation between the specific activities at the left side of the component. The specific activity of the deflector reaches a minimum at the bottom, which is made out of iron. Although there is no vertical variation in the left side of the component (017 – 019), a general overview of the centre of the deflector area indicates that the specific activity drops significantly over a vertical distance of 0.5 m.

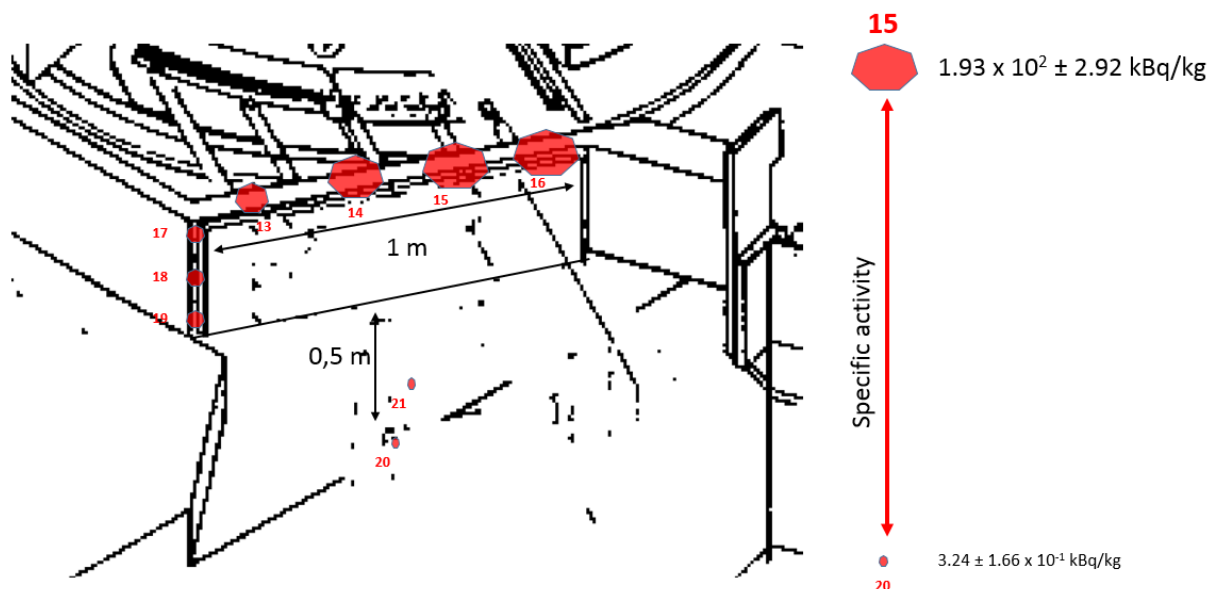


Figure 43 - Activation at the centre of deflector area

Table 14 - Specific activities [kBq/kg] at centre of deflector area

Sample n°	Average spec. act. (kBq/kg)	Uncertainty spec. act. (kBq/kg)
013	9.41×10^1	1.55
014	1.31×10^2	2.05
015	1.93×10^2	2.92
016	1.91×10^2	2.90
017	1.63×10^1	4.21×10^{-1}
018	1.87×10^1	4.50×10^{-1}
019	1.67×10^1	4.23×10^{-1}
020	3.24	1.66×10^{-1}
021	3.98	1.79×10^{-1}

To check if the specific activity levels are lower when measured deeper in the material, two additional samples with increasing depth were drilled in the same hole as sample 020. The result of this experiment is shown in Figure 44. As illustrated in the figure, the specific activity decreases slowly with increasing depth.

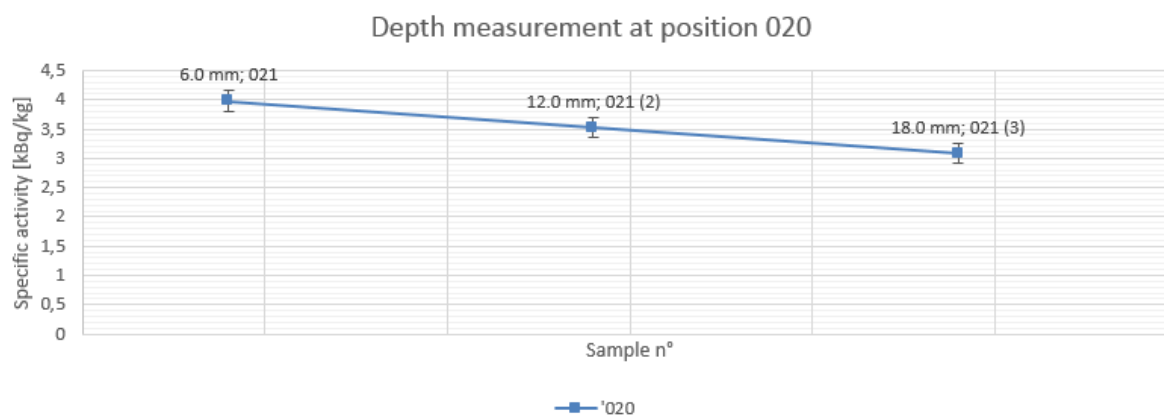


Figure 44 - Variation of specific activities with depth at position 020

The third and final zone of interest is the right side of the deflector area, as shown in Figure 45.

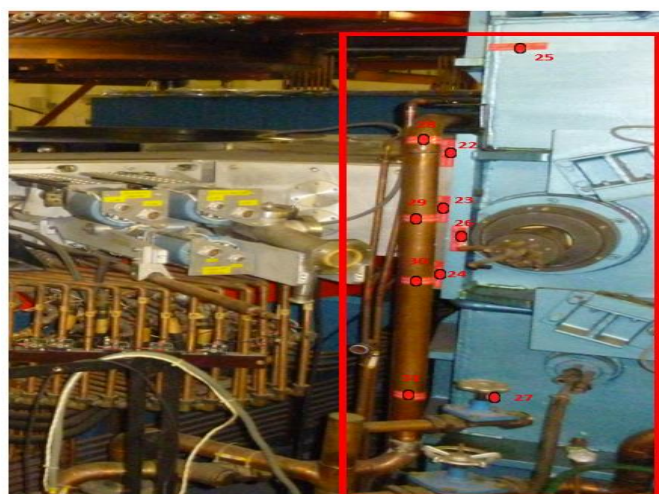


Figure 45 - Right side of the deflector area

The maximum specific activity was measured in sample 023 with a value of $4.16 \times 10^{-1} \pm 8.03 \times 10^{-1}$ kBq/kg and the minimum value of $2.19 \times 10^{-1} \pm 3.88 \times 10^{-2}$ kBq/kg was found in sample 031. Compared with the specific activity levels at the left side of the deflector area, the values at the right side are higher. A very interesting feature of this side is that many samples are taken from different materials that are positioned very close to each other. This makes it possible to see the influence of the type of material on the activation levels. A good example of this is seen in sample 022 and 028, which are respectively taken from stainless steel and copper. Although the distance between the two sample points is only 11 cm, there is a great difference in specific activity: $3.30 \times 10^1 \pm 6.79 \times 10^{-1}$ kBq/kg in 022 and $7.04 \times 10^{-1} \pm 7.97 \times 10^{-2}$ kBq/kg in 028. The same can be observed in the comparison between the samples shown in Table 15.

Table 15 - Comparison between specific activity of copper (Cu) and stainless steel (SS) at right side of the deflector area

Sample n°	Average specific activity [kBq/kg]	Average specific activity [kBq/kg]	Sample n°
022 (SS)	$3.30 \times 10^1 \pm 6.79E-01$	$7.04 \times 10^{-1} \pm 7.97 \times 10^{-2}$	028 (Cu)
023 (SS)	$4.16 \times 10^1 \pm 8.03E-01$	$2.94 \pm 1.56 \times 10^{-1}$	029 (Cu)
024 (SS)	$3.71 \times 10^1 \pm 7.31E-01$	$2.18 \pm 1.32 \times 10^{-1}$	030 (Cu)

Because each pair of copper and stainless steel samples is located at approximately the same distance from the deflector, they have been irradiated under the same conditions. This means that the difference in specific activity results from the difference in material properties. From Table 15 it is possible to see that activation of stainless steels results in higher specific activity levels than in copper, provided that the irradiation conditions are the same for the two materials.

Additionally, sample 026 was taken from the high frequency cavity to check the specific activity in aluminium. This sample is located approximately 10 cm from position 023. The specific activity in the aluminium sample is $9.61 \times 10^{-1} \pm 9.25 \times 10^{-2}$ kBq/kg. This lower value is probably a result from the attenuation by the stainless steel between the aluminium and the deflector, but also from the fact that aluminium is less activated than stainless steel under the same irradiation conditions. It is possible to conclude that copper and aluminium are less activated than steel under the same irradiation conditions.

To obtain the vertical variation of the specific activity in this right area of the deflector it is useful to compare the results between the samples 028 – 031 on the copper tube. The variation is shown in the right side of Figure 46. The graph shows that the specific activity presents a maximum in the middle of the tube. The middle of the tube is approximately on the same height as the deflector. This indicates that the level of activation is highest at the height of the deflector. Sample 028 is taken from the top of the tube and 031 from the bottom, which can also be seen in Figure 45. The distance between 028 and 031 is 90 cm. The same tendency is seen in the stainless steel plate on the left side of Figure 46. The distance between the top (022) of the plate and the bottom (024) is 50 cm.

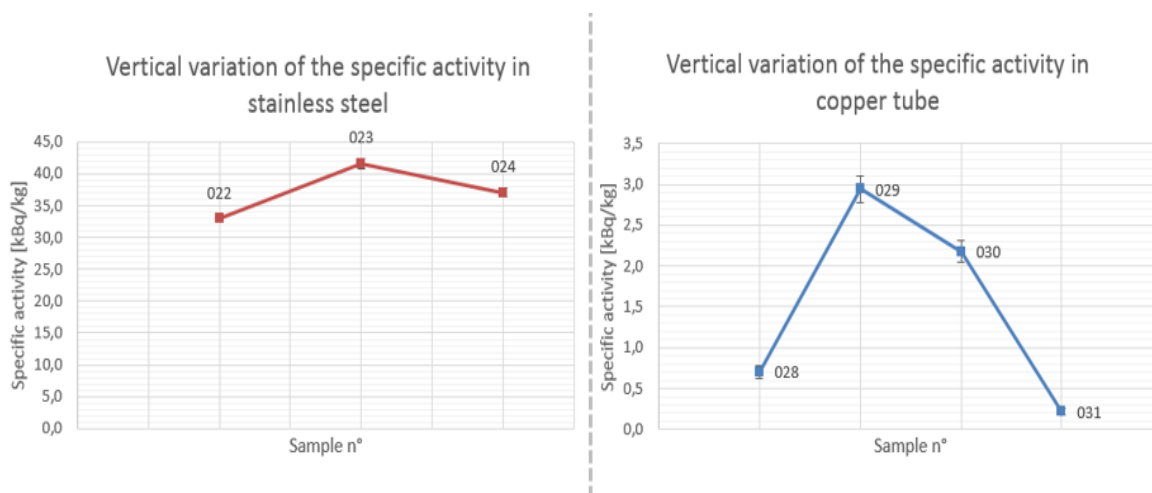


Figure 46 - Vertical variation of the specific activity [kBq/kg] in stainless steel and copper

Similar to the left side and the centre area of the deflector area, a depth measurement was executed in sample 023. The results of these drillings are shown below in Figure 47. It shows that the specific activity decreases 6 % over a distance of 13.5 mm in the plate made of stainless steel.

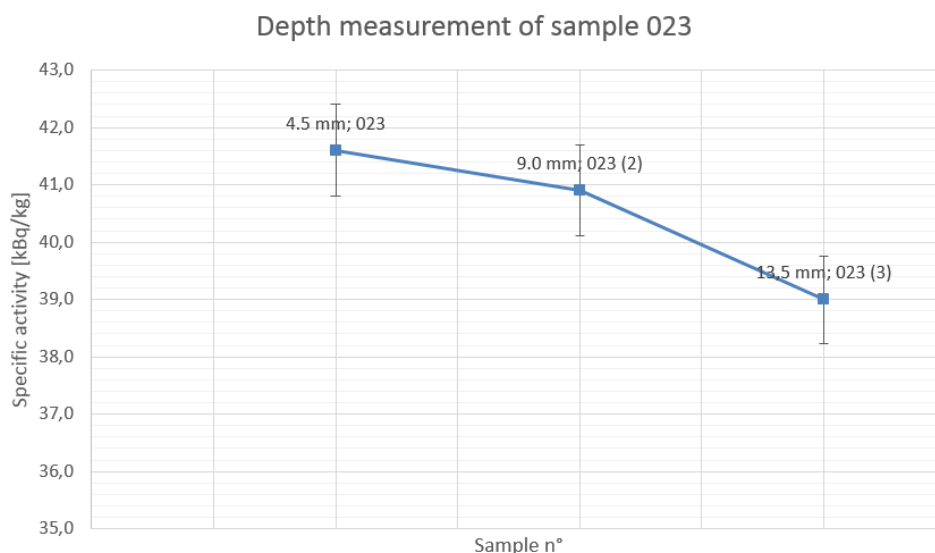


Figure 47 - Depth measurement of sample 023

To conclude the measurements in the deflector area, a sample (065) was taken from the top of the cyclotron, 1.10 m above the deflector. The specific activity measured in the sample is $3.11 \times 10^{-1} \pm 1.88 \times 10^{-2}$ kBq/kg. This is a rather low value for the specific activity in comparison with other samples in the deflector area.

9.2.2 Magnetic channel

The next area of interest is the magnetic channel. This component is located next to the deflector and was responsible for focussing the particle beam after extraction in the deflector. Samples 034 – 037 were taken from this component, as shown in Figure 48. The specific activities vary between $3.13 \times 10^{-1} \pm 4.48 \times 10^{-2}$ kBq/kg and $2.17 \times 10^1 \pm 5.05 \times 10^{-1}$ kBq/kg. The lowest level of specific activity corresponds to sample 034, which was taken from a copper component. This is similar to the deflector area, where copper samples also showed lower specific activities in comparison with other materials. The samples

035 – 037 were taken from stainless steel and the results show, as illustrated in Figure 48, that there is an increase of specific activity in the stainless steel. This increase is probably the result of the fact that 037 is located the closest to the deflector and thus more exposed to neutrons and beam particles.

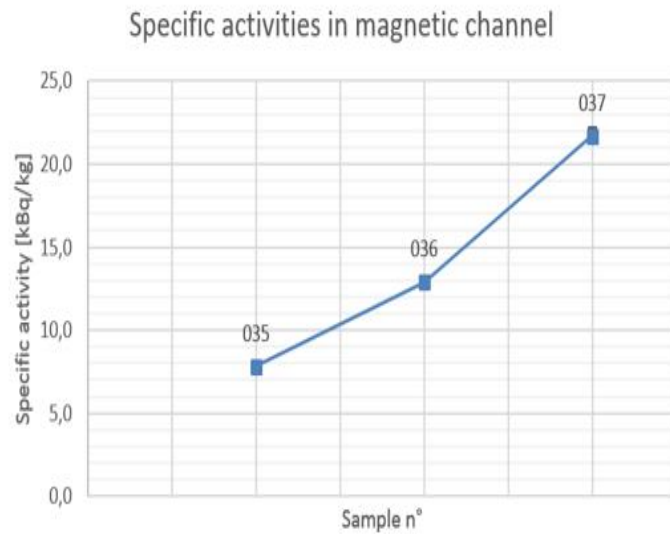


Figure 48 - Samples and specific activities in the magnetic channel

9.2.3 Beam exit area

The following component of interest is the beam exit area. Here the accelerated protons leave the cyclotron and are transported towards the irradiation rooms. Figure 49 shows this component. The highest level of specific activity was found in sample 044 and is $3.28 \times 10^2 \pm 4.78$ kBq/kg.

Sample 044 was taken in the copper cylinder, which is seen on top of the component. During operation the cylinder was mounted on the front end of the beam exit, indicated with an arrow. Sample 041, which was taken from the stainless steel tube that transports the beam, has a specific activity of $1.61 \times 10^2 \pm 2.48$ kBq/kg. This is 50% less than sample 044, which was located only a few centimetres above 041. These results are opposite to those obtained from the deflector area and the magnetic channel, where the specific activities in copper were lower than in stainless steel for components located at the same position. The activity in the copper cylinder is higher, because that piece was directly in the beam line. The right side of Figure 49 shows that the copper cylinder is narrower than the stainless steel tube and consequently there were more interactions in the copper than in the stainless steel. The remaining two samples, 042 and 043, were both taken in iron. Because sample 042 was taken closer to the beam area it has a higher level of specific activity than 043: $2.59 \times 10^1 \pm 5.75 \times 10^{-1}$ kBq/kg for 042 and $2.25 \pm 1.37 \times 10^{-1}$ kBq/kg for 043.



Figure 49 - Beam exit area

After the beam exit area, the accelerated particles were transported over a beam line of 2.40 m until the beam arrived at the switching magnet. The transport tubes were already removed before they could be sampled, but the iron structure that served as a support for the beam transport tubes still remains. From the support structure between the beam exit area and the switching magnet, 3 samples were taken. The variation of the specific activity is shown below in Figure 50.

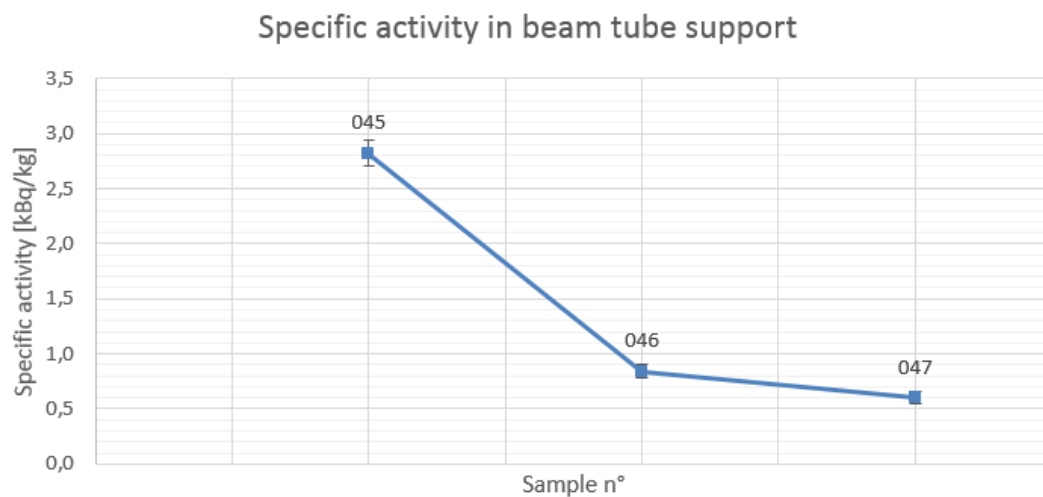


Figure 50 - Specific activity in beam tube support between beam exit area and switching magnet

Sample 045 was taken approximately 0.5 m from the beam exit area. Sample 046 and 047 were taken each time 0.8 m further. As seen in Figure 50, the specific activity in the steel support system decreases further from the exit area. As 045 is located closest to the exit area, it was more exposed to the secondary neutrons produced in that area. Over a distance of 2.40 m, the specific activity between 045 and 047 decreases by 78%, because the influence of the secondary neutrons decreases with distance and thus a decrease of specific activity is observed when going further along the beam transport track.

9.2.4 Switching magnet

The switching magnet was also sampled. In total 6 samples were taken from this component, three on the side facing the cyclotron and three on the other side. On each side two samples were taken from the iron box that surrounds the switching magnets and one was taken from the copper component of the magnet. Figure 51 shows the two sides of the switching magnet, the left one is the side facing the cyclotron. As shown in Table 16, the specific activities in the 3 sample points taken from the side that faces the cyclotron are higher than on the other side.



Figure 51 - Samples taken from the switching magnet

Table 16 - Specific activities measured in the switching magnet

Sample n°	Average specific activity [kBq/kg]	Uncertainty specific activity [kBq/kg]
048	1.44	3.82×10^{-2}
049	1.35×10^{-1}	1.74×10^{-2}
050	1.90×10^{-1}	1.62×10^{-2}
051	5.11×10^{-2}	1.25×10^{-3}
052	3.58×10^{-2}	6.03×10^{-3}
053	6.56×10^{-2}	1.17×10^{-2}

After the switching magnet there are three possible trajectories for the beam, depending on the settings of the switching magnet. Only on one of the three trajectories the stainless steel beam pipe still stands in its original position along with the magnetic lens to focus the beam. This set-up is shown in Figure 52. The specific activity from this part of the pipe was measured in sample 054 and indicated a value of $4.25 \pm 1.44 \times 10^{-1}$ kBq/kg. As this part was the only one remaining in the whole cyclotron vault, it is difficult to compare this value with other measurements at different locations.

However, it is expected that the specific activity measured in sample 054 is a good indication of the level of activation in the rest of the beam transport pipes. At location 054, the source of activation is the beam inside the pipe, but it is possible that parts of the transport pipes closer to the cyclotron are slightly more activated as a result from the secondary neutrons coming from the cyclotron.



Figure 52 - Beam transport set-up at the track 1

Similar to the transport pipe, the magnetic lens (location 55) is also the only one remaining in its original location. The measurement indicates a specific activity of $4.83 \times 10^{-2} \pm 6.84 \times 10^{-3}$ kBq/kg. This level of specific activity indicates that few interactions took place in the material of the magnetic lens. As seen in Figure 52, three samples were taken alongside the iron supports that stretch from the switching magnet to the end of the cyclotron vault. As seen from Table 17, the specific activities along the support structure are approximately the same.

Table 17 - Specific activities in beam pipe supports after the switching magnet

Sample n°	Average specific activity [kBq/kg]	Uncertainty specific activity [kBq/kg]
056	3.36×10^{-1}	3.76×10^{-2}
057	3.74×10^{-1}	3.69×10^{-2}
058	3.64×10^{-1}	1.92×10^{-2}

On track 2 of the switching magnet there were 3 samples taken from two interesting components: two from a box that was used to stop the beam in an emergency situation and one from a component made out of cast iron which was used to focus the beam during transport. The set-up is shown in Figure 53. The specific activity measured in the cast-iron focus lens is $7.77 \times 10^{-2} \pm 1.20 \times 10^{-2}$ kBq/kg. This level of specific activity is of the same order than the specific activity measured in the magnetic lens on track 1. It can be expected that other magnetic lenses and similar components on other positions of the beam transport have similar specific activities.

The component that blocks the beam during emergency consists out of a hollow box with a hole in the front to let the beam through during normal operation. To immediately stop the beam, a solid iron block drops in the beam during emergency. A sample was taken from the stainless steel box and one from the solid iron block that used to block the beam. The specific activity measured in the box is $3.31 \pm 1.63 \times 10^{-1}$ kBq/kg and $1.13 \times 10^{-1} \pm 1.51 \times 10^{-2}$ kBq/kg in the solid iron block. The latter value seems low for a component that used to be directly in the beam. After some research with the technical staff that used to operate the cyclotron, it turned out that the emergency block was never used during operation. The value of the specific activity in the box itself is in the same order as the specific activity in the beam transport pipe.



Figure 53 - Sample locations in cast-iron focus lens and box to stop the beam during emergency

9.2.5 Ventilation units

As mentioned earlier, three sample points were taken from the ventilation units in the cyclotron vault. Because these ventilation units are a large piece of metal over a large portion of the length of the cyclotron vault, they are a good indication of the variation of the activation at further distances from the cyclotron. The locations of the samples are shown in Figure 54. Table 18 shows that the specific activity in all the three locations is approximately the same. These results indicate that the level of activation on the left side of the cyclotron vault is hardly different at further distances.

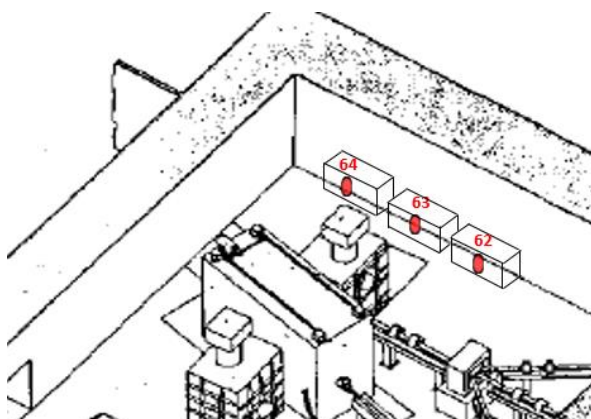


Figure 54 - Sample locations at the ventilation units of the cyclotron vault

Table 18 - Specific activation in the ventilation unit

Sample n°	Average specific activity [kBq/kg]	Uncertainty specific activity [kBq/kg]
062	1.09×10^{-1}	1.38×10^{-2}
063	1.11×10^{-1}	1.49×10^{-2}
064	1.04×10^{-1}	1.05×10^{-2}

9.2.6 Internal target area

The internal target area is an interesting area because here a target was inserted into the cyclotron and into the circular trajectory of the protons. This resulted in the production of ^{201}Tl , but also in a lot of secondary neutrons that activated surrounding materials. However, the energy of the beam was “only” 34 MeV and not the usual 67 MeV. The internal target area and the sample location are shown in Figure 55.

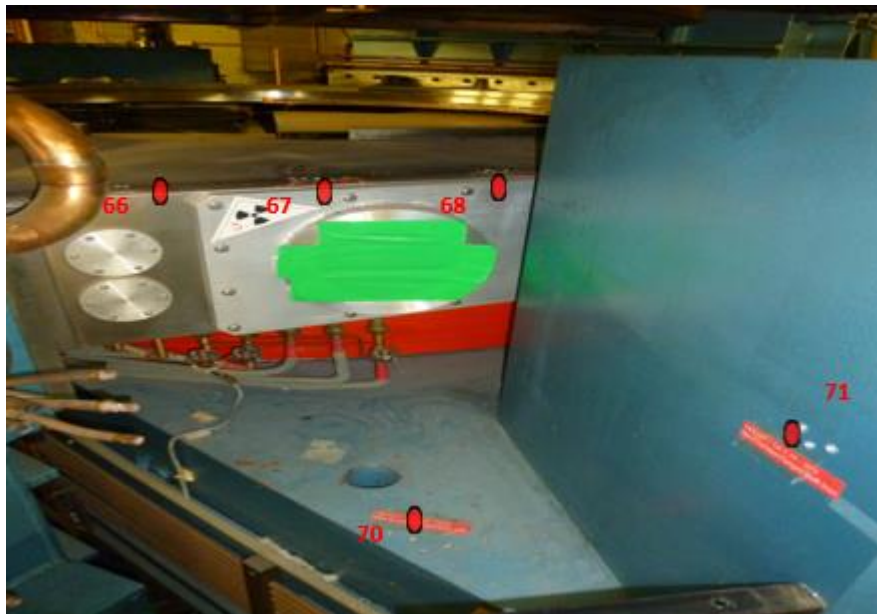


Figure 55 - Internal target area and sample locations

Three samples were taken at the stainless steel component closest to the area where the internal target was put into the beam. The results are shown below in Figure 56. The specific activity of the samples increases as they are located closer to the area where the internal target was put into the beam. Of the three samples, sample 068 is closest to the internal target and has consequently the largest specific activity of the samples taken in the area: $8.44 \times 10^1 \pm 1.41$ kBq/kg. The distance between 066 and 068 is 0.60 m.

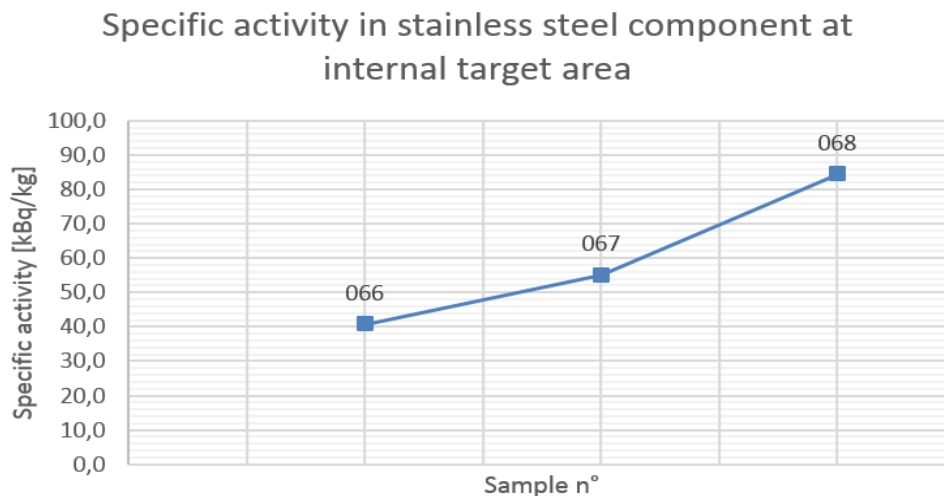


Figure 56 - Specific activities in stainless steel component at internal target area

Just below the stainless steel component, sample 070 was taken in an iron structure. Its specific activity is $2.82 \pm 1.49 \times 10^{-1}$ kBq/kg, which is more than a factor 10 less than in the stainless steel just 0.50 m in height and 0.59 m in length away. Additionally, sample 071 was also taken in iron, but in a structure at the same height as the stainless steel component. The specific activity at this location is $1.00 \pm 9.51 \times 10^{-2}$ kBq/kg, which does not differ that much from location 070.

To conclude the drilling at the internal target area, sample 072 was taken at the backside of the iron structure in which 071 was taken. Between these two samples there is approximately 0.90 m of solid iron. The specific activity in 072 is $2.24 \times 10^{-1} \pm 2.78 \times 10^{-2}$ kBq/kg and is thus a bit less than the specific activity at location 070.

9.2.7 High frequency cavity

The last location of interest is the high frequency cavity at the left side of the cyclotron. It is in every way identical to HF cavity 2 at the right side. The location of sample 069 on HF cavity 1 can be seen in Figure 57. The specific activity measured in the sample is $3.95 \times 10^{-2} \pm 9.76 \times 10^{-3}$ kBq/kg. When compared with the values of the specific activity at the second cavity, it seems that the specific activity at the outside panel of the first HF cavity is higher than in the second one. However, sample 069 was measured for 24 hours and the samples at the second cavity was measured for 12 hours.

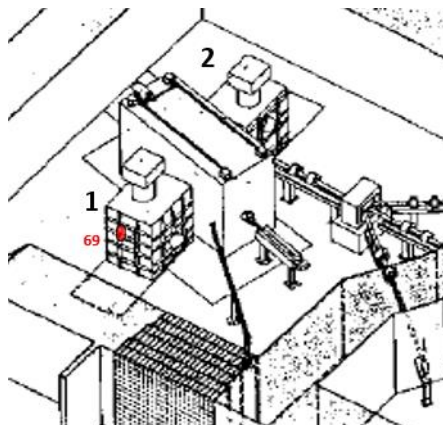


Figure 57 - Sample 069 at HF cavity 1

9.2.8 Identified hotspots

Based on what was discussed above, it is possible to identify three areas (Figure 58) that show a high level of activation in comparison with other areas in the cyclotron and the cyclotron vault. These areas are called hotspots of the cyclotron vault. Table 19 below shows an overview of these three hotspots and the maximum specific activity measured in each area.

Table 19 - Overview of the three hotspots identified in the cyclotron

Hotspot area	Maximum specific activity [kBq/kg]
Deflector area (1)	1.93E+02 ± 2.92
Beam exit area (2)	3.28E+02 ± 4.78
Internal target area (3)	8.44E+01 ± 1.41

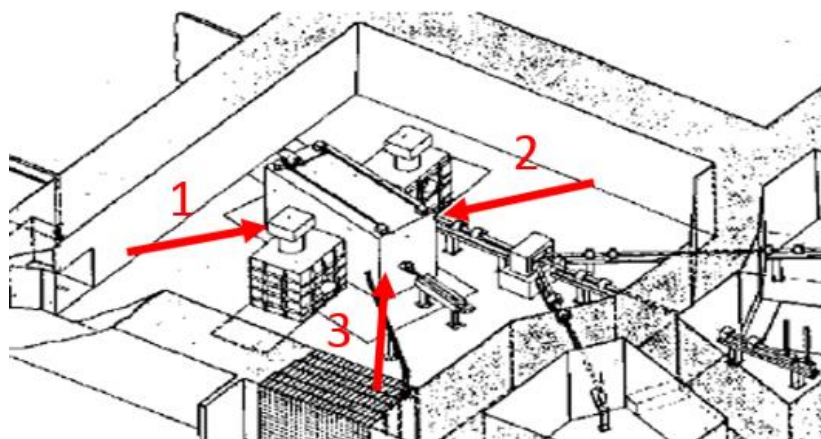


Figure 58 - Overview of the three hotspots identified in the cyclotron

It is not surprising that these three areas are the most activated of the entire cyclotron and cyclotron vault. During operation of the accelerator, these areas were subjected to interactions with high energy protons and secondary neutrons.

Out of these three hotspots, the beam exit area is the most activated and the internal target area the least. However, the beam exit area is a rather small area in comparison with the deflector area or the internal target area.

9.3 Elaboration of the final disposal scenarios of the activated metallic components

⁶⁰Co is the only radionuclide identified in the metallic components of the cyclotron as a result of activation during the operation of the cyclotron. Consequently, it is the only radionuclide to be taken into account regarding the Belgian limits for unconditional release, acceptance criteria for specialized melting or final storage as category A radioactive waste. The specific activities being known for the most important metallic components of the cyclotron and cyclotron vault, it is now possible to determine the most suitable final disposal option for each of these components.

To properly determine the optimal option for final disposal of each component it is important to take the uncertainty of the measurement into account. The uncertainty allows to calculate the minimum and maximum value of the range of the specific activity of a sample. The possible options for final disposal were already discussed in chapter 6, but a short overview is given below in Table 20.

Table 20 - Acceptance criteria for final disposal options

Category	Final disposal option	Acceptance criteria
1	Unconditional clearance based on Belgian release levels	≤ 0.1 kBq/kg for ^{60}Co
2	Specialized nuclear melting facility at Studsvik, Sweden	≤ 1.2 kBq/kg for ^{60}Co
3	Specialized nuclear melting facility at <i>EnergySolutions</i> , USA	≤ 1421 kBq/kg for ^{60}Co in stainless steel
4	Category A radioactive waste	> 1421 kBq/kg ³

With the range of specific activity for each sample and the acceptance criteria for each disposal option, it is possible to determine the optimal final disposal option for the component in which the sample was taken. With the assistance of Excel, three columns were made for each option. The program shows “OK” when a certain option is allowed and “NOT OK” when the option is not possible for the sample of interest. When both the minimum and maximum value of a specific activity interval were clearly under or above an acceptance criterion of a final disposal option, there was no problem. However, when the specific activity interval of a sample balanced at the criterion, it was not possible to designate the sample to a certain final disposal scenario. Excel indicated this with “Check”. In that case, it was chosen to allocate the sample to the next final disposal category with a higher tolerance level for specific activity. When there is doubt that the specific acidity exceeds an acceptance criterion, it is decided that the specific activity is indeed higher than that certain limit. An example of the functioning of the program and the evaluation of each sample with regard to the final disposal options is shown in Table 21.

Table 21 - Example of the final disposal evaluation for samples

Sample n°	Average specific activity [kBq/kg]	Uncertainty specific activity [kBq/kg]	Minimum value specific activity interval [kBq/kg]	Maximum value specific activity interval [kBq/kg]	Unconditional clearance OK?	Melting Studsvik OK?	Melting Energy solution OK?
001	2.41	1.44×10^{-1}	2.27	2.55	NOT OK	NOT OK	OK
005 (2)	1.27	1.08×10^{-1}	1.16	1.38	NOT OK	CHECK	OK
007	8.44×10^{-1}	9.22×10^{-2}	7.52×10^{-1}	9.36×10^{-1}	NOT OK	OK	OK
051	5.11×10^{-2}	1.25×10^{-2}	3.86×10^{-2}	6.36×10^{-2}	OK	OK	OK
059	1.13×10^{-1}	1.51×10^{-2}	9.79×10^{-2}	1.28×10^{-1}	CHECK	OK	OK

The table shows 5 different samples with 5 different allowed final disposal options. Sample 001 has a specific activity interval which is too high for unconditional release as well as for melting at Studsvik. However, the specific activity is less than 1421 kBq/kg and thus this sample is cleared for melting at *EnergySolutions*. The second sample in the table is also not cleared for unconditional release. As a result from the uncertainty, the minimum and maximum value of the specific activity interval are just under, respectively above the acceptance criterion of 1.2 kBq/kg for melting at Studsvik. As mentioned above no risks are taken in the case of doubt, so sample 005 (2) is assigned to melting at *EnergySolutions*. Sample 007 has a specific activity that is too high for unconditional release, but the

³ Cat. A accepts radioactive wastes with lower specific activities than 1421 kBq/kg. However, within the context of this study, it is the last option when the waste is not qualified for any other scenario.

interval is well defined to assign the sample for melting at Studsvik. The next sample, 051, is an example in which case the minimum and maximum value of the interval are both under the Belgian release limit of 0.1 kBq/kg. As a result, sample 055 can be released unconditionally. The final sample of Table 21 is an example in which the limit for unconditional clearance is situated in the interval of the specific activity. Once again, no risks are taken and consequently sample 059 is assigned to melting at Studsvik.

Based on that, the optimal final disposal option for each metallic component will be discussed in the next chapter.

9.3.1 Deflector area

First there is the left side of the deflector area, shown in Figure 38. All of the samples drilled in the iron structure show a specific activity that is higher than 0.1 kBq/kg. So it can be said that, based on the samples drilled in the surface, this component cannot be assigned for unconditional release. Next, the first two rows of samples taken in the component (001 – 006) show a specific activity that is also too high for being allowed in the melting facility at Studsvik, but it is low enough to be allowed for melting at *EnergySolutions*. However, starting from the third row of samples (007 – 012), approximately 0.5 m of the deflector, the specific activity is low enough to be qualified for melting at Studsvik. So the results show that the left side of the component can be divided into 2 categories for final disposal: the right half can be assigned to *EnergySolutions* and the other half to Studsvik.

As mentioned earlier, depth measurements were done at three points in the left side of the deflector area. The results of these measurements are again given in Figure 59. The drillings in sample 002 indicate that even after three times the initial depth, the specific activity remains above Studsvik's acceptance limit of 1.2 kBq/kg. Next, the depth measurements of location 005 indicate that after 24.6 mm the specific activity is below the limit of 1.2 kBq/kg. This means that it is necessary to remove the first 24.6 mm of iron, which is intended for melting at *EnergySolutions*, to arrive at the part where the specific activity allows for melting at Studsvik. This operation is time-consuming and it is probably easier to melt the component as a whole at *EnergySolutions*. Finally, the drilling at location 011 indicates that after 12 mm of depth, there is no change with regard to the final disposal option.

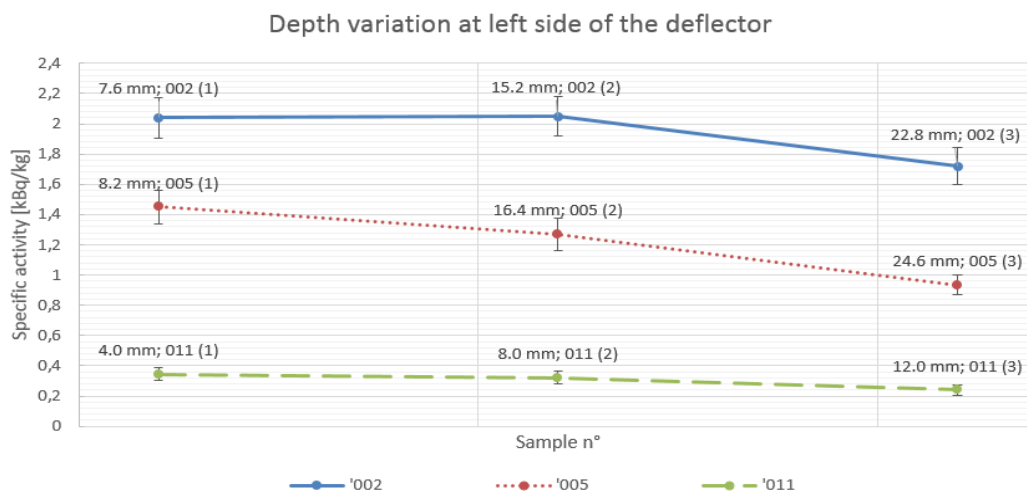


Figure 59 - Variation of specific activity with depth

This is also confirmed with the samples 032 and 033 drilled at the back side of the left deflector area, as shown in Figure 41. Their specific activities also indicate that the left half of this area could be approved for melting at Studsvik.

Next, there is the central area of the deflector area with the deflector itself. The specific activities measured in this area show that all of the samples have specific activities higher than both the acceptance criteria for unconditional release and melting at Studsvik. Furthermore, the depth measurement at location 021 shown that even 18 mm deeper into the iron component, the specific activity is still too high for being accepted at Studsvik. So it can be concluded that all the components from the central deflector area will be assigned to melting at *EnergySolutions*.

Thereafter, there is the right side of the deflector area. Similar to the central area, every sample in this area indicates that no component will be approved for unconditional clearance. With regard to melting at Studsvik, there are some differences between the different parts of this area. The samples 022 – 024 in the stainless steel plate (Figure 45) indicate that the specific activity is too high to be considered for melting at Studsvik. Furthermore, the depth measurement at location 023 gives no new insights in this decision. However, the samples 025 - 027 taken in HF cavity 1, right next to the stainless steel plate, show a specific activity that is low enough to be qualified for melting at Studsvik. Next there is the copper tube that runs along the whole height of the right side of the deflector area. The samples 028 – 031 indicate that the top and the bottom (028 and 031) are cleared for melting in Sweden, but the centre of the tube (029 and 030) must be melted at *EnergySolutions* because the specific activity levels are too high in this part of the tube. Because the copper tube is well accessible, it is not unthinkable to cut the tube in different parts for the different melting facilities. This operation needs to be checked for its financial advantage but it is possible from a technical point of view.

Finally, there is the top of the deflector. Sample 065 indicates a specific activity that is low enough to be qualified for melting at Studsvik. However, this sample was taken at the top of the cyclotron where the distance to the deflector is the largest. It is expected that samples drilled deeper in the top of the cyclotron will show a gradual increase of specific activity because the distance to the deflector becomes smaller. Additional depth measurements must be taken to determine if the specific activity in the component increases above 1.2 kBq/kg. When this is the case it is possible to consider *EnergySolutions* as the optimal disposal scenario for this component. As shown below in Figure 60, the top of the cyclotron is one unit and difficult to disassemble or cut into different parts with regard to their optimal final disposal category.



Figure 60 - Top of the cyclotron above the deflector area

9.3.2 Magnetic channel

Next there is the magnetic channel to be discussed in terms of final disposal options. Of the four samples taken at this area, none of them have specific activities low enough to be qualified for unconditional release. Furthermore, only sample 034 taken from a copper part of the magnetic channel shows a specific activity low enough to be melted at Studsvik. All of the 3 samples taken at the stainless steel part of the magnetic channel will be assigned to melting at *EnergySolutions*.

9.3.3 High frequency cavity 2

The second high frequency cavity of the cyclotron was sampled at three locations. Those three samples, which were taken from the rear of the cavity, indicated a non-detectable specific activity during a measurement of 12 hours. The details of those measurements are discussed above. In terms of final disposal it is possible to qualify the aluminium backside of the second HF cavity for unconditional release. Given that the cavities are hollow, it seems possible to cut or dismantle the second cavity to isolate the backside for unconditional clearance.

However, to make such a decision it is necessary to take more samples at many different locations in the cavity to have an exact idea of the variation of the specific activity in it and to consider whether cutting parts of the cavity is more advantageous in terms of resources. More details about this area are given below in 9.3.8.

9.3.4 Beam exit area

From the measurements it is clear that the beam exit area holds the maximum specific activity measured in the entire cyclotron and cyclotron vault. None of the 4 samples in the area indicate that the specific activity is low enough to be qualified for melting at Studsvik and obviously not for unconditional clearance. So the entire beam exit component can be assigned for melting in the United States. An advantage with this component is that this represents a small area compared with other components. Furthermore, all of the samples in the beam exit area indicate a specific activity level that makes it possible to group all the components of that area into one final disposal category. This is not the case with the deflector area, which is a much larger area and has samples that are categorized into different final disposal options. As a result it is much easier to isolate the beam exit component from the cyclotron and categorize it as an entire piece for melting at *EnergySolutions*.

Next there is the beam tube support infrastructure that stretches from the beam exit area to the switching magnet over a length of 2.40 m. The support structure is shown in Figure 61. Only the sample 045, which is located closest to the beam exit, shows a specific activity that is too high to qualify for melting at Studsvik. However, the majority of the 2.40 m long support infrastructure is qualified for melting at Studsvik as the specific activities of 46 and 047 are below 1.2 kBq/kg. Furthermore, it is easy to cut the support infrastructure into different parts corresponding to the proper category of final disposal.



Figure 61 - Beam tube support structure from beam exit to switching magnet

9.3.5 Switching magnet area

The switching magnet is a large cubic component. From the 6 samples taken at both front and back sides of the component, only one indicates a specific activity that is too high to be qualified for melting at Studsvik. It concerns sample 048, taken from the copper part at the front side of the switching magnet. The remaining two samples at the front side indicate lower specific activities that qualify for melting at Studsvik. The 3 samples at the back side show specific activities that allow for unconditional clearance. Nevertheless, there are no samples taken from the beam tubes inside the switching magnet. If the specific activity of those tubes inside the component are activated in a similar level as sample 054, taken from a beam tube further down the beam trajectory, it should be expected that those tubes are also not cleared for melting at Studsvik. To decide which final disposal option is best, it is necessary to determine to what extent it is possible to disassemble the switching magnet and to isolate the different parts for their own final disposal. When it later becomes clear that it is not feasible to disassemble the component, it is still possible to send the piece as a whole to the melting facility at *EnergySolutions*.

The sample taken at location 055, in the magnetic lens indicates that the specific activity at the top of the component is low enough to be qualified for unconditional release. However, to be sure that the lens is qualified for unconditional release, it is necessary to take more samples of the component. Next there is the beam pipe support infrastructure that stretches from the switching magnet to the wall of the cyclotron vault. The measurements of samples 056 – 058 indicate that the infrastructure cannot be released unconditionally, but it qualifies for melting at Studsvik. This is the same final disposal option as the beam pipe support structure from the beam exit to the switching magnet. Based on the results from those two identical structures, but at different locations in the cyclotron vault, it is possible to say that similar beam pipe support structures in the vault can also be categorized for melting at Studsvik.

The component that stop the beam during emergencies, located on track 2, consists out of two different parts: the stainless steel box and the solid iron block to stop the beam. The specific activity of the stainless steel box shows that it has to be categorized for melting at *EnergySolutions*. However, the solid iron block shows a specific activity range that falls between the unconditional release limit of 0.1 kBq/kg. As explained above, no risk is to be taken and as a result the solid iron can be categorized for melting at Studsvik. However, the sample taken at the front of the solid iron part is maybe not

conclusive for the whole part. The underside of the part was during the operation much closer to the beam than the front. As a result, the level of specific activity can be higher at the bottom. So to properly categorize the part into one of the scenarios for final disposal, more samples are needed in the solid iron part. In case that the final disposal category of the two parts is different, it is an easy operation to disassemble the component into two parts: the box and the solid iron block. Those two parts are respectively shown on the left and right sides of Figure 62.



Figure 62 - Box and solid iron structure to stop the beam during emergency

Also located on track two is the galvanised iron lens. The specific activity in the external part of the component is low enough to be qualified for unconditional release. However, to make sure that the internal parts of the component are also qualified to be released unconditionally, additional samples must be taken.

9.3.6 Ventilation units

All the ventilation units at the left side of the cyclotron vault have approximately the same specific activity level, as shown in Table 18. Table 22 shows that the specific activity interval of the three samples do not provide enough information to take a decision whether the unconditional clearance is allowed. Because no safety risks are to be taken, the ventilations units should be categorized for melting at Studsvik.

Table 22 - Specific activities at the ventilation units and final disposal options

Sample n°	Average specific activity [kBq/kg]	Uncertainty specific activity [kBq/kg]	Minimum value specific activity interval [kBq/kg]	Maximum value specific activity interval [kBq/kg]	Unconditional clearance OK?	Melting Studsvik OK?	Melting Energy solution OK?
062	1.09×10^{-1}	1.38×10^{-2}	9.52×10^{-2}	1.23×10^{-1}	CHECK	OK	OK
063	1.11×10^{-1}	1.49×10^{-2}	9.61×10^{-2}	1.26×10^{-1}	CHECK	OK	OK
064	1.04×10^{-1}	1.05×10^{-2}	9.35×10^{-2}	1.15×10^{-1}	CHECK	OK	OK

9.3.7 Internal target area

The specific activities of samples 066 – 068, which were taken from the stainless steel component closest to the internal target, show that the component cannot be qualified for unconditional release or melting at Studsvik. However, the specific activity is low enough to comply with the acceptance criteria for melting at *EnergySolutions*.

Sample 070 was drilled in iron 0.50 m lower and 0.59 m further away from the stainless steel part. The specific activity in this sample also indicates that melting at *EnergySolutions* is the optimal final disposal option for this part. Next there is location 071, which is located 0.70 m further away from the stainless steel block, but at the same height. The specific activity in that part of the internal target area shows a value that complies with the acceptance criteria for melting at Studsvik. This is also the case with location 072, which is at the back end of the iron component where 071 was drilled into.

However, some additional samples are needed to determine the specific activity of the iron part closer to the internal target. As the distance to the internal target becomes smaller, it is expected that the specific activity increases in the direction of the arrow shown in Figure 63. When those additional measurements show that the specific activity is too high to be accepted at Studsvik, a decision should be taken whether the part is sent as one entity to *EnergySolutions* or it is disassembled. The different parts that result from the disassembling process can then be sent separately to the different melting facilities.

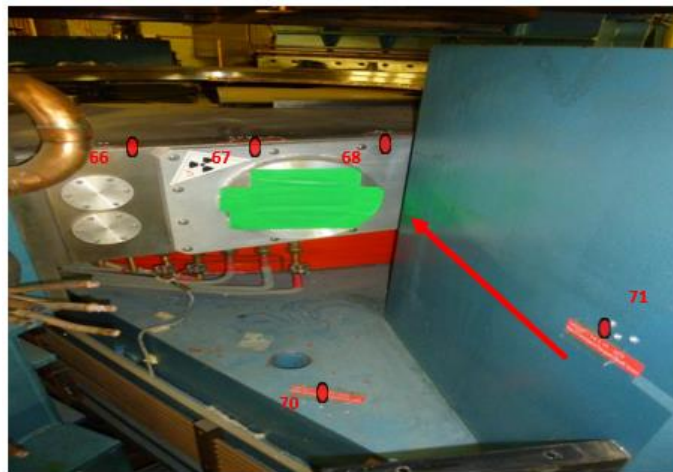


Figure 63 - Direction of additional samples at internal target area

9.3.8 High frequency cavity 1

The final component in the cyclotron vault to discuss with regard to the final disposal scenarios is the HF cavity at the left side of the cyclotron. Sample 069 taken at the most left side, indicates that the specific activity is low enough to be qualified for unconditional release. However, this sample only indicates that the back panel of the cavity is qualified to be released unconditionally. This back panel is indicated with a green arrow in Figure 64. Indicated in red is the left panel of the cavity where the samples 025 – 027 show that the most left side of left panel is to be categorized for melting at Studsvik. From those results it becomes clear that some additional samples are needed to determine the variation of the specific activity in the panels of the cavity. Based on those additional measurements it has to be decided whether the hollow cavity is cut into different pieces with regard to

their optimal final disposal option or to process and send the cavity as a whole to Studsvik. Similar to previous components, this decision depends on financial aspects and the availability of resources.

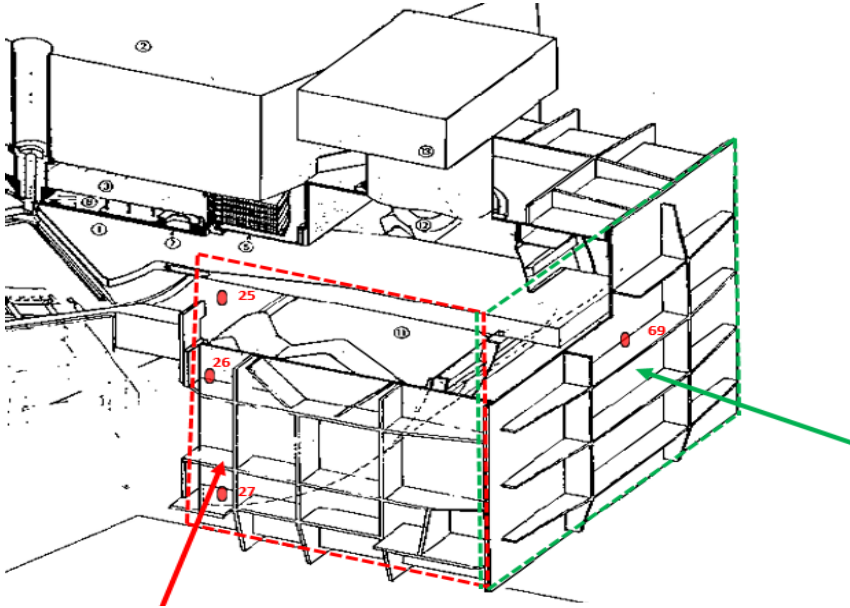


Figure 64 - HF cavity 1

9.3.9 Overview of the final disposal options

After the determination of the final disposal options for each component in the cyclotron and cyclotron vault, the following table gives an overview of what was discussed above.

Table 23 - Overview of the optimal final disposal options for each component

Area	Subarea	Unconditional release	Melting at Studsvik	Melting at EnergySolutions	Category A radioactive waste
Deflector area	Left side		X (> 0.5 m from deflector)	X (< 0.5 m from deflector)	
	Centre			X	
	Right side		X (Copper and aluminium)	X (Stainless steel plate and copper)	
	Top of cyclotron (*)		X		
Magnetic channel	/		X (Copper part)	X (Stainless steel component)	
HF cavity 2 (*)	/	X			
Beam exit area	Beam exit			X	
	Beam pipe support		X	X (Right below beam exit)	
Switching magnet area	Switching magnet (*)	X (whole backside)	X (Iron at cyclotron side)	X (Copper at cyclotron side)	
	Beam pipe support		X		
	Beam Pipe		X		
	Magnetic lens (*)	X			
	Box to block beam during emergency (*)		X (Solid iron block)	X (Stainless steel box)	

(*) Additional samples are needed in the component

Table 24 - Overview of the optimal final disposal options for each component – continued

Area	Subarea	Unconditional release	Melting at Studsvik	Melting at EnergySolutions	Radioactive category A waste
Switching magnet area	Galvanised iron lens (*)	X			
Ventilations units			X		
Internal target area (*)	/		X (iron)	X (Stainless steel and iron)	
HF cavity 1	/	X			

(*) Additional samples are needed in the component

It is worth mentioning that the optimal final disposal categories in the table above are based on the specific activities measured in the samples. For certain components, additional samples are needed to properly determine the optimal final disposal option, but the samples already taken provide good indications to define which category of final disposal is the most interesting. On the contrary, for some components the samples allow to make a clear decision with regard to final disposal and no further samples are thus required.

Based on the optimal final disposal options for each area, Figure 65 below gives a quantitative overview of the final disposal of the metallic components present in the cyclotron and cyclotron vault.

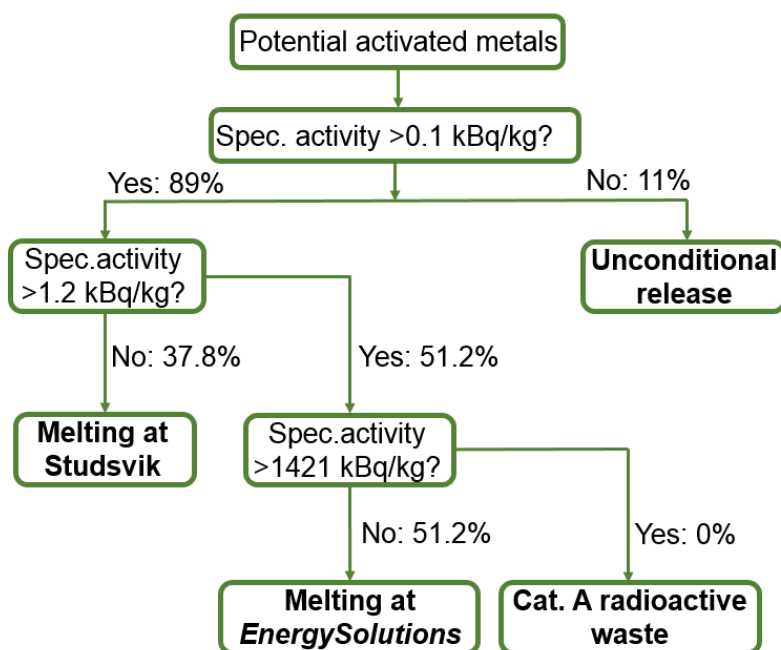


Figure 65 - Quantitative overview of the final disposal option

The figure shows that 11% of the samples taken in metallic components are potentially qualified for unconditional release in Belgium, taken into account that some of the components will need further samples to verify if the limit of 0.1 kBq/kg is not exceeded. These 11% is therefore a first quantitative indication of metallic components to be released unconditionally. From the remaining 89%, 37.8% has a specific activity that is lower than the limit for melting at Studsvik. Similar to unconditional release, these 37.8% is a first quantitative indication. This percentage could vary if the averaging method is accepted by Studsvik or when additional samples give more insight into the specific activity in certain components. The remaining 51.2% of samples are qualified for melting at *EnergySolutions*. This means that 0% of the samples give an indication that the specific activity is too high to be qualified for melting and that the component has to be treated as radioactive waste of category A. In other words, this study indicates that the dismantling of the metallic components of the cyclotron and present in the cyclotron vault will not result in direct radioactive waste of category A. However, there is some secondary radioactive waste expected from Studsvik's melting facility. As explained in 7.3.1 the residual products from the melting process (slag, dust from the ventilation filters, cutting and blasting residues) are returned back to Belgium. These residual products are probably to be treated as radioactive waste category A by ONDRAF/NIRAS.

Next to the residual melting products that will be sent back from Sweden, the metal ingots that are the final products of the melting process have to be taken into account. When the specific activity of those metal ingots is too high to be released unconditionally in Sweden (limit of 1 kBq/kg), Studsvik will temporarily store the ingots for maximum 10 years until the ⁶⁰Co is sufficiently decayed. However, when the ⁶⁰Co is not sufficiently decayed or when the weight of the stored metal ingots exceeds 20 tonnes per year, the metal ingots are also to be returned. Consequently, these metals ingots must be stored as radioactive category A waste or, if possible, to be released conditionally for reuse and recycling in the nuclear industry.

It was mentioned above that it was necessary to disassemble a component into different pieces, because the samples taken into the component or area indicate that certain pieces of the component must be categorized into different final disposal categories. Cutting or disassembling a component depends on whether there is a financial advantage and that the resources (working hours, personnel, materials, etc.) are available.

Another method that can be used when a certain component is divided in different final disposal categories is to work with the average specific activity in that component. Figure 66 below shows an example of a component that is divided into two zones of specific activity. The left zone has specific activity of 0.7 kBq/kg and the right one 1.3 kBq/kg. This means that the right zone is not allowed for melting at Studsvik. Consequently the average specific activity of the block is 1 kBq/kg. This average value is in accordance with acceptance limit of Studsvik. However, in reality the component geometry is much more complicated and such an averaging method must be discussed with Studsvik for approval.

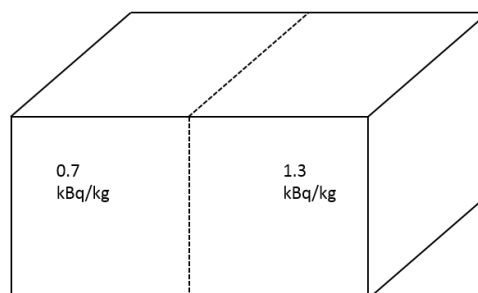


Figure 66 - Example of method to average specific activity

Up to now, the value of 1.2 kBq/kg was treated as the upper limit not to be exceeded for the acceptance of activated metals at Studsvik. However, this limit is maintained for routine acceptance procedures. In reference [41] Studsvik specifies that higher specific activity values are discussable for acceptance. When it later becomes clear that Studsvik will accept higher activated metallic components from the cyclotron vault, more components can be sent to Sweden. This must only be taken into consideration when there is a financial advantage in comparison with sending the higher activated materials to *EnergySolutions*.

If Studsvik decides to accept higher activated materials, it has to be taken into account that more metal ingots can be sent back from Sweden because they have specific activities that are still too high for unconditional release in Sweden or to be temporarily stored at Studsvik. Those metal ingots that are sent back could possibly increase the overall cost because they will likely to be treated in Belgium as radioactive category A waste.

9.3.10 Additional acceptance criteria for final disposal options

As discussed in chapter 7 Final disposal, there are also other acceptance criteria to be taken into account next to the specific activity of ^{60}Co with regard to the final disposal options.

Firstly, it has to be verified that for the components that are qualified for unconditional release the effective dose per year that a civilian would receive from the release of the component is not exceeding 10 $\mu\text{Sv/a}$. Furthermore, it has to be verified that the annual collective dose does not exceed 1 man-sievert. These doses have to be verified when the components are isolated from the cyclotron. Next, it is necessary to perform a surface contamination measurement if the components will later be manipulated. As all the components that were sampled during this study were already decontaminated and cleaned, no further contamination is expected. This is also valid for the acceptance criteria of Studsvik and *EnergySolutions* with regard to a fixed or removable contamination.

For components that will be sent to Studsvik, it must be verified that the surface dose rate in contact with the part does not exceed 0.2 mSv/h and that hotspots are smaller than 0.5 mSv/h. Components that are qualified for melting at Studsvik have typical surface dose rate values of the order of $\mu\text{Sv/h}$. However these values are measured in the cyclotron vault where there is a large interference from the surroundings. When the dismantling will start and the components will be disassembled and isolated, their surface dose rate should be checked again. In its acceptance criteria, Studsvik mentions that metallic pieces larger than 0.6 m diameter/width and 1.2 m length need segmentation. Some parts from the cyclotron will exceed those dimensions, but Studsvik offer to do the segmentation in Sweden prior to melting. Studsvik also specifies that galvanised materials are not allowed to be melted. The beam focus lens is the only component in the cyclotron vault that is made out of galvanised iron. As mentioned before, the samples taken from this component give a first indication that it can be released unconditionally. However, more samples from inside the component are needed and these can indicate that the specific activity is too high to be qualified for unconditional release. The acceptance of the galvanised iron can always be discussed with Studsvik, otherwise it must be sent to *EnergySolutions*.

Finally there are the acceptance criteria of *EnergySolutions*. They specify that non-ferrous metals are not accepted to be melted. However, *EnergySolutions* mentions that a case-by-case study of accidental quantities of these materials is always possible. This means that copper components can be accepted. The same is valid for aluminium parts. Similar to the melting facility at Studsvik, *EnergySolutions* sets a limit of 200 $\mu\text{Sv/h}$ for the surface dose rate of the metallic components. Certain components of the

cyclotron that are considered to be sent to *EnergySolutions* exceed this limit. These cases have to be discussed with the melting facility otherwise they have to be considered as category A radioactive waste.

10 Conclusion and future work

10.1 Conclusions

This study's focus was on the radiological characterization of internal and external metallic components present in the cyclotron and cyclotron vault. The measurements performed in this study gave insight into the radionuclides present as a result of activation in the different components. They also serve as a first indication of the specific activity of those radionuclides into these components. Based on those measurements it was possible to determine the current optimal final disposal option for each metallic component that was sampled.

Based on 5 different parameters, 82 samples were taken from different metallic components present in the cyclotron and the cyclotron vault. An additional 3 samples were drilled from the concrete shield surrounding the accelerator. All of the samples were measured in the same geometry with a HPGe detector. The only radionuclide that was identified in the 82 metallic samples was ^{60}Co . However, the concrete samples contain besides ^{60}Co ($t_{1/2} = 5.27$ a) also ^{152}Eu ($t_{1/2} = 13.33$ a).

So, after more than 20 years of inactivity, ^{60}Co is the only radionuclide that is still detectable as a result from the activation during the operation of the cyclotron. All of the other radionuclides in the metallic pieces are fully decayed and are not detectable anymore. Owing to circumstances, the cyclotron is an example of the dismantling strategy 'storage under surveillance', although it was not the intention to implement this strategy. However, the period of 20 years was enough to decay all of the radionuclides, except one: ^{60}Co . This makes the radiological characterization and the dismantling easier, because only one radionuclide has to be taken into account.

A small part of the samples was taken from components near the proton beam where proton induced nuclear reactions were possible. However, the presence of ^{60}Co in the components all over the cyclotron vault is mainly the result of activation through secondary neutron reactions. The specific activity of the ^{60}Co varies between non-detectable and 328 kBq/kg. Based on those specific activities, three hotspots were identified in the cyclotron: the deflector area, the beam exit area and the internal target area.

Finally, based on the specific activities measured in the samples, 4 different disposal scenarios were elaborated: unconditional release, melting at Studsvik, melting at *EnergySolutions* and disposal as radioactive category A waste. 11% of the samples show a specific activity that is lower than 0.1 kBq/kg. So those samples give the indication that those components can be qualified for unconditional reuse and recycling. The remaining 89% can be sent to Studsvik and *EnergySolutions* to be melted. The metallic samples give a first indication that none of the components present in the cyclotron vault are to be disposed of as radioactive category A waste. However, secondary wastes and metal ingots with specific activities too high to be released unconditionally, can be returned from Studsvik after melting.

10.2 Recommendations and future work

During this study some components, materials and areas in the vault were excluded. In what follows, an overview is given of recommendations for future research with regard to the radiological characterization and the preparation of the dismantling of the CGR-MEV cyclotron.

First of all, some areas of the cyclotron and cyclotron were not sampled, because some of those areas were difficult to access or are still contaminated. An example of such a contaminated area is the centre of the cyclotron in which the particles were accelerated. Due to the contamination it was not justified in terms of radiological protection to sample that area. Therefore it was not possible to sample the copper septum, which is part of the deflector, the dees and the bending magnets. Once those parts will also have been decontaminated it will be possible to characterize them. It is expected that high levels of activation will be found in this centre area of the accelerator, especially in the copper septum. The levels of specific activity are expected to be in the same order of the specific activity (328 kBq/kg) measured in the copper ring at the beam exit. For future studies it will also be interesting to take samples of these components at different distances from the ion source to the outside of the orbital trajectory. Because one sample was already taken from the top of the accelerator, it is interesting to see if the level of specific activity (0.311 kBq/kg) is comparable with different materials in the basement under the cyclotron. In that basement, there are also a lot of different metallic parts present that need to be characterized and categorized into an optimal final disposal option. Based on the measurements that were carried out for this study, it is expected that ^{60}Co will also be the only present radionuclide – as a result from activation – in the metallic parts that were not yet sampled.

Another interesting area to take samples of, is the structure on which the internal target was connected. This area is shown below in Figure 67. It is recommended to take samples from the yellow support structure as well from the tube at different distances.



Figure 67 - Structure on which the internal target was mounted

Beside metallic components, there are also parts made out of PVC, rubber, etc. Those parts were excluded from the study, but to perform a full radiological characterization of the cyclotron vault as a preparation for the dismantling, these components must be included in future studies.

Concrete is a material that is abundantly present in the cyclotron vault. As the focus was on the metallic components, the concrete walls were not considered for characterization in this study. However, as mentioned in 9.1.2, three samples were taken at three different locations in the concrete walls surrounding the accelerator (see Figure 25). In those three samples, ^{152}Eu and ^{60}Co were identified. The specific activities of these identified radionuclides are given below in Figure 68. The graph shows that ^{152}Eu is the dominant radionuclide in the concrete. Samples 074 and 075 show a larger quantity of ^{152}Eu in comparison with sample 073. This could be due to the position of the samples, as shown in Figure 25. 073 was taken the furthest from the cyclotron with several components in between. Sample 074 was taken in the concrete wall the closest to the deflector with nothing in between. This could explain the fact that the specific activity in 074 is slightly higher than in 075, which was also taken close to the deflector, but with the HF cavity 1 in between. Based on the values it is possible to conclude that the specific activity of ^{60}Co is below the limit for unconditional release (0.1 kBq/kg), but the levels of ^{152}Eu are too high for the concrete to be released unconditionally.

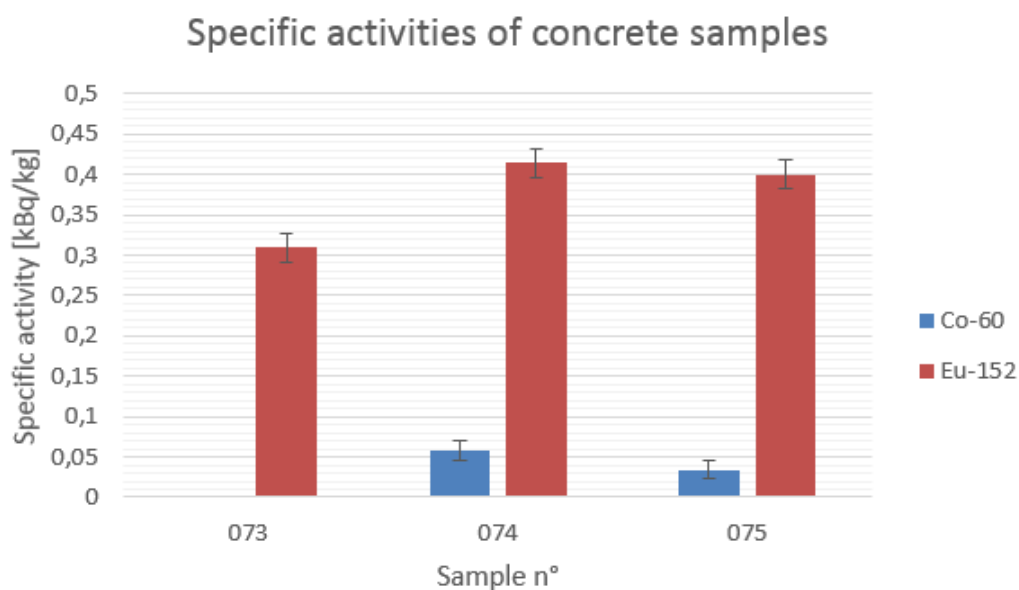


Figure 68 - Specific activities of the concrete samples

The three samples were only drilled in the surface of the concrete walls with an average depth of 5.3 cm. To properly characterize all of the concrete walls in the cyclotron vault it is necessary to take samples at different locations in the vault, at different heights and at different depths. Nevertheless, the 3 samples already serve as a good indication of the radionuclides present in the concrete and the order of specific activities. Finally, disposal scenarios for the activated concrete have to be determined when the dismantling operations start.

As mentioned in 9.3, additional samples of some components are necessary to determine the optimal final disposal option. The samples that were already taken from the components are a good indication which category of final disposal is the most interesting. Table 25 gives an overview of these components.

Table 25 - Components that need additional sampling

Top of cyclotron	HF cavity 2
HF cavity 1	Switching magnet
Magnetic lens	Box to block beam during emergency
Galvanised iron lens	Internal target area

Because the inventory of components intended for each final disposal category is not complete yet, it is difficult to give an overview of the cost to process the activated wastes that will be produced during the dismantling of the cyclotron and cyclotron vault. A document of ONDRAF/NIRAS claims that the cost for melting is in the order of 5 to 20 €/kg [58]. However, the tariffs of Studsvik and *EnergySolutions* can be higher when case-by-case studies must be done. For instance higher measured specific activities than mentioned in the acceptance criteria, types of metals that normally are not accepted in large quantities, etc. The tariff for disposal of the radioactive wastes category A in a surface repository is approximately 37 000 €/m³ [59]. As it is not yet known which quantities of secondary wastes or metal ingots will be returned from Studsvik, it is difficult to make a estimation of the cost for disposal of the radioactive category A wastes. Furthermore, it is recommended to investigate if there is a possibility to release conditionally some of the activated materials in the nuclear industry

Finally, some of the sampled components have specific activities that are just above the Belgian limit for unconditional release. For instance the ventilations units (sample 062 – 064). They have been categorized for melting at Studsvik, but a suggestion could be to wait until the specific activity is below the limit. The time needed for this is calculated below, starting from the maximum value of the specific activity range.

$$A = A_0 \times e^{-\lambda \Delta t}$$

$$0.126 \frac{\text{kBq}}{\text{kg}} = 0.1 \frac{\text{kBq}}{\text{kg}} \times e^{-\frac{\ln(2)}{5.2a} \Delta t}$$

$$\Delta t = \frac{\ln\left(\frac{0.126 \frac{\text{kBq}}{\text{kg}}}{0.1 \frac{\text{kBq}}{\text{kg}}}\right)}{\frac{\ln(2)}{5.2a}}$$

$$\Delta t = 2 a$$

So after maximum 2 years it is possible to release the ventilations units unconditionally, which is cheaper than melting at Studsvik or *EnergySolutions*. The possibility of this option depends on the dismantling strategy of ONDRAF/NIRAS. Table 26 gives an overview of the samples of which the maximum value of the specific activity range is low enough to decay under the limit of 0.1 kBq/kg within 5 years. If the dismantling operation starts later than the values given in the table, these components will be qualified for unconditional release at the time the dismantling starts. Otherwise it is possible to store these parts temporarily to let the ⁶⁰Co decay.

Table 26 - Components with decay times to 0.1 kBq/kg lower than 5 years

Sample ID	component	Upper value of specific activity range (kBq/kg)	time to decay to 0.1 kBq/kg (years)
033	Left side deflector area	1.53×10^{-1}	3
049	Switching magnet	1.52×10^{-1}	3
059	Box to block beam	1.28×10^{-1}	2
062	Ventilation unit	1.23×10^{-1}	2
063	Ventilation unit	1.26×10^{-1}	2
064	Ventilation unit	1.15×10^{-1}	1

References

- [1] ONDRAF/NIRAS, “1982-2012 L'ONDRAF a trente ans,” 2012.
- [2] ONDRAF/NIRAS, “Nationale instelling voor radioactief afval en verrijkte splijtstoffen,” [Online]. Available: <http://www.niras.be/content/nationale-instelling-voor-radioactief-afval-en-verrijkte-splijtstoffen>. [Accessed 13 February 2015].
- [3] ONDRAF/NIRAS, “Opdrachten,” [Online]. Available: <http://www.niras.be/content/opdrachten>. [Accessed 15 February 2015].
- [4] ONDRAF/NIRAS, “Stroomopwaarts' beheer,” [Online]. Available: <http://www.niras.be/content/stroomopwaarts-beheer>. [Accessed 17 February 2015].
- [5] ONDRAF/NIRAS, “Courant beheer,” [Online]. Available: <http://www.niras.be/content/courant-beheer>. [Accessed 17 February 2015].
- [6] ONDRAF/NIRAS, “NIRAS en Belgoproces investeren in de Kempen,” [Online]. Available: <http://www.niras.be/content/niras-en-belgoproces-investeren-de-kempen-0>. [Accessed 17 February 2015].
- [7] NIRAS/ONDRAF, “ONDRAF/NIRAS and its main partners,” in *ONDRAF/NIRAS, responsible management of radioactive waste*, 2012, p. 23.
- [8] ONDRAF/NIRAS, “Beheer op lange termijn,” [Online]. Available: <http://www.niras.be/content/beheer-op-lange-termijn>. [Accessed 17 February 2015].
- [9] K. S. Krane, “15.2 Cyclotron accelerators,” in *Introductory Nuclear Physics*, United States of America, John Wiley & Sons, 1988, pp. 571-581.
- [10] Daesalus Isodar, “Cyclotrons,” [Online]. Available: <http://www.nevis.columbia.edu/daedalus/exp/cyclo.html>. [Accessed 27 February 2015].
- [11] IAEA, “Radiopharmaceutical Production: Cyclotron basics,” 2011. [Online]. Available: http://www.iaea.org/googleResult.html?cx=004828748078731094376%3Am_jpm98tdns&cof=FORID%3A11&q=cyclotron+basics&submit.x=0&submit.y=0&submit=Search. [Accessed 27 February 2015].
- [12] IAEA, “Directory of Cyclotrons used for Radionuclide Production in Member States,” IAEA, Austria, 2006.
- [13] M. Braeckeveldt, “Hergebruik en recyclage van ijzer/staal en beton afkomstig van de ntmanteling van nucleaire installaties in België,” Katholieke Universiteit Leuven Faculteit Toegepaste Wetenschappen Centrum Nucleaire Techniek, Leuven, 1994-1995.
- [14] V. Massaut, “Nuclear Reactor Decommissioning? Yes we can!,” SCK•CEN, 2014.
- [15] World Nuclear Association, “Decommissioning Nuclear Facilities,” 2015. [Online]. Available: <http://www.world-nuclear.org/info/Nuclear-Fuel-Cycle/Nuclear-Wastes/Decommissioning-Nuclear-Facilities/>. [Accessed 5 April 2015].
- [16] M. Hotat, I. Verstraeten and J. Cantarella, “Plan de Déclassement initial: Révision 2004,” 2004.
- [17] IRE, “Inhuldiging van het eerste productiecyclotron van het Nationaal Instituut voor Radio-Elementen (I.R.E.),” *Revue IRE tijdschrift*, vol. Vol.7 N°4, p. 29, 1983.
- [18] NIRAS, “Annexe 1 - Historique casemate CGR,” Fleurus.
- [19] European Commission Nuclear Safety and the Environment, “Evaluation of the Radiological and Economic Consequences of Decommissioning Particle Accelerators,” Vrij Universiteit Brussel Cyclotron department, Brussel, 1999.

- [20] B. Craybeck, "Premières contributions à l'étude du déclassement des accélérateurs," Université catholique de Louvain, 1991-1992.
- [21] NIRAS/ONDRAF, "Rapports de production - cyclotron CGR (du 23/03/01987 au 15/09/1993)," 2014.
- [22] Nederlands-Normalisatie-instituut, "Kernwetenschappen en kerntechniek," in *Termen en definities*, 1985, p. 115.
- [23] K. S. Krane, "Nuclear reactions," in *Introductory Nuclear Physics*, United States of America, John Wiley & Sons, 1988, pp. 378-379.
- [24] R. E. Cohen and P. Giacomo, "Nomenclature conventions in nuclear physics," in *Symbols, units, nomenclature and fundamental constants in physics*, Sèvres, France, 1987, p. 16.
- [25] K. S. Krane, "Radioactive decay," in *Introductory Nuclear Physics*, United States of America, John Wiley & Sons, 1988, p. 16.
- [26] H. Janssens, "Kernreacties," in *Industriële ingenieurswetenschappen: 2691 Kernfysica en stralingsfysica*, Hasselt, 2013-204, pp. 1-64.
- [27] N. Soppera, E. Dupont and M. Bossant, JANIS Book of proton-induced cross-section, OECD NEA Data Bank, 2012.
- [28] K. S. Krane, "Neutron Physics," in *Introductory Nuclear Physics*, United States of America, John Wiley & Sons, 1988, p. 445.
- [29] K. Holbert, "EEE 562 Nuclear Reactor Theory and Design," 22 June 2011. [Online]. Available: <http://holbert.faculty.asu.edu/eee562/ThermalNeutronFlux.pdf>. [Accessed 17 March 2015].
- [30] K. Mukhin, Experimental Nuclear Physics, Vol.I: Physics of Atomic Nucleus, Moscow: Mir Publishers, 1987.
- [31] N. Soppera, E. Dupont and M. Bossant, JANIS Book of neutron - induced cross sections, OECD NEA Data Bank, 2012.
- [32] ONDRAF/NIRAS, "Annexe 1 - Historique casemate CGR," Fleurus.
- [33] MIT Department of Civil and Environmental Engineering, "Chemical Composition of Structural Steels," 1999. [Online]. Available: <http://web.mit.edu/1.51/www/pdf/chemical.pdf>. [Accessed 19 March 2015].
- [34] The London Metal Exchange, "Special Contract Rules for High Grade Primary Aluminium," [Online]. Available: <http://www.lme.com/~media/Files/Branding/Chemical%20composition/Non%20ferrous/Chemical%20composition%20-%20aluminium.pdf>. [Accessed 21 March 2015].
- [35] N. Soppera, E. Dupont and M. Bossant, JANIS Book of neutron - induced cross sections, OECD NEA Data Bank, 2012.
- [36] S. Nijst, "Masterproef: Improving the radionuclide Inventory Determination of the Irradiated Graphite from BR1 in Mol," Faculteit industriële wetenschappen, UHasselt, 2013-2014.
- [37] JURION, "Koninklijk besluit van 30 maart 1981 houdende bepaling van de opdrachten en de werkingsmodaliteiten van de openbare instelling voor het beheer van radioactief afval en splijtstoffen," 30 March 1981. [Online]. Available: <http://www.jurion.fanc.fgov.be/jurdb-consult/consultatieLink?wettekstId=7460&appLang=nl>. [Accessed 28 March 2015].
- [38] JURION, "20/07/01 ARBIS - Bijlage IB, Koninklijk besluit van 20 juli 2001 houdende algemeen reglement op de bescherming van de bevolking, van de werknemers en het leefmilieu tegen het gevaar van de ioniserende stralingen," 20 July 2001. [Online]. Available: <http://www.jurion.fanc.fgov.be/jurdb-consult/consultatieLink?wettekstId=7460&appLang=nl>. [Accessed 29 March 2015].

- [39] IAEA, “Technical Report Series no. 462, Managing Low Radioactivity Material from the Decommissioning of Nuclear Facilities,” IAEA, Austria, 2008.
- [40] Studsvik Nuclear AB, “Containerized Scrap: Steel, Aluminium, Copper and Brass,” 2007.
- [41] B. Wirendal, A. Stenmark and G. Krause, “Metallic Scrap Acceptance Criteria,” 2009.
- [42] Bruce Stephenson Energy Solutions, “International Radioactive Material Acceptance Guidelines,” 2012.
- [43] The engineering toolbox, “Metals and Alloys - densities,” [Online]. Available: http://www.engineeringtoolbox.com/metal-alloys-densities-d_50.html. [Accessed 13 March 2015].
- [44] EnergySolutions, “Waste Management Facilities,” [Online]. Available: <http://www.energysolutions.com/waste-management/facilities/>. [Accessed 2 April 2015].
- [45] NIRAS/ONDRAF, “Our mission? To protect you,” in *ONDRAF/NIRAS, responsible management of radioactive waste*, 2012, p. 23.
- [46] NIRAS/ONDRAF, “cAt; Berging categorie A-afval,” 2011. [Online]. Available: <http://www.niras-cat.be/nl/getpage.php?i=26>. [Accessed 3 April 2015].
- [47] ONDRAF/NIRAS, “cAt - Berging categorie A-afval,” 2011. [Online]. Available: <http://www.niras-cat.be/nl/getpage.php?i=26>. [Accessed 3 April 2015].
- [48] NIRAS/ONDRAF, “Acceptatiecriteria en erkenningen,” [Online]. Available: <http://www.niras.be/content/acceptatiecriteria-en-erkenning>. [Accessed 3 April 2015].
- [49] (NIRAS/ONDRAF), Joris Lenssens, “ACRIA-NGA-A14/A24,” NIRAS, 2008.
- [50] Joris Lenssens (NIRAS/ONDRAF), “ACRIA-NGA-A17/A27,” NIRAS/ONDRAF, 2008.
- [51] I. Rittersdorf, “Gamma Ray Spectroscopy,” 2007.
- [52] Canberra Industries inc, “Extended Range Coaxial Ge detectors (XtRa),” 2013.
- [53] T. Shiomi, Y. Azeyanagi, A. Yamadera and T. Nakamura, “Measurement of Residual Radioactivity of Machine Elements,” *Journal of Nuclear Science and Technology*, vol. 37, no. Sup 1, pp. 357-361, 2000.
- [54] Canberra industries Inc., The Genie 2000 Customization Tools Manual - ICN 9233653G, United States of America, 2006.
- [55] L. Ekström, S. Chu and R. Firestone, “The Lund/LBNL Nuclear Data Search,” February 1999. [Online]. Available: <http://nucleardata.nuclear.lu.se/toi/index.asp>. [Accessed February 2015].
- [56] CERCA LEA, “Calibration Certificate N° CT/140626/14/1382,” 2014.
- [57] J. Magill, G. Pfennig, R. Dreher and Z. Soti, “Karlsruher Nuklidekarte,” Nucleonica, Germany, 2012.
- [58] R. S. (ONDRAF/NIRAS), “Missies/Taken NIRAS/ONDRAF i.v.m. Ontmanteling Installaties Klasse IIa,” Brussels, 2014.
- [59] ONDRAF/NIRAS, “Dekking van de kosten van het courant beheer,” ONDRAF/NIRAS, [Online]. Available: <http://www.niras.be/content/dekking-van-de-kosten-van-het-courant-beheer>. [Accessed 16 May 2015].

List of appendices

Appendix 1: unconditional release levels of radionuclides113
Appendix 2: certificate multi-gamma calibrations source.....115
Appendix 3: radioactive decay chains of naturally occurring radionuclides.....119

Appendix 1: Unconditional release levels of radionuclides

Table 27 - Release levels of radionuclides [38]

Nuclide ⁽¹⁾	Clearance levels f, l [kBq/kg]	Nuclide ⁽¹⁾	Clearance levels f, l [kBq/kg]	Nuclide ⁽¹⁾	Clearance levels f, l [kBq/kg]	Nuclide ⁽¹⁾	Clearance levels f, l [kBq/kg]	Nuclide ⁽¹⁾	Clearance levels f, l [kBq/kg]	Nuclide ⁽¹⁾	Clearance levels f, l [kBq/kg]
H-3	100	Sr-90+	1	Tc-132+	0.1	Hf-181	1	Th-234+	10	Cf-251	0.1
Be-7	10	Y-90	100	Tc-134	0.1	Ta-182	0.1	Po-230	1	Cf-252	0.1
C-14	10	Y-91	10	I-125	1	W-181	10	Pa-231	0.01	Cf-253	1
Na-22	0.1	Zr-93	10	I-126	1	W-185	100	Po-233	1	Cf-254	0.1
P-32	100	Zr-95+	0.1	I-129	0.1	Rc-186	10	U-230+	1	Es-253	1
P-33	100	Nb-93m	100	I-131	1	Os-185	1	U-231	10	Es-254+	0.1
S-35	100	Nb-94	0.1	Cs-129	1	Os-191	10	U-232+	0.1	Es-254m+	1
Cl-36	1	Nb-95	1	Cs-131	1000	Os-193	10	U-233	1		
K-40	1	Mo-93	10	Cs-132	1	Ir-190	0.1	U-234	1		
Ca-45	100	Mo-93+	1	Cs-134	0.1	Ir-192	0.1	U-235+	1		
Ca-47	1	Tc-96	0.1	Cs-135	10	Pt-191	1	U-236	1		
Sc-46	0.1	Tc-97	10	Cs-136	0.1	Pt-193m	100	U-237	10		
Sc-47	10	Tc-97m	10	Cs-137+	1	Au-196	1	U-238+	1		
Sc-48	0.1	Tc-99	1	Ba-131	1	Au-198	10	Np-237+	0.1		
V-48	0.1	Ru-97	1	Ba-140	0.1	Hg-197	10	Np-239	1		
Cr-51	10	Ru-103+	1	La-140	0.1	Hg-203	1	Pu-236	0.1		
Mn-52	0.1	Ru-106+	1	Ce-139	1	Tl-200	1	Pu-237	10		
Mn-53	1000	Rh-105	10	Ce-141	10	Tl-201	10	Pu-238	0.1		
Mn-54	0.1	Pd-103+	1000	Ce-143	1	Tl-202	1	Pu-239	0.1		
Fe-55	100	Ag-105	1	Ce-144+	10	Tl-204	10	Pu-240	0.1		
Fe-59	0.1	Ag-108m+	0.1	Pr-143	100	Pb-203	1	Pu-241	1		
Co-56	0.1	Ag-110m+	0.1	Nd-147	10	Pb-210+	0.01	Pu-242	0.1		
Co-57	1	Ag-111	10	Pm-147	100	Pb-206	0.1	Pu-244+	0.1		
Co-58	0.1	Cd-103+	10	Pm-149	100	Bi-207	0.1	Am-241	0.1		
Co-60	0.1	Cd-115+	1	Sm-151	100	Bi-210	10	Am-242m+	0.1		
Ni-59	100	Cd-115m+	10	Sm-153	10	Po-210	0.01	Am-243+	0.1		
Ni-63	100	In-111	1	Eu-152	0.1	Ra-223+	1	Cm-242	1		
Zn-65	1	In-114m+	1	Eu-154	0.1	Ra-224+	1	Cm-243	0.1		
Ge-71	10000	Sn-113+	1	Eu-155	10	Ra-225	1	Cm-244	0.1		
As-73	100	Sn-125	1	Gd-153	10	Ra-226+	0.01	Cm-245	0.1		
As-74	1	Sb-122	1	Tb-160	0.1	Ra-228+	0.01	Cm-246	0.1		
As-76	1	Sb-124	0.1	Dy-166	10	Ac-227+	0.01	Cm-247+	0.1		
As-77	100	Sb-125+	1	Ho-166	10	Th-227	1	Cm-248	0.1		
Se-75	1	Tc-123m	1	Er-169	100	Th-228+	0.1	Bk-243	10		
Br-82	0.1	Tc-125m	100	Tm-170	10	Th-229+	0.1	Cf-246	10		
Rb-86	10	Tc-127m+	10	Tm-171	100	Th-230	0.1	Cf-248	1		
Sr-85	1	Tc-128m+	10	Yb-175	10	Th-231	100	Cf-249	0.1		
Sr-89	10	Tc-131m+	0.1	Lu-177	10	Th-232+	0.01	Cf-250	0.1		

The radionuclides marked with an +, means that the daughter nuclides are taken into account in the release level. [38]

Appendix 2: certificate multi-gamma calibration source



CHAINE D'ETALONNAGE

RAYONNEMENT IONISANT
IONIZING RADIATION

LABORATOIRE D'ETALONNAGE ACCREDITE
ACCREDITED CALIBRATION LABORATORY

ACCREDITATION N° 2-1529

CERCA LEA

LEA Laboratoire Etalons d'Activité
Site du Tricastin
B.P. 75 - 28701 Pierrelatte Cedex
Tél. : (33) 04 75 96 56 00
Fax : (33) 04 75 96 56 40
Internet : www.lea-cerca.com
CERCA, filiale de AREVA NP

COMMANDE : BE30842-01 / 29.07.2014

Order :

CERTIFICAT D'ETALONNAGE CALIBRATION CERTIFICATE N° CT/140626/14/1382

DELIVRE A : **CANBERRA BENELUX N.V. / S.A.**
ISSUED FOR : 1731 ZELLIK

INSTRUMENT ETALONNE
CALIBRATION INSTRUMENT

Désignation : **ETALON MULTIGAMMA SOLUTION**
Designation : MULTIGAMMA STANDARD SOLUTION

Constructeur : **L.E.A.**
Manufacturer :

Type : **9ML01ELMA[60]**
Type :

N° d'identification : **7962/9**
Identification number

Ce certificat comprend **3 pages**
This certificate includes pages

Date d'émission : **06/10/2014**
Date of issue : day/month/year

LE RESPONSABLE DU LABORATOIRE
THE HEAD OF THE LABORATORY


Laetitia MARCHAND
CERCA LEA



LA REPRODUCTION DE CE CERTIFICAT N'EST AUTORISEE QUE
SOUS LA FORME DE FAC-SIMILE PHOTOGRAPHIQUE INTEGRAL
THIS CERTIFICATE MAY NOT BE REPRODUCED OTHER THAN IN
FULL BY PHOTOGRAPHIC PROCESS

1 Means and methods

Type of calibration	Photon flux
Unit	s ⁻¹
Detector used	Solid state detectors Ge-HP (N)
Reference of the measurement equipment	CSGHP1/5
Method employed	γ-ray spectrometer

The environmental conditions have no influence on the results of the measurement.

2 Nominal characteristics delivered standards

Reference	Multigamma reference : 9ML01ELMA60, N° 7962/9
Type of container(*)	A
Daughter products	¹¹³ In ^m , ¹⁰⁹ Ag ^m , ¹³⁷ Ba ^m
Volume	1 cm ³
Density	1,016 g.cm ⁻³
Chemical composition	Chloride of each component + EuCl ₃ for ²⁴¹ Am in HCl 1N
Reference date	24/11/2014 at 12 h UTC
Classification	No sealed source
No surface contamination (**)	Wipe test : 10/09/2014 OK
Operator	E. ARMAING

(*) See product characteristics in LEA catalogue (www.lea-cerca.com).

(**) According to NF M61-003 / ISO 9978.

Only the original copy is valid.

1 Means and methods

Type of calibration	Photon flux
Unit	s ⁻¹
Detector used	Solid state detectors Ge-HP (N)
Reference of the measurement equipment	CSGHP1/5
Method employed	γ-ray spectrometer

The environmental conditions have no influence on the results of the measurement.

2 Nominal characteristics delivered standards

Reference	Multigamma reference : 9ML01ELMA60, N° 7962/9
Type of container(*)	A
Daughter products	¹¹³ In ^m , ¹⁰⁶ Ag ^m , ¹³⁷ Ba ^m
Volume	1 cm ³
Density	1,016 g.cm ⁻³
Chemical composition	Chloride of each component + EuCl ₃ for ²⁴¹ Am in HCl 1N
Reference date	24/11/2014 at 12 h UTC
Classification	No sealed source
No surface contamination (**)	Wipe test : 10/09/2014 OK
Operator	E. ARMAING

(*) See product characteristics in LEA catalogue (www.lea-cerca.com).
 (**) According to NF M61-003 / ISO 9978.

Only the original copy is valid.

3 Results

3-1 Photonic flux

Standard multigamma type : 9ML01ELMA60, reference : 7962/9				
Radionuclide	Energy in keV(***)	Number of photons per 100 disintegrations (***)	Photonic flux in $s^{-1} g^{-1}$ 4II sr	Extended relative uncertainty (k=2, %)
²⁴¹ Am	59,5409 ± 0,0001	35,92 ± 0,17	1,138E+04	± 4
¹⁰⁹ Cd	88,0336 ± 0,0001	3,626 ± 0,026	1,009E+04	± 5
⁵⁷ Co	122,06065 ± 0,00012	85,51 ± 0,06	1,334E+04	± 3
⁵⁷ Co	136,47356 ± 0,00029	10,71 ± 0,15	1,671E+03	± 4
¹³⁹ Ce	165,8575 ± 0,0011	79,90 ± 0,04	1,314E+04	± 3,5
⁵¹ Cr	320,0835 ± 0,0004	9,89 ± 0,02	2,32E+04	± 4,5
¹¹³ Sn	391,698 ± 0,003	64,97 ± 0,17	3,00E+04	± 4
⁸⁵ Sr	514,0048 ± 0,0022	98,5 ± 0,4	4,82E+04	± 3,5
¹³⁷ Cs	661,657 ± 0,003	84,99 ± 0,2	5,17E+04	± 3
⁸⁸ Y	898,036 ± 0,004	93,90 ± 0,23	9,03E+04	± 3
⁶⁰ Co	1173,228 ± 0,003	99,85 ± 0,03	8,77E+04	± 3
⁶⁰ Co	1332,492 ± 0,004	99,9826 ± 0,0006	8,78E+04	± 3
⁸⁸ Y	1836,052 ± 0,013	99,32 ± 0,03	9,55E+04	± 3

(***)Values recommended by the LNHB (<http://www.nucleide.org>).

3-2 Specific activity by radionuclide

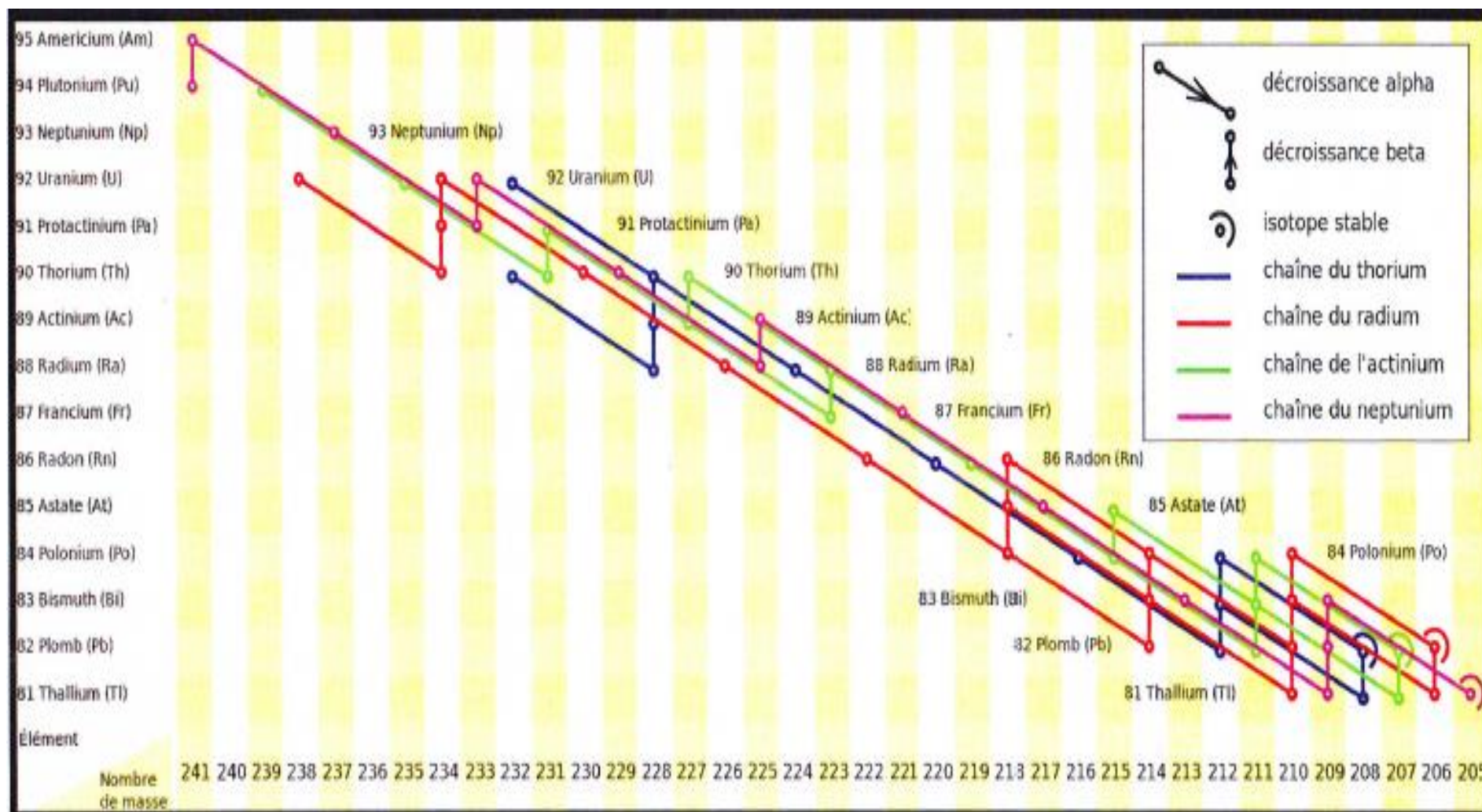
Radionuclide	Specific activity (kBq.g ⁻¹)	Extended relative uncertainty (k=2, %)
Americium 241	3,17E+01	± 4
Cadmium 109	2,78E+02	± 5
Cobalt 57	1,560E+01	± 3
Cerium 139	1,645E+01	± 4
Chromium 51	2,35E+02	± 4,5
Tin 113	4,62E+01	± 4
Strontium 85	4,89E+01	± 3,5
Cesium 137	6,08E+01	± 3
Cobalt 60	8,78E+01	± 3
Yttrium 88	9,62E+01	± 3

The extended uncertainties mentioned are those corresponding to two incertitude composed type. The uncertainties types have been calculated taking into account the different uncertainties components: reference standards, means if calibration, environmental conditions, the data of the calibrated instrument, repeatability...

The delivery of a certificate calibration with logotype COFRAC guarantees the traceability of the calibration results according to the international unity system.

Only the original copy is valid.

Appendix 3: radioactive decay chains of naturally occurring radionuclides



Auteursrechtelijke overeenkomst

Ik/wij verlenen het wereldwijde auteursrecht voor de ingediende eindverhandeling:

Radiological characterization of a cyclotron in view of its dismantling and final disposal

Richting: **master in de industriële wetenschappen: nucleaire technologie-nucleaire technieken / medisch nucleaire technieken**

Jaar: **2015**

in alle mogelijke mediaformaten, - bestaande en in de toekomst te ontwikkelen - , aan de Universiteit Hasselt.

Niet tegenstaand deze toekenning van het auteursrecht aan de Universiteit Hasselt behoud ik als auteur het recht om de eindverhandeling, - in zijn geheel of gedeeltelijk -, vrij te reproduceren, (her)publiceren of distribueren zonder de toelating te moeten verkrijgen van de Universiteit Hasselt.

Ik bevestig dat de eindverhandeling mijn origineel werk is, en dat ik het recht heb om de rechten te verlenen die in deze overeenkomst worden beschreven. Ik verklaar tevens dat de eindverhandeling, naar mijn weten, het auteursrecht van anderen niet overtreedt.

Ik verklaar tevens dat ik voor het materiaal in de eindverhandeling dat beschermd wordt door het auteursrecht, de nodige toelatingen heb verkregen zodat ik deze ook aan de Universiteit Hasselt kan overdragen en dat dit duidelijk in de tekst en inhoud van de eindverhandeling werd genotificeerd.

Universiteit Hasselt zal mij als auteur(s) van de eindverhandeling identificeren en zal geen wijzigingen aanbrengen aan de eindverhandeling, uitgezonderd deze toegelaten door deze overeenkomst.

Voor akkoord,

Van Raemdonck, Nathan

Datum: **31/05/2015**